AD-A259 642

REPORT DOCUMENTATION PAG

1. AGENCY USE ONLY (Leave blank)	2. REPORT DATE	3. REPORT TYPE AND DATES COVERED
		FINAL 01/01/90 - 12/31/91

4. TITLE AND SUBTITLE

Radiation Effects in HEMTS

5. FUNDING NUMBERS

AFOSR-90-0086

6. AUTHOR(S)

Professor G.J.Papaioannou

7. PERFORMING ORGANIZATION NAME(S) AND ADDRESS(ES)

University of Athens
Solid State Section, Physics Department
Panepistimiopolis
GR-157 84 ZOGRAFOS Athens GREECE

8. PERFORMING ORGANIZATION REPORT NUMBER

9. SPONSORING/MONITORING AGENCY NAME(S) AND ADDRESS(ES)

European Office of Aerospace Research and Development
PSC 802 Box 14,
FPO AE 09499-0200

10. SPONSORING/MONITORING AGENCY REPORT NUMBER

11. SUPPLEMENTARY NOTES

12a. DISTRIBUTION/AVAILABILITY STATEMENT

Approved for puplic release;
Distribution unlimited

12b. DISTRIBUTION CODE

13. ABSTRACT (Maximum 200 words)

Various structure HEMTs have been irradiated with He irons (MeV alpha particle), fast neutrons and Co60 gamma rays. The radiation doze was varied up to 10^{13}a/cm^2, 10^{16}n/cm^2 and 10^7rads Si. The investigation has been extended on GaAs layers and AlGaAs/GaAs heterojuctions in order to determine the defects that are induced by radiation in GaAs and AlGaAs. The degradation sources of HEMTs and their dependence on the device layer structure have been determined. A charge control model was, also, employed in order to separate the contribution of donor and buffer layers on the 2DEG degradation. Finally the investigation included a comparative study of MESFET radiation degradation.

14. SUBJECT TERMS	15. NUMBER OF PAGES
Radiation, Gallium Arsenide, Reliability, HEMTS	106
	16. PRICE CODE

17. SECURITY CLASSIFICATION OF REPORT	18. SECURITY CLASSIFICATION OF THIS PAGE	19. SECURITY CLASSIFICATION OF ABSTRACT	20. LIMITATION OF ABSTRACT
UNCLASSIFIED	UNCLASSIFIED	UNCLASSIFIED	

RADIATION EFFECTS IN HEMTs

University of Athens

Solid State Physics Section

Physics Dpt

Project Leader

Assis. Prof. G J Papaioannou

Grant No : AFOSR 90-0086

CONTENTS

SUMMARY

The effect of particle and electromagnetic radiation on HEMTs has been investigated. The particle irradiation consisted of He ions and neutrons while the electromagnetic one consisted of Co60 gamma rays. Total radiation doses in the case of He ions was $10^{13}cm^{-2}$, in the case of neutrons was $10^{16}cm^{-2}$ and in the case of gamma rays was $3x10^{7}$rads. The investigation included HEMT with conventional structures as also structures which included an AlGaAs buffer layer or a low temperature grown AlGaAs donor layer. The present study showed that the introduction of an AlGaAs buffer does not improve considerably the device radiation hardness. In contrast it was found that the use of a low temperature grown AlGaAs donor layer enhances significantly the HEMT radiation hardness. Comparative studies including MESFETs have shown that HEMTs are more radiation hard. Only MBE MESFETs fabricated on highly doped channels whic were grown on LT buffers are radiation hard as HEMTs.

1. INTRODUCTION

Radiation generates defects in the crystal lattice by displacing lattice constituents, thus introducing additional energy states in the energy band of the semiconducting material. These defects may act as recombination centers which reduce the minority carrier lifetime. On the other hand, the displacement defects do introduce additional fixed charges, which have the same effect as a change in the net dopant concentration. Therefore the semiconductor material always becomes more intrinsic as a result of radiation damage. Moreover, the carrier mobilities are reduced due to scattering by the radiation induced defect centers.

The AlGaAs/GaAs high electron mobility FET (HEMT) is an important component for applications involving high speed digital and microwave/millimeter wave integrated circuits for data and signal processing and communication systems. These devices have demonstrated higher frequency, lower power dissipation, higher gain, and lower noise over the GaAs MESFETs. For many applications in environments fraught with radiation hazards, such as outer space and nuclear reactors, HEMTs must perform satisfactorly. Thus the understanding of the performance of HEMTs under exposure to radiation is required. HEMTs consist of many layers which thickness, composition and doping level must be precisely controled during growth. The introduction of charged states, in addition to the above mentioned electrical parameters, decreases the band bending slo-

pe of the barriers between the various layers. This results into an additional source of degradation of the 2DEG and hence the device performance. Considering all these parameters it becomes obvious that the radiation induced degradation in these devices is a composit effect.

A significant effort was payed for the determination of the degradation sources in the device structure. The result of this effort was the publication of a significant number of papers dealing with different nature radiations and device structures, including also microwave monolithic integrated circuits (MMICs). These investigations showed that under exposure to neutron [1,2] or gamma [3,4] radiation, HEMTs are susceptible to displacement and ionization damage. The response of HEMTs to transient ionizing radiation [5] and the dependence of the magnitude of induced, persisting, currents on the concentration of deep traps was also studied in [5]. Finally the radiation degradation induced by heavy ions, such as H, He, O and Si was investigated and the threshold dose for significant damage, induced by each ion species, was determined and reported in [6]. In all previous studies the effort was concentrated, mainly, on the determination of the dependence of the threshold voltage on the radiation dose. Other device parameters such as the transconductance, the drain saturation current, the noise and frequency respone were also considered. Regarding the modeling of the device gegradation that has been introduced relatively recently in the literature and that to a limited scale. A comprehensive work

on the dependence of the threshold voltage on the radiation dose, taking into account the carrier removal rate in the AlGaAs layer and the introduction rate of electron and hole traps in the GaAs buffer layer, was done only for neutron irradiated HEMTs [1,2].

The aim of the present project is to obtain a better knowledge on the radiation effects in HEMTs. This is achieved by investigating the effect of various radiations in these devices. So both particle and electromagnetic radiation were employed. The particle radiation consisted of either heavy ions (He^{2+}, alpha particles) or fast neutrons and the electromagnetic one consisted of Co60 gamma rays.

In the present project the irradiation has been performed initially on GaAs layers with different doping levels in order to determine the traps that are introduced by different kind radiation, the traps introduction rate and relation to the background doping. This was necessary in order to obtain information about the carrier removal rate in both the contact and buffer layer of the HEMTs. AlGaAs/GaAs heterojunctions have been irradiated in order to determine the carrier removal rate in both the AlGaAs layer and the quantum well. The main work was focused on HEMTs part of which were commertially available while the others have been fabricated by IESL FORTH (Crete, Greece). So devices with different structures were irradiated and the effect of radiation on the 2DEG carrier concentration, carrier mobility and the device characteristics were investigated as a function of the total

dose. A charge control model has been applied to determine the radiation effects in the various layers. Finally some radiation study has been performed on MESFETs in order to compare their performance to that of the HEMTs.

2. EXPERIMENT

2.1 Samples

The samples used in the present work were GaAs MBE layers, AlGaAs/GaAs heterojunctions and HEMTs. In addition a few MESFETs have been assessed simultaneously with the HEMTs.

The GaAs layers were grown by MBE method and doped with Si. The carrier concentration in these samples varyed from $10^{15}cm^{-3}$ to $10^{18}cm^{-3}$. All layers were grown on undoped semi-insulating substrates so all contacts were made on the epi-layer. The test structures were simple Au Schottky diodes for the samples with carrier concntrations lower than $10^{17}cm^{-3}$ and MESFETs for those with carrier concentrations larger than that. The layer thickness was about 5μm for the low carrier concentraion samples and about 0.1μm to 0.2μm for the high concentration ones, presented in Fig.1a and 1b respectively.

The AlGaAs/GaAs heterojunctions were grown in order to simulate the HEMT quantum well although the carrier concentration in all layers were quite differed from those of HEMTs. The structure of these samples is presented in Table 1 and consists of an N^+ GaAs substrate for the deposition of a back ohmic contact. The doping level in both GaAs and AlGaAs layers wass chosed so that the samples to be assessed by a conventional C-V method, using a 1MHz Boonton bridge. On top a thin GaAs capping layer was deposited to avoid the oxidation of the AlGaAs one. Finally an Al Schottky contact was made on the upper layer.

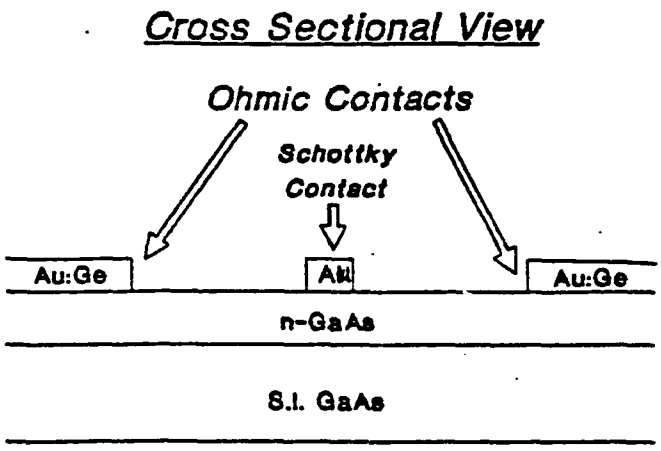

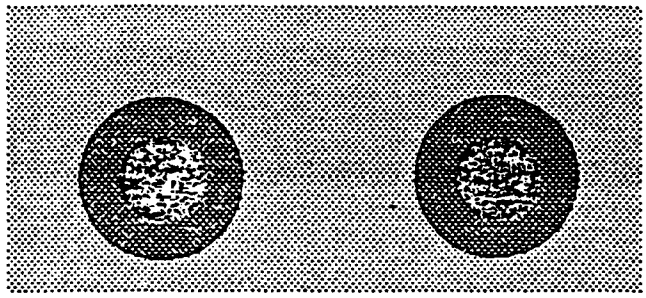

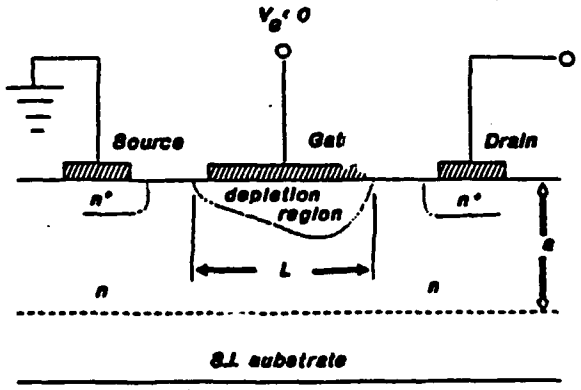

Fig.1 Cross section of (a) Schottky diodes on the low doping level samples and (b) MESFETs on the high doping level ones

Table 1. AlGaAs heterojunction layer structure

Layer	Doping	Thickness
n GaAs	$10^{16}cm^{-3}$	0.1μm
n AlGaAs	$2x10^{16}cm^{-3}$	0.5μm
n GaAs	$10^{15}cm^{-3}$	0.5μm
n+ GaAs	substrate	

The layer structure of the HEMTs used in this project is summarized in Table 2. Commertially available HEMTs as well as non conventional ones have been employed. In the case of the commertially available HEMTs the layer structure was possible to be definrd. Only the devices geometry was determined by SEM. So it was assumed their structure was was similar to structure A in Table 2. HEMTs with a second AlGaAs buffer layer under the GaAs one, structure B, have been also used since these structures exhibit a lower "photoconductivity" when they are exposed to ionizing electromagnetic radiation [5]. Finally HEMTs (structure C) in which the AlGaAs space and donor layers as also the GaAs contact layers were grown at lower temperatures Tg=510°C (nominally 650°C), as in the case of GaAs pseudomorphic HEMTs.

The study has been completed by assessing the MESFETs which are already mentioned above and presented in Fig.1b. Some additional MESFETs fabricated on low temperature buffers (Tg=250°C) have been assessed simultaneously with the HEMTs in order to compare their radiation hardness to that of the HEMTs and of the conventional MESFETs.

Table 2. HEMT layer structure

Layer	Doping	Thickness Struct.A*	Struct.B+	Struct.C#
n^+ GaAs	$2x10^{18}cm^{-3}$	100A	100A	100A
n^+ AlGaAs	$2x10^{18}cm^{-3}$	450A	500A	450A
AlGaAs	-	30A	100A	30A
GaAs	-	1μm	1μm	1μm
AlGaAs	-	-	2μm	-
GaAs	SI	substrate	substrate	substrate

* AlGaAs Al mole fraction 28%
\+ AlGaAs Al mole fraction 30%
\# AlGaAs growth temperature was 510°C and Al mole fraction 28%

2.2 Radiation Sources and Assessement

All samples have been irradiated with either particle or electromagnetic radiation. The electromagnetic radiation consisted of gamma rays obtained from a Co60 source while the particle one consisted of either heavy ions He^{2+}, that is alpha particles obtained from an Am source, or fast neutrons obtained from the reactor of NRCPS Demokritos (Athens, Greece).

The alpha particles had an average energy of 5MeV and the samles irradiation fluence covered the range of $10^{10}cm^{-2}$ to about $10^{13}cm^{-2}$. The neutrons, as already mentioned were obtained from a nuclear reactor, and their energy spectrum was continuous above 10KeV. The sampes have been irradiated with doses covering the range of $10^{13}cm^{-2}$ to $10^{16}cm^{-2}$. Finally the gamma ray total radiation dose did not exceeded the dose of $3x10^7$ rad Si due to extremelly large radiation time.

All devices were characterised before and after each

successive dose. In the case of Schottky diodes the assessment was restricted on C-V and Deep Level Transient Spectroscopy (DLTS) measurements. In the case of MESFETs and HEMTs it consisted of obtaining the I_{DS}-V_{DS} or V_{GS} and on long gate devices the C-V characteristics. From those the G_m, G_D and N_s characteristics were furthere calculated. Additionally DLTS measurements of either the gate capacitance or drain current were performed in order to monitor the background trap concentration and the introduction of new traps by radiation. In all cases the HEMT aluminum mole fraction was greater than 22% so the DX center was present in all DLTS specctra. The dependence of the devices drift mobility on the sheet carrier concentration was also determined for various radiation doses. That was obtained from both geometrical magnetoresistance and linear region I_{DS}-V_{DS} measurements.

3 He^+ ION RADIATION

3.1 Radiation Effects in GaAs Layers

The study of radiation damage in GaAs was considered to be of great importance since this was not investigated in detail previously. Although there have been reports in the literature on He ion radiation damage in MESFETs [16] and HEMTs [7], they did not investigated these effects in such detail as in the case of neutrons. So there is only one report [17] which investgates the degradation factor in GaAs and that in ion implanted layers which were exposed to 65MeV He ions.

The samples used in this investigation were Si doped molecular beam epitaxy (MBE) layers with carrier concentrations ranging from $10^{15}cm^{-3}$ to $10^{18}cm^{-3}$. Defect characterisation was performed by means of capacitance DLTS, in Schottky diodes for low carrier concentration samples, or drain current DLTS, in MESFETs for high carrier concentration samples. In each case these measurements were combined with free carrier profiling, the last were obtained by a differential C-V method.

A. Schottky Diodes ($n<10^{17}cm^{-3}$)

Samples with carrier concentrations $3x10^{15}cm^{-3}$ (S1) and $2x10^{16}cm^{-3}$ (S2) have been used for Schottky diodes. The DLTS characterisation before irradiation revealed two traps which have been introduced during the material growth. These traps have been identified by comparing their Arrhenious plots, si-

grnatures, to those of well known ones that are introduced during the MBE growth. The identification has shown that in all samples they are the EB5 and the EB7 with concentrations ranging between $3x10^{-4}$ and 10^{-3} with respect to the background doping. A spectrum of these traps is presented in Fig.2a.

The free carrier concentration and DLTS spectra were not affected by irradiation doses bellow $10^{10}cm^{-2}$. Beyond that dose only the concentration and the patern of EB7 started to change while EB5 remained unaffected. This suggested that the threshold dose for 5MeV alpha particle radiation induced damage for low carrier concentration GaAs can be considered to be close to $10^{10}cm^{-2}$ which is in good agreement with the reported level of $2x10^{9}cm^{-2}$ [7] obtained from radiation studies on MESFETs.

The free carrier concentration of samples S1 decreased to $10^{15}cm^{-3}$ after a total dose of $2x10^{12}cm^{-2}$ and the DLTS spectra revealed the introduction of five traps labeled Ea1 to Ea5 (fig.2b) with activation energies of 0.19eV, 0.26eV, 0.39eV, 0.45eV and 0.61eV (Table 3) respectively. On the other hand the same total dose decreased the free carrier concentration of samples S2 to $8x10^{15}cm^{-3}$ and introduced clearly four traps the Ea2 to Ea5 (fig.2c), while the trap Ea1 was observed within the detection limits of the DLTS system which for the background concentration of the presend samples was about $10^{12}cm^{-3}$. In the samples S1 only the trap Ea4 was not clearly resolved while in S2 the same trap appeared as a

structure associated to Ea5 trap. That resulted in an inaccurate calculation of its activation energy from the Arrhenius plot. Another feature of the introduced defects is the fact that their concentrations, hence the introduction rate, depend on the background doping of the unirradiated material. So in sample S2, where the doping is larger, the introduction rates of the traps Ea3 and Ea5 have increased considerably over the introduction rate of the trap Ea2.

In order to get more insight on the origin of these traps isochronal annealings for 10min. were performed up to 300°C and the DLTS spectra were found to remain similar to the as-irradiated ones. That indicated that these traps are not related with simple primary damages such as those introduced by electron irradiation [8-11]. This is in agreement with the fact that alpha particles, due to their large mass, must produce significant disturbances through the whole irradiated layer. The lattice atoms, recoiled into the semiconductor, will leave the near-surface region with a significant concentration of As and Ga vacancies, while the displaced As and Ga atoms must lie several atomic planes of the simultaneously created vacancies. So the primary point defects, vacancies and displaced atoms, will be on average much more widely separated than they are in the electron irradiated GaAs. As a result of the large distance over which the primary defects must migrate before they recombine, other point defects acting as sinks for the diffusing interstitials and vacancies should be considered. Thus impurities may combine with dif-

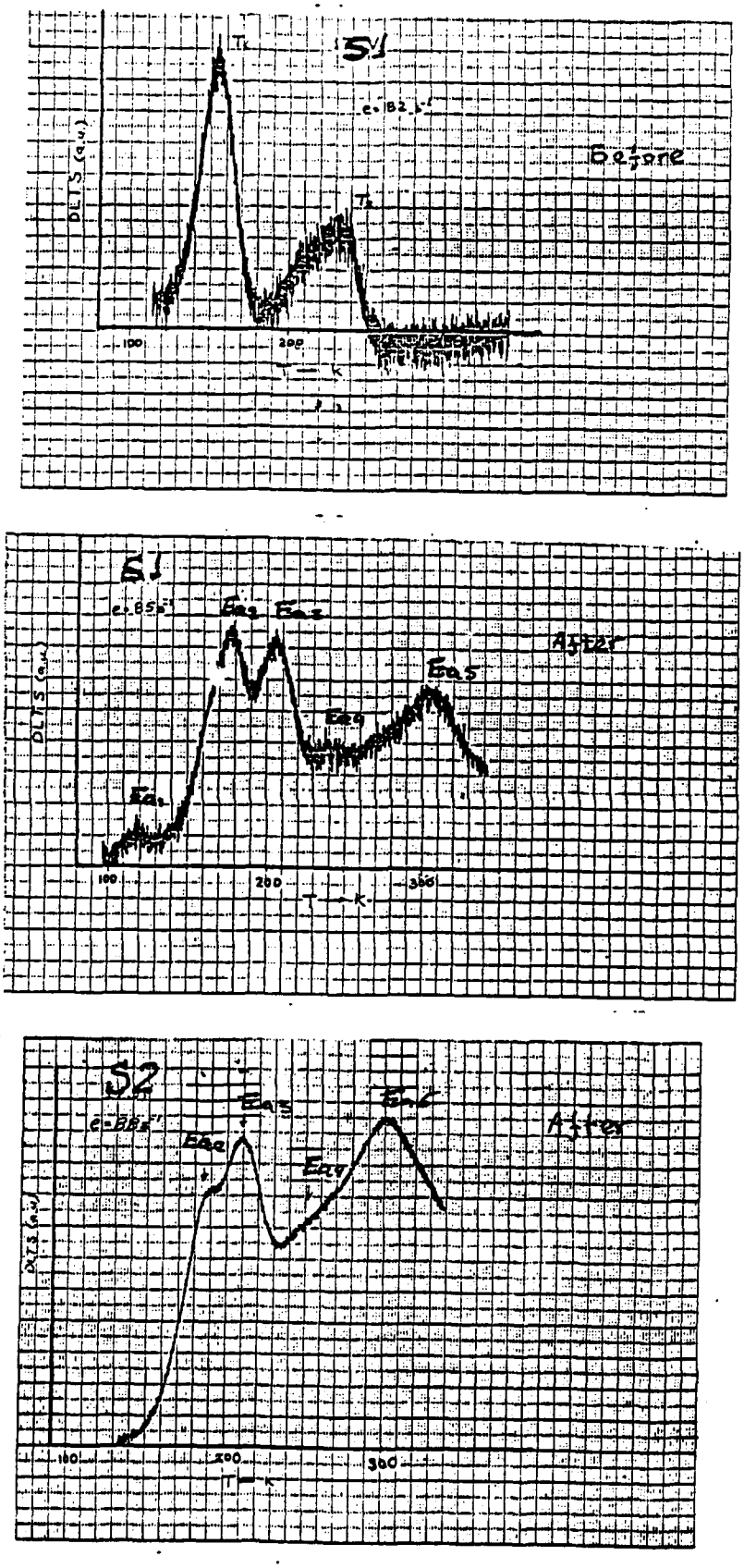

Fig.2 DLTS spectra of (a) deffects introduced in samples during growth and after 2x1012cm-2 total dose He+ irradiation in sampe (b) S1 and (c) S2

fusing vacancies and form complexes involving displaced atoms from the same sublattice. Therefore the observed different increases in the introduction rates with the increase of the background doping must be attributed to this mechanism. On the other hand the trap Ea1 must be attributed to defects which do not the involve material doping since their concentration, hence the introduction rate, is almost the same in both samples.

In order to identify the induced defects or to find other traps with similar characteristic parameters the signatures of the Ea1 to Ea5 traps were compared to those of well known ones. The comparison has assigned Ea1 to I6 [12] which is more probable since there is no report on the dependence of the I6 concentration on the material doping. The other defects were assigned the Ea2 to I5 [12] and Ea3 and Ea5 to L1p and L2p [13] respectively. Since the Ea2 introduction rate

Table 3. Electron traps introduced after 2×10^{12} cm^{-2} radiation dose with 5MeV alpha particles

Trap	Ea (eV)	Nt (10^{13} cm^{-3})		Assignement
		S1 N_D (10^{15} cm^{-3})	S2 N_D (10^{16} cm^{-3})	
Ea1	0.19	0.2	- -	I6[12]
Ea2	0.26	1.6	5.6	I5[12]
Ea3	0.39	1.4	8	L1p[13]
Ea4	0.45	0.7	4	-
Ea5	0.61	1.2	8.5	L2p[13]

depends on the material doping this suggests that Ea2 is more probably a defect with characteristics similar to those of I5 than being the I5 itself. Regarding the other candidates the defects L1p and L2p are induced by 2MeV proton irradiation [13]. Annealing studies have shown that the L2p concentration remains alsmost constant after isochronal annealings up to 300°C while L1p showes a two step annealing behavior with the first step taking place bellow 300°C. Comparing this behavior to the one exhibited by Ea3 and Ea5 it is concluded that Ea5 may be considered to have a closer relation to L2p than Ea3 to L1p. These results are summarized in Table 3.

B. MESFETs ($n>10^{17}cm^{-3}$)

The doping level of the samples on which MESFETs were processed were $1.5x10^{17}cm^{-3}$ (S3) and $2x10^{18}cm^{-3}$ (S4). MESFETs with gate lengths of 1μm to 20μm and widths of 250μm were processed. The devices were assessed by I-V and C-V characteristics and drain current DLTS. The C-V profiles revealed that alpha particle irradiation of $2x10^{12}cm^{-2}$ total dose decreases the initial carrier concentration of sample S3 from $1.5x10^{17}cm^{-3}$ to about $10^{17}cm^{-3}$ and that of sample S4 from $2x10^{18}cm^{-3}$ to about $1.4x10^{18}cm^{-3}$. Only two traps have been detected before irradiation. These were native traps, namely the M2 and E5A, which are introduced during MBE growth. In

Table 4. Electron traps introduced by alpha particles in samples with $10^{17}cm^{-3}$ carrier concentration

Trap	Ea eV	Nt $10^{14}cm^{-3}$	Assignement
Ea6	0.31	1.4	-
Ea3	0.41	1.6	L1p [13]
Ea5	0.66	1.5	L2p[13]
Ea7	0.89	1.5	L3p [13]

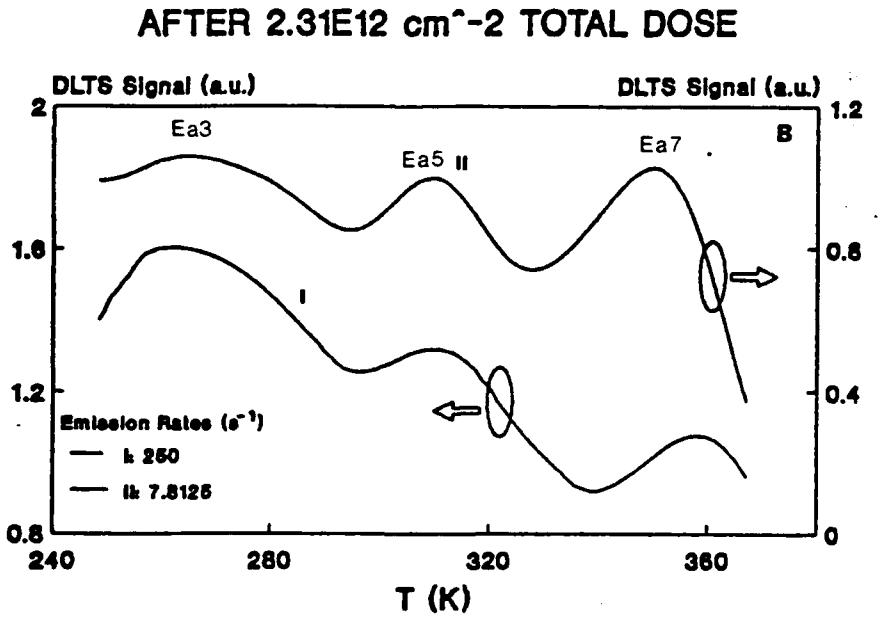

Fig.3 S3 samples IDS-DLTS spectra obtained after a radiation dose of $2.3x10^{12}cm^{-2}$ He ions.

these samples it was found that alpha particle irradiation introduces only four traps. These were easily detected in sample S3 (fig.3) and the results from their Arrhenious plots are summurised in Table 4. Very noisy spectra were obtained from samples S4 due to excess leackage in the FATFET gate . Smoothed spectra are presented in Fig.4 and an indication of their activation energies and concentrations are presented in Table 5. Each trap identity was determined by the method already described above.

Table 5. Electron traps introduced by alpha particles in samples with $10^{18}cm^{-3}$ carrier concentration

Trap	Ea eV	Nt $10^{14}cm^{-3}$	Assignement
Ea8	0.22	2.2	? I6[12]
Ea3	0.36	2.1	L1p[13]
Ea7	0.89	2.0	L3p[13]

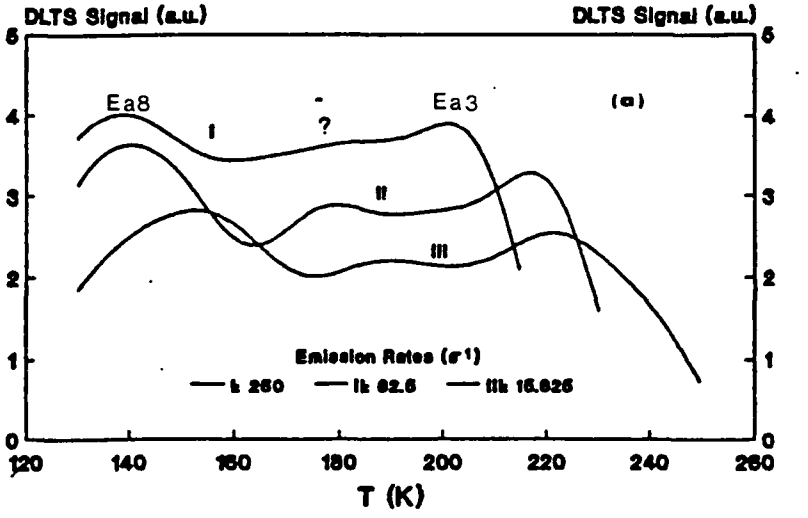

Fig.4 S4 samples IDS-DLTS spectra obtained after a radiation dose of $3.8x10^{12}cm^{-2}$ He ions.

The study of these structures leads to usefull conclusions about the He ion induced degradation of GaAs buffers and contact layers of HEMTs. It is well known that the carrier concentration in a semiconductors decrease when they are exposed to radiation. The rate of carrier removal can be described by a simple differential equation

$$\frac{dN}{dD} = - \beta N_o$$

where D is the radiation dose, N_o the carrier concentration of the unirradiated material and ß the degradation parameter which depends on the initial carrier concentration. Previous investigations in GaAs [14] have shown that for neutron radiation the degradation parameter depends on the background doping as

$$\beta(cm^2) = 7.2x10^{-4} N_o^{-0.77}$$

The mass and charge of He ions is much different of that of neutrons so the degradation parameter is expected to be different too. In Fig.5 is presented the variation of the degradation parameter as a function of the GaAs layer initial doping. From that plot the it was found that in the case of 5MeV He ions the degradation parameter is given by

$$\beta(cm^2) = 1.4x10^{-11} N_o^{-0.095}$$

The relation which was obtained from the carrier removal rate in Ref.17 in ion implanted resistors was quite different

$$\beta(cm^2) = 2.1x10^{-4} N_o^{-0.62}$$

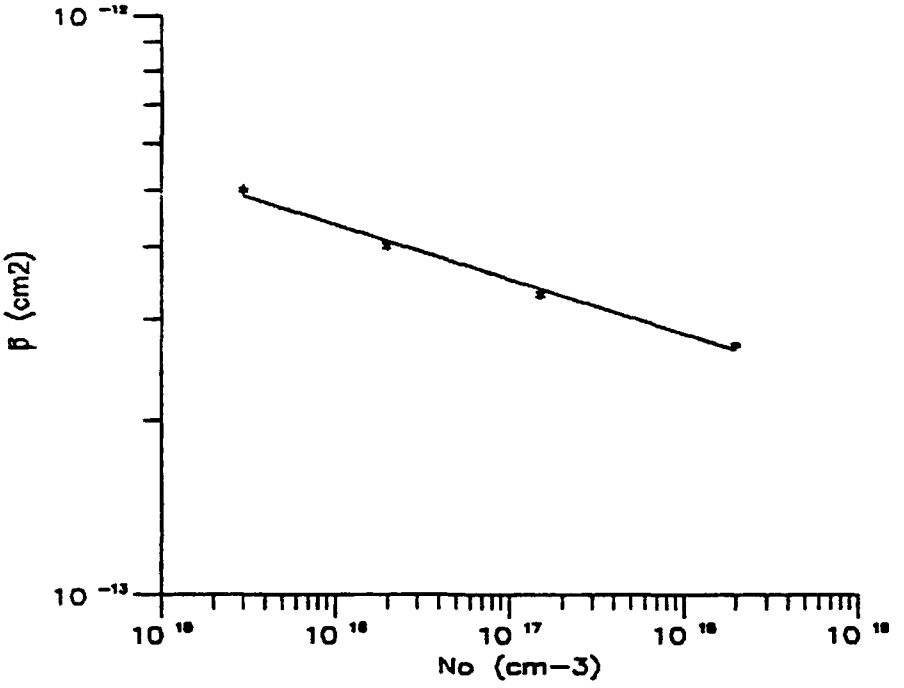

Fig. 5 Dependence of the degradation parameter on the semiconductor background doping. Data obtained from GaAs irradiated with 5MeV He ions.

but it must be pointed out that the He ion energy was much larger (65MeV) than the one in the present investigation and the GaAs layers were ion implanted ones, which as found from our experiments degrade faster than the MBE ones. From additional experiments on the shift of the threshold voltage of MBE grown MESFETs which were exposed to 5MeV He ions [15] we obtained a similar result. In that case the degradation parameter was found to given by the relation

$$\beta(cm^2) = 3.3x10^{-11}N_o^{-0.11}$$

This is in very good agreement with the present results if we take into account that in the case of MESFETs the threshold voltage is affected also by other parameters such as the substrate doping and the doping uniformity of the channel.

Heavy ion radiation introduces in GaAs complex traps which introduction rate, as shown in Figs. 2-4, depends on the Si donor concentration. Among eight traps, detected in all samples, three of them, namely Ea3, Ea5 and Ea7, were most frequently encountered. The dependence of the concentration of these traps on the background Si donor concentration

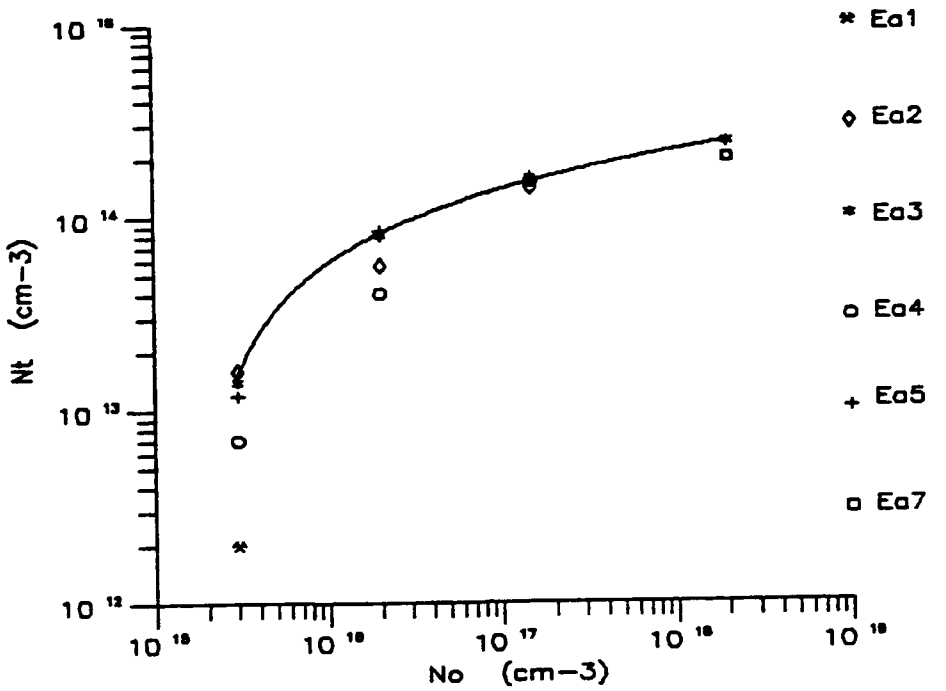

Fig. 6 Dependence of the trap concentration on the background doping in GaAs irradiated with 2×10^{12} cm^{-2} He ions.

for a radiation dose of $2x10^{12}cm^{-2}$ is ploted in Fig.6. In the same figure the concentration of the other five detected traps is presented. It is important to notice the sublinear relation of the trap concentration. This indicates that the background impurities, in the present case Si, combine with the diffusing vacancies at room temperature and form complexes. It must be mentioned that other point defects are also involved acting as sinks for the diffusing interstitials and vacancies. Such a defect may be considered the EL2 although there has been no indication of the involvement of this trap. In conclusion the carrier removal in GaAs exposed to He ions shows a smaller dependence on the background doping compared to neutron radiation and the introduce electron traps show a sublinear dependence on the background concentration.

3.2 Radiation Effects in Heterojunctions

The carrier concentration in both the donor layer and the 2DEG of an AlGaAs/GaAs heterojunction can be determined by C-V profiling [18]. The structure of the heterojunctions used in this project has been already presented in Table 1. The carrier profile of these structures shows a minimum of carrier concentration on the AlGaAs side and a peak on the GaAs side of the heterojunction. The samples were irradiated up to $10^{13}cm^{-2}$ dose. The radiation of these samples with He ions resulted into a simoultaneuous decrease of the carrier concentration in the AlGaAs donor layer and in the 2DEG. This

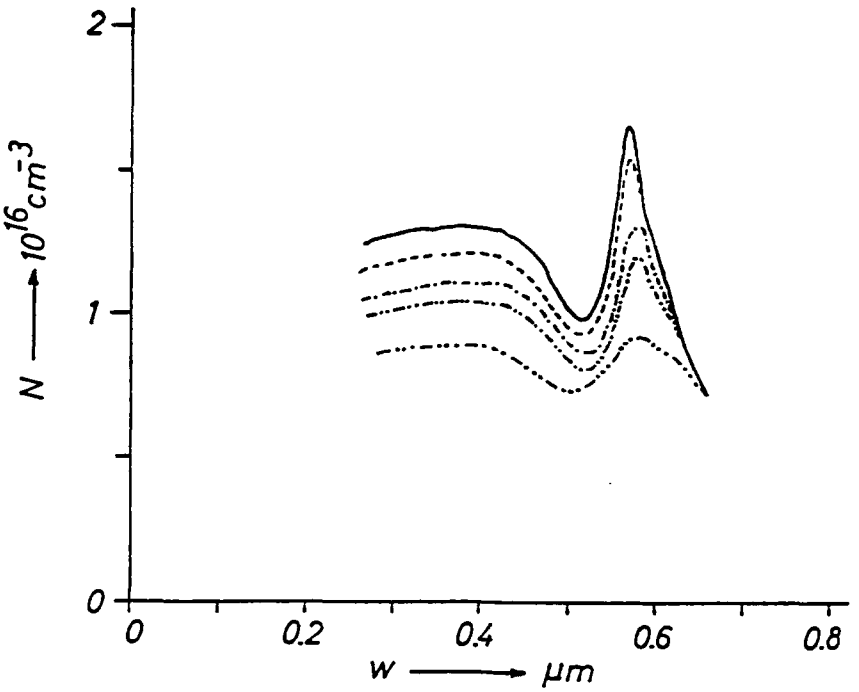

Fig. 7 Profile of an AlGaAs/GaAs heterojunction obtained from the C-V characteristic. The continuous line corresponds to the characteristic before irradiation, (···) after a dose of $1.5 \times 10^{12}\,cm^{-2}$, (- -) a dose of $3 \times 10^{12}\,cm^{-2}$, (-·-·-) a dose of $4.7 \times 10^{12}\,cm^{-2}$ and (-···-···-) after a dose of $6.6 \times 10^{12}\,cm^{-2}$.

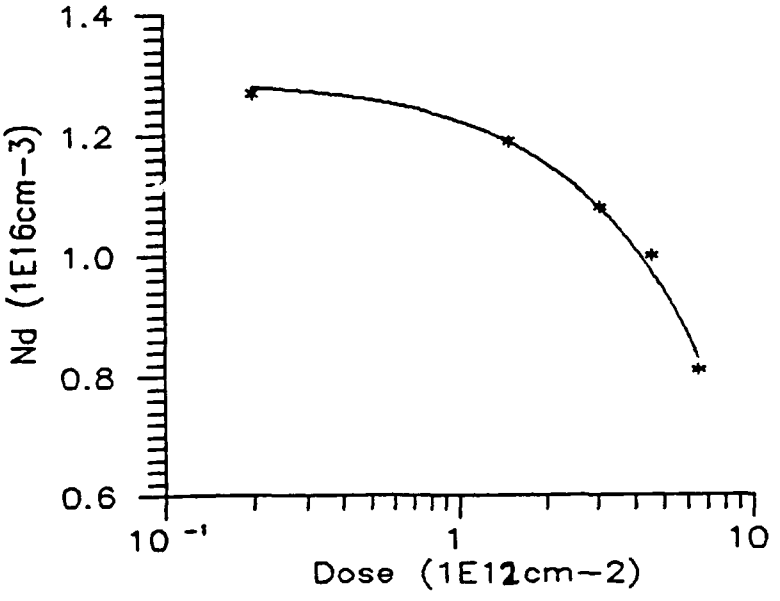

Fig. 8 Dependence of AlGaAs carrier concentration on the radiation dose.

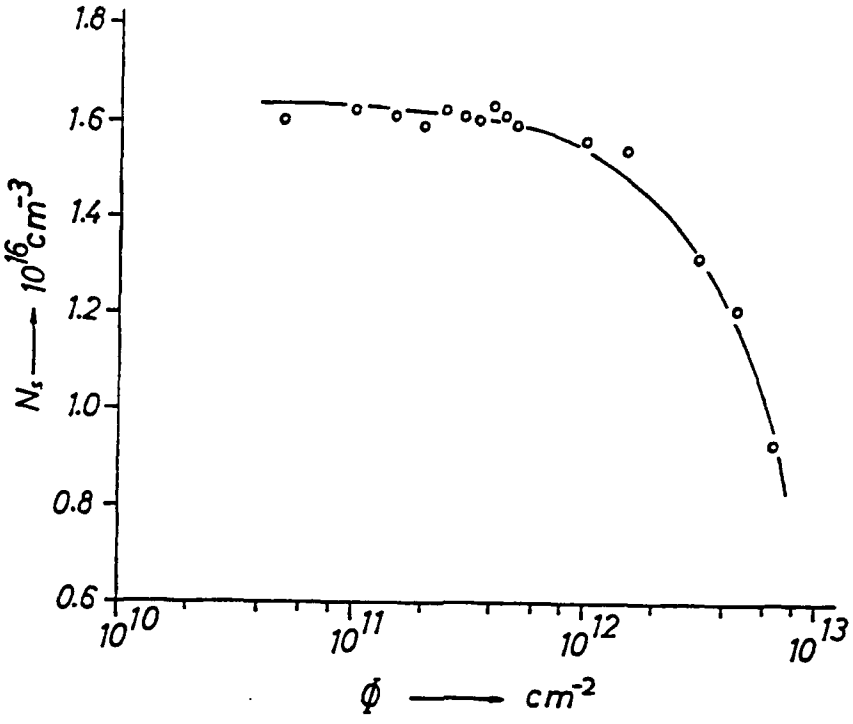

Fig. 9 Dependence of the 2DEG carrier concentration on the radiation dose.

is shown, for severalradiarion doses, in Fig.7. The carrier removal was found to follow a linear relation with the radiation dose in both the AlGaAs and 2DEG and are presented in Fig.8 and 9 respectively. The data in both cases were fited to the general equation

$$N(D) = N_o\ (1-\beta D)$$

where β is the degradation parameter. The degradation parameters were not the same, that is in the case of

* AlGaAs $\beta = 5.5\times10^{-14}\,cm^2$

and

* 2DEG $\beta = 6.3\times10^{-14}\,cm^2$

This clearly suggests that the decrease of carrier concentration in the 2DEG must not be attributed only to the decrease of carrier concentration in the AlGaAs but also to other reasons such as the introduction of charges into the GaAs layer, as shown above, and the generation of interface states. Hear it must be mentioned that in these samples the carrier concentration in the GaAs is much larger than that in a conventional HEMT and also that the depth of the well is not as large as in HEMTs. Therefore the effect of introduction of charges in the GaAs layer must be considered as a less significant effect which suggests that the generation of interfece traps is a more significant one. This is also supported from mobility measurements in HEMTs.

DLTS measurements did not reveal any significant trap concentration comparable to that of the DX center. This was also supported by the DLTS spectra of HEMTs. Hear it must be pointed that these results do not suggest that He ion irradiation does not introduces traps in AlGaAs. In contrast traps are introduced but their concentration is much lower than that of the DX center such as that presented in Fig.10. The origin of this trap was not possible to be traced due to its low concentration.

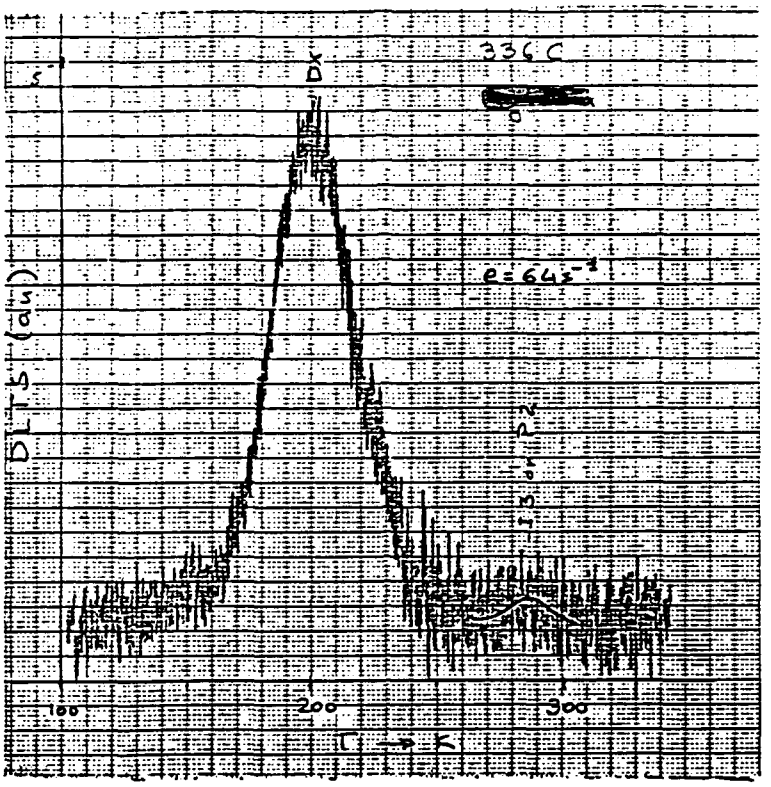

Fig.10 Electron trap detected in HEMTs after a $10^{12}cm^{-2}$ dose

3.3 Radiation Effects in HEMTs

Ionizing radiation degrades the performance of MESFETs and HEMTs. This is manifested primarly through the degradation of their I-V characteristics which in turn is the result of the degradation of the mobility and carrier concentration in the semiconductor, the decrease of the electric field in the junctions and the variation of other parameters such as the series resistances. Starting from the I-V characteristics we shall attempt to understand the degradation mechanisms by evaluating and studying the variation of each parameter with radiation.

I-V Characteristics

The effect of He ion irradiation on the I_{DS}-V_{DS} characteristic, of 1μm gate length devices, is shown in Figs.11a and 11b for structure A and C respectively. The behavior of structure B HEMTs was similar to that of structure A, thus it is not presented. The evolution of the I-V characteristcs with the radiation dose indicates that the device performance is not significantly affected for radiation doses lower than about $10^{12}cm^{-2}$. Beyond this level the devices degradation rate becomes significant. So the drain current drops to almost 20% of its pre-irrradiation value at a total dose of about $1.4x10^{12}cm^{-2}$ on structures A and B and at $2.6x10^{12}cm^{-2}$ on structure C. A comparison of the degradation rates of these structures leads to the conclusion that the devices in which the AlGaAs donor and spacer layers was grown at lower temperatures, that is the donor layer contains more defects, are more resistant than those in which the AlGaAs layers was grown at higher temperatures. On the other hand the presence of an AlGaAs buffer layer seems to play a minor role on the device radiation hardness although experiments on transient ionizing radiation response have shown an improved performance of MESFETs [16] with AlGaAs buffer layers and HEMTs with superlattice buffer layers [19]. In general the degradation of the I_{DS}-V_{DS} characteristics may result from:

a) the decrease of the 2DEG carrier concentration

b) the decrease of the mobility or saturation velocity, when the device operates in the linear or saturation

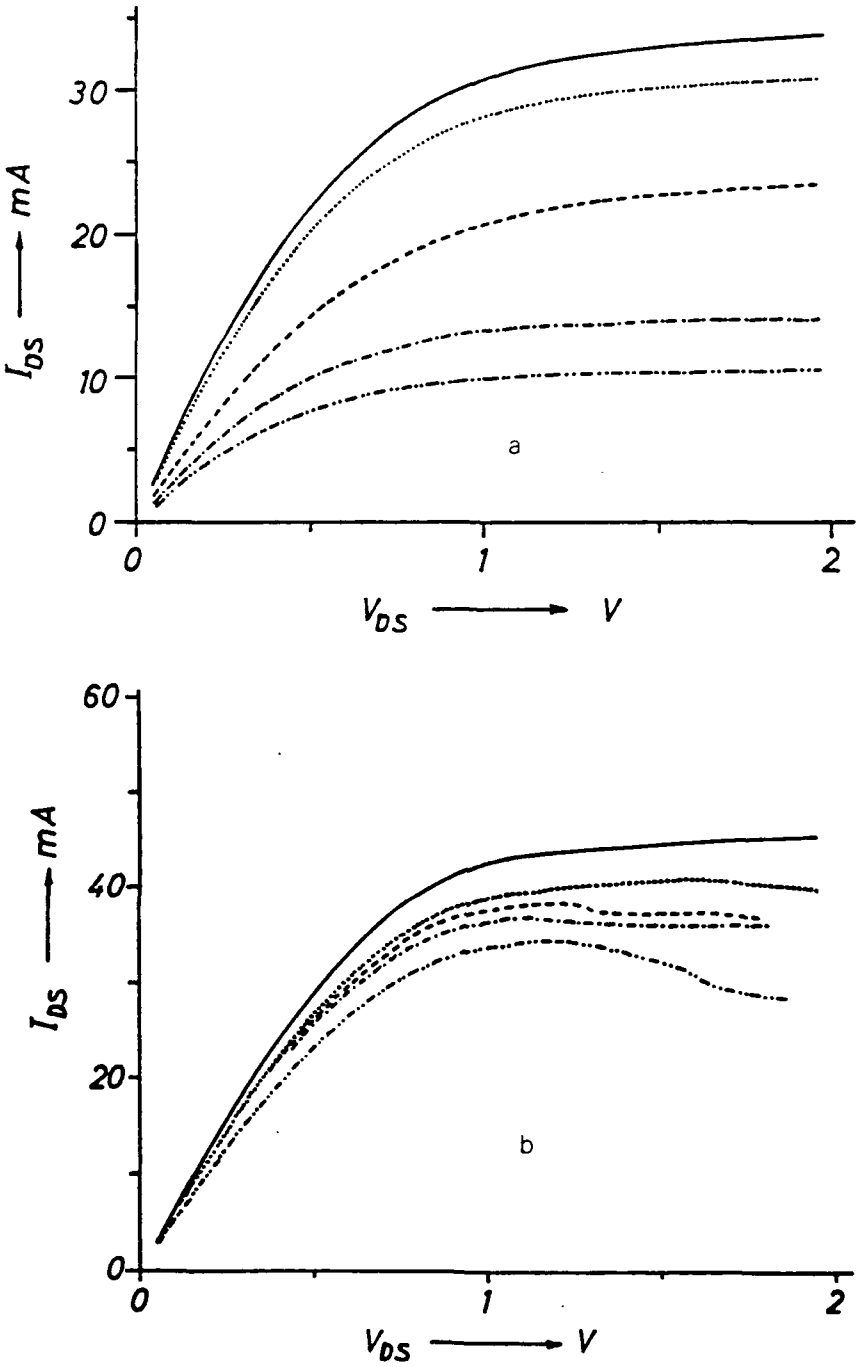

Fig.11 Degradation of I_{DS}-V_{DS} characteristics (V_{GS}=0V) of:
(a) structure A: continuous line corresponds to the characteristic before irradiation, (···) after a dose of $5x10^{11}cm^{-2}$, (- -) after a dose of $3x10^{12}cm^{-2}$, (-·-·-) after a dose of $4.5x10^{12}cm^{-2}$ and (-···-···-) after a dose of $5.7x10^{12}cm^{-2}$.
(b) structure C: continuous line corresponds to the characteristic before irradiation, (···) after a dose of $1.2x10^{12}cm^{-2}$, (- -) after a dose of $1.6x10^{12}cm^{-2}$, (-·-·-) after a dose of $2.6x10^{12}cm^{-2}$ and (-···-···-) after a dose of $3.2x10^{12}cm^{-2}$. The drain current instabilities beyond V^{DS}=1V are caused bu oscillations.

region

c) the increrase of the threshold voltage

d) the increase of the source series resistance.

Since all these occur simultaneously the determination of the magnitude of each one is necessary for the understunding of degradation mechanisms of HEMTs.

The effect of radiation on the I_{DS}-V_{GS} characteristics becomes more evident if instead of studying them we study the transconductance ones. The Gm-V_{GS} characteristics give different information, that depending on whether they have been obtained when the device is biased in the linear region (fig.12) or at saturation (fig.13). In the first case the extrinsic transconductance Gme, that is the experimentally measured one, is practically equal to to the intrinsic Gmi one, because the low value of the source series resistance Rs plays no significant role in the equation which relates the extrinsic and the intrinsic trasconductances

$$Gmi = \frac{Gme}{1 + Gme \cdot Rs}$$

In the linear region the 2DEG mobility is always much larger than that of the heavily doped AlGaAs donor layer. Furthere we can assume that this is valid also for all radiation doses used in our experiments. On the other hand, as it will be shown later, the 2DEG mobility does not vary significantly with the carrier concentration at gate bias levels well above threshold. The current-voltage characteristics of

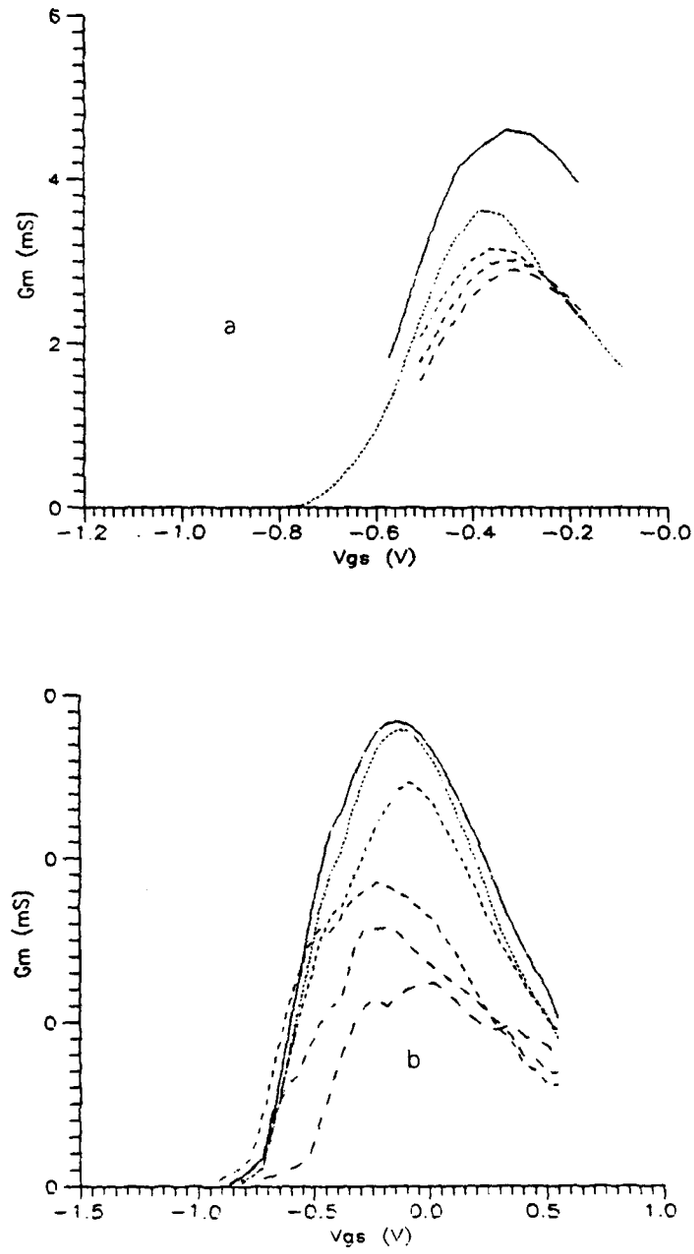

Fig.12 Degradation of linear region transconductance for
(a) structure A: continuous line corresponds to the characteristic before irradiation. The others correspond to doses of $8x10^{11}cm^{-2}$, $1.2x10^{12}cm^{-2}$, $1.8x10^{12}cm^{-2}$, $2.2x10^{12}cm^{-2}$ and $2.6x10^{12}cm^{-2}$.
(b) structure C: continuous line corresponds to the characteristic before irradiation. The others correspond to doses of $0.8x10^{12}cm^{-2}$, $1.6x10^{12}cm^{-2}$, $3.1x10^{12}cm^{-2}$, $4.5x10^{12}cm^{-2}$ and $5.7x10^{12}cm^{-2}$.

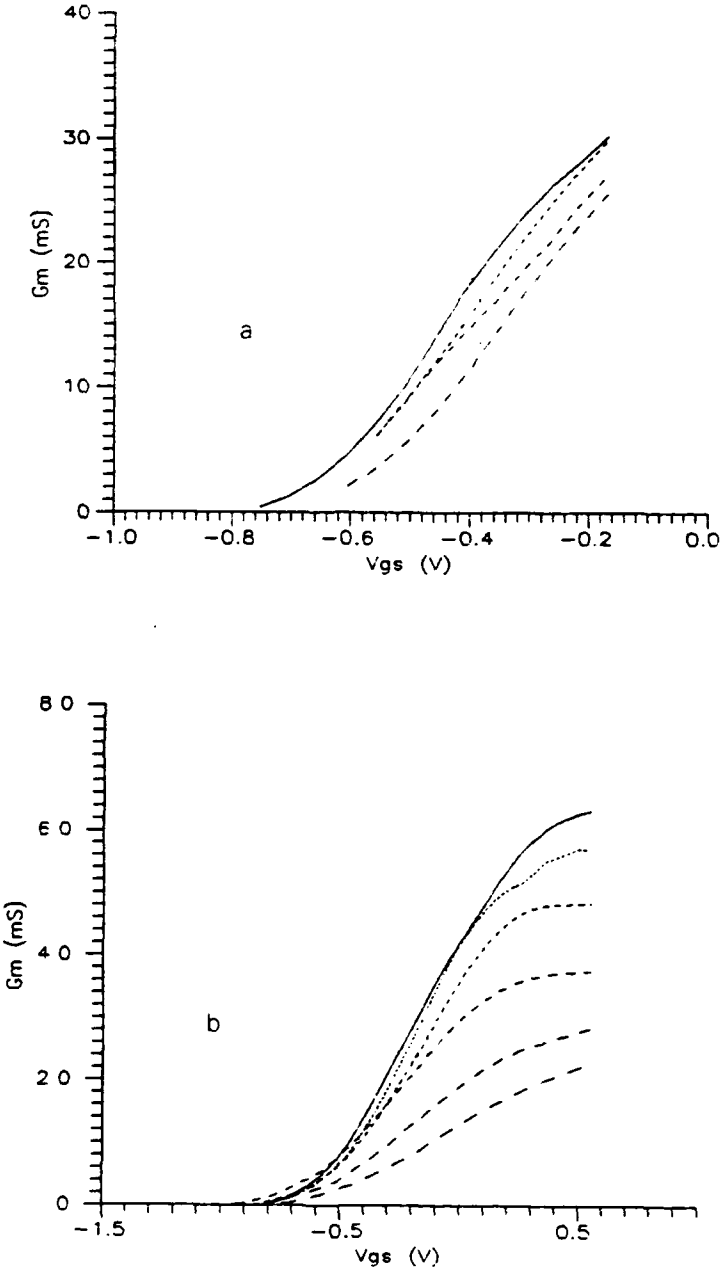

Fig.13 Degradation of saturation region transconductance for
(a) structure A: continuous line corresponds to the characteristic before irradiation. The others correspond to doses of $1.2\times10^{12}cm^{-2}$, $2.2\times10^{12}cm^{-2}$ and $2.6\times10^{12}cm^{-2}$.
(b) structure C: continuous line corresponds to the characteristic before irradiation.The others correspond to doses of $0.8\times10^{12}cm^{-2}$, $1.6\times10^{12}cm^{-2}$, $3.1\times10^{12}cm^{-2}$, $4.5\times10^{12}cm^{-2}$ and $5.7\times10^{12}cm^{-2}$.

a HEMT may be found based on the charge control model, using the gradual channel approximation [20]. This implies that the carrier concentration in the 2DEG is given by

$$Ns(x) = \frac{\varepsilon}{d_t} [V_{GS} - V_{th} - V(x)]$$

where d_t is the thickness of the AlGaAs layer, x the space coordinate along the channel and V(x) is the channel potential. If a very low potential is applied between the drain and source contacts the carrier concentration is almost constant. Then the transconductance of the linear region of operation can be written in a simple form:

$$Gm = q \cdot \mu \cdot W \cdot V_{DS} \frac{dNs}{dV_{GS}}$$

where W is the channel width. This denotes that the transconductance is in fact determined by the device charge control efficiency. Figure 12 shows a shift of the threshold voltage towards more positive gate bias levels with increasing the radiation dose. The origin of this shift will be discussed later. Another feature of Fig.12 is that the peak of Gm, which represents the maximum efficiency of charge control of the 2DEG , does not shift with radiation. This means that although the 2DEG is affected by the He ion radiation, its modulation starts at almost the same gate voltage and this is almost independent of the radiation dose. Such a behavior can be obtained only if the pinch-off voltage, V_P, of the donor layer remains almost constant or at least it varies slowly

with the He ion dose. More information can be obtained if the gate bias, for total donor layer depletion, is written as

$$V_{GS} = V_P - V_{bi}$$

where V_{bi} is the Schottky gate junction build in potential. The height of the build in potential is determined by the surface potential Φ_b, the net donor concentration N_D and the conduction band density of states N_c by

$$V_{bi} = \Phi_b + kT \cdot \ln(N_D/N_c)$$

Upon radiation the build in voltage decreases with increasing the dose due to carrier removal. Assuming a carrier reremoval rate β we can determine the variation of V_{bi} with the radiation dose

$$\Delta V_{bi} = kT \cdot \beta \cdot D$$

On the other hand the pinch-off voltage is given by

$$V_P = \frac{qd^2}{2\varepsilon} N_D$$

where d is the thickness of the donor layer. Assuming again a constant carrier removal rate we can calculate the variation of the pinch-off voltage as a function of the radiation dose and obtain

$$\Delta V_P = V_P \cdot \beta \cdot D$$

Finally the change in the gate bias for totam depletion of the donor layer will be given by

$$\Delta V_{GS} = (V_P - kT) \cdot \beta \cdot D$$

The last equation in connection with the characteristics presented in Fig.12 lead to the conclusion that for He ion radiation the degradation factor of highly doped AlGaAs is ve-

ry small and it seems that it does not constitutes an important source for a HEMT degradation.

In the saturation region the source series resistance plays a significant role so any interpretation based on the transconductance characteristics have to be treated with care. In this region the charge control model based on a two-piece linear approximation for the electron velocity versus electric field curve, leads to the following expression for the maximum intrinsic transconductance of a HEMT [21]:

$$Gmi_{max} = \frac{q\mu N_{so}}{\{1+[q\mu N_{so} d_t / \varepsilon v_s L_g]^2\}^{1/2}}$$

where N_{so} is the equilibrium interface carrier concentration [22]. For devices with structures like those of Table 1 if we assume a mobility of $\mu=4000 cm^2/Vsec$, an $N_{so}=10^{12} cm^{-2}$, a saturation velocity $v_s=2x10^7 cm/sec$ and a gate length $L_g=2\mu m$, we obtain

$$v_s = \frac{Gmi_{max} d_t}{\varepsilon L_g}$$

Further the saturation velocity can be calculated taking into account the source series resistance. So

$$v_s = \frac{Gme_{max} d_t}{\varepsilon L_g} \quad \frac{1}{1 - RsGme_{max}}$$

The source series resistance, as will be shown later, constitutes an important source of degradation in HEMTs because its

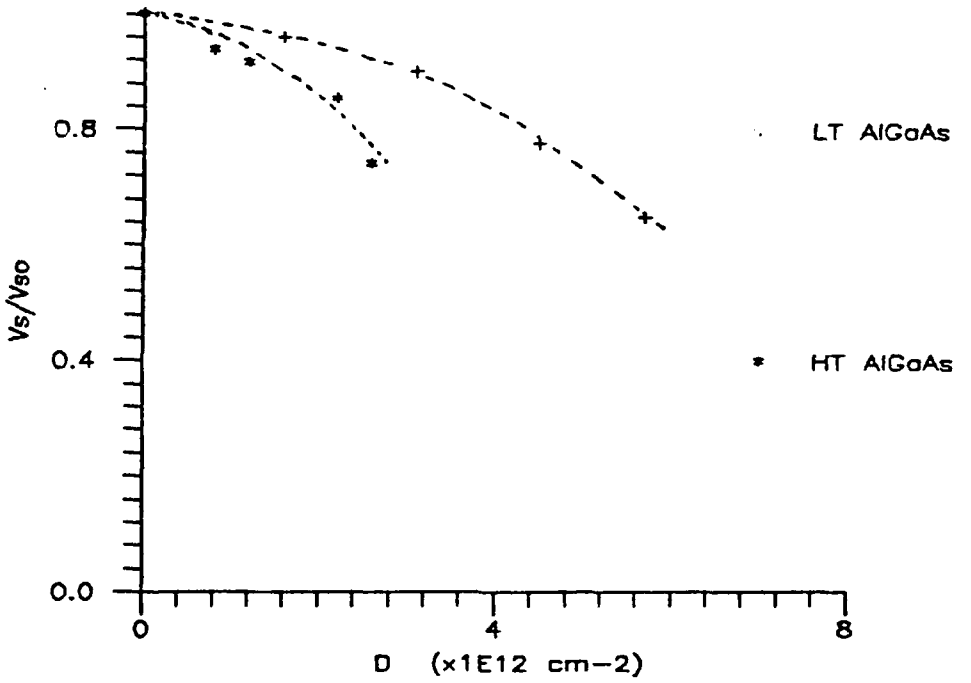

Fig.14 Dependence of the ratio of saturation velocity to its pre-irradiation value on the radiation dose.

value increases significantly with radiation. In order to minimise the error that is induced by neglecting Rs we calculated the saturation velocity at low Gme values, that is at gate bias levels well beyond the transconductance peak. This method permitted the estimation of variation of saturation velocity with radiation dose. A better investigation is achieved if the series resitance is used in the calculations. By choosing properly the gate bias the estimated error can be decreased to less than 10%. For such gate bias levels the saturation velocities of 1μm gate length devices was found to be about $8x10^6$ cm/sec for structure A, $7x10^6$ cm/sec for B and about $3x10^6$ cm/sec for C. The ratio of the velocity after irradiation to its pre-irradiation one is plotted in Fig.14.

The decrease of the saturation velocity with radiation may attributed to an increase of the hetero-junction interface roughness due to atom displacement by the He ions. Such a hypothesis is supposed by the fact that the degradation rate of the saturation velocity in structure C is lower than that of strucutre A. As already mentioned the AlGaAs layer, in C, was grown at a relatively low temperature 510°C and it is well known that such growth conditions give rise to very rough interfaces. So for these strucures large radiation doses are needed to increase furthere the already existing interface roughness. In normal structures, such as A,the interface roughness has to be very low. So upon radiation these interfaces degrade faster and at lower doses. Finally the increase of the interface roughness has been monitored in electrical measurements as will be discussed later.

I-T Characteristics

In HEMTs the drain current increases when the temperature decreases. This behavior originates from the spatial separation of the conduction and the donor layer. In such a structure the dominant scattering mechanism is on phonons which leads to an increase of mobility when the temperature decreases. The introduction of lattice defects in the buffer and spacer layers, with irradiation, increases the concentration of charged centers which are both bulk and interface ones. This furthere increases the scattering on ionized impurities and decreases the 2DEG mobility at low temperatures. At room

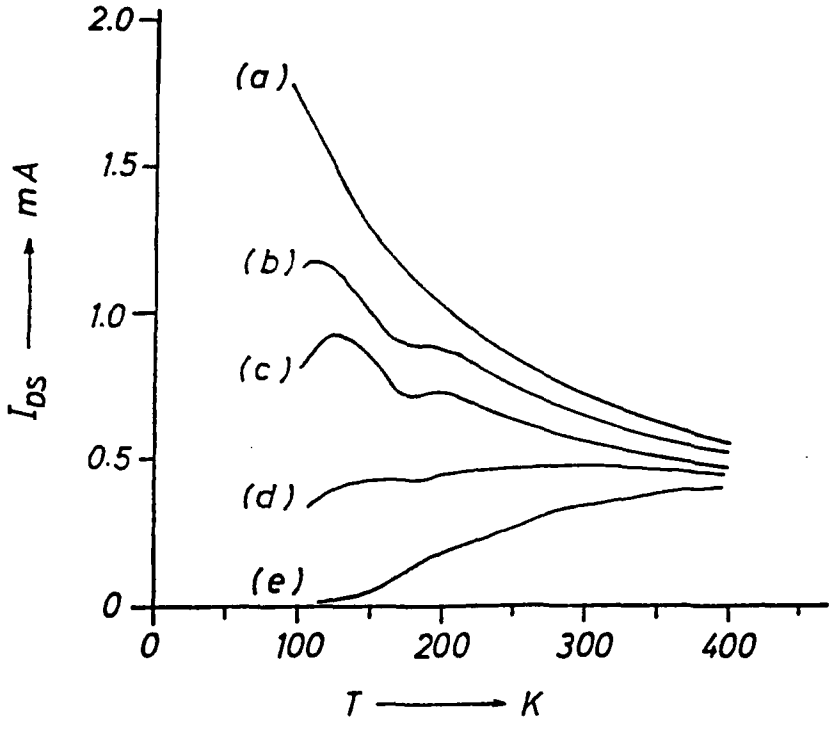

Fig.15 Temperature dependence of drain current (a) before irradiation and for radiation doses of (b) $10^{12}cm^{-2}$, (c) $3x10^{12}cm^{-2}$, (d) $4.5x10^{12}cm^{-2}$, (e) $5.7x10^{12}cm^{-2}$

temperature the leading scattering mechanism is on phonons so the effect of radiation is less prominent. This and the carrier removal, due to the introduction of electron traps in both the donor and the buffer layers, decrease the device current at low temperatures. Concequently at low radiation doses these effects will be less prominent and the device current will collapse at low temperatures mainly due to the presence of the DX center. At large radiation doses the lattice defects will be the leading ones and the device drain current will vanish gradually with the temperature decrea-

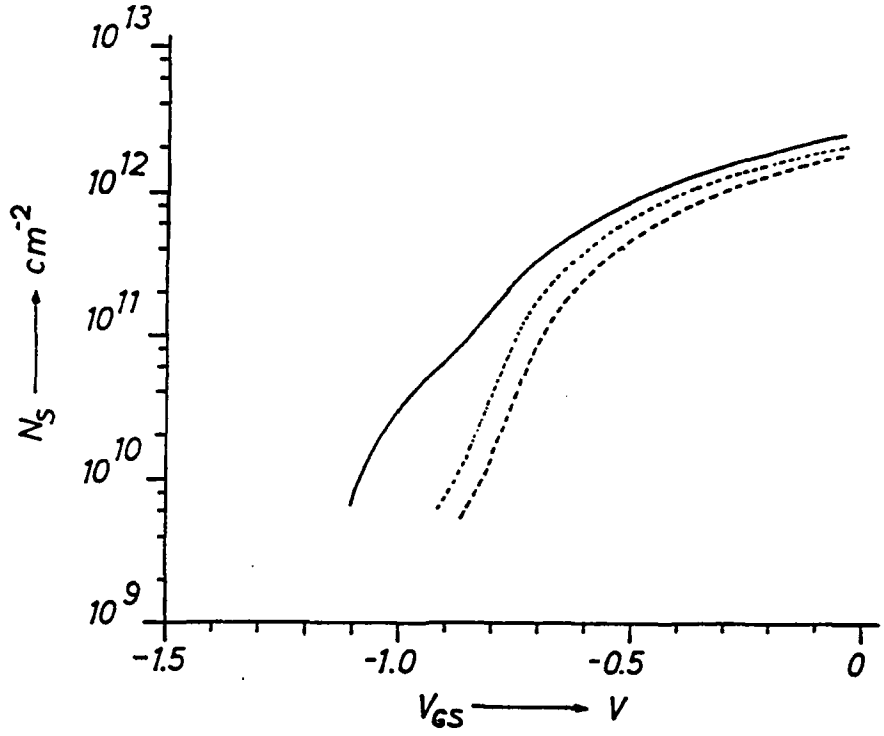

Fig.16 Sheet carrier concentration, including that of the AlGaAs donor layer, vs gate bias (—) before irradiation, (···) after a dose of $2x10^{12}cm^{-2}$ and (- - -) after a dose of $4.5x10^{12}cm^{-2}$

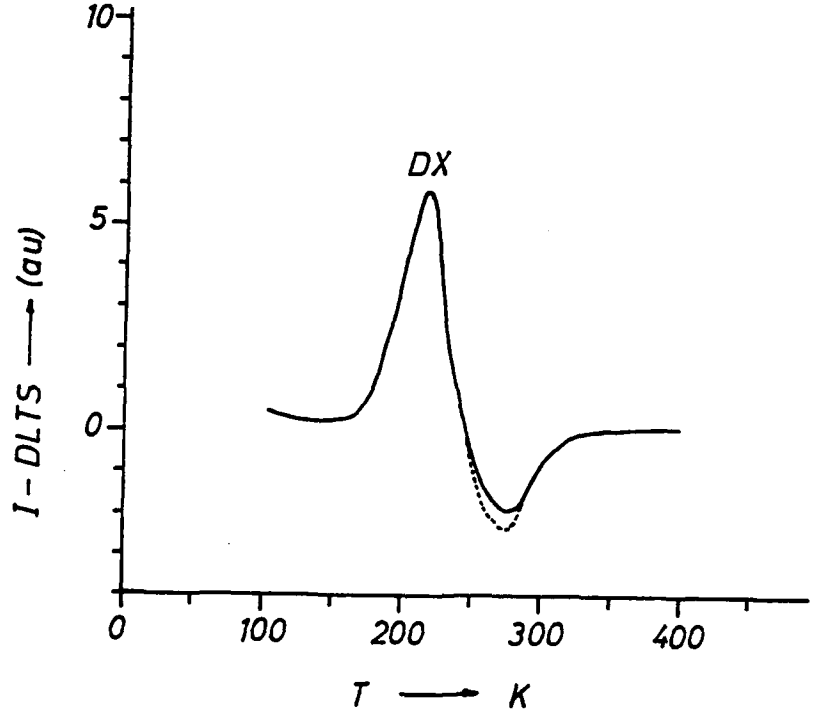

Fig.17 Typical drain current DLTS before irradiation (continuous line) and after a dose of $3x10^{12}cm^{-2}$ (dashed line)

sing. The temperature dependence of the drain current for various radiation doses, with the device biassed in the linear region, is shown in Fig.15. The experimental results were found to be very in good agreement with the predicted behavior. So for doses up to about $3x10^{12}cm^{-2}$ the drain current still increases at low temperatures indicating a low scattering rate on ionized centers. Above this dose the scattering on ionized centers seems becomes the dominant mechanism. This in conection with the carrier trapping effect decreases smoothly the drain current at low temperatures.

Ns-V Characteristics

The concentration of the 2DEG was calculated from C-V measurements of FATFET gate capacitance. Experimental results are presented in Fig.16. In the lower part of each Ns-V these characteristic the concentration is determined by the 2DEG while in the upper part there is some contribution from the donors of the AlGaAs layer. The 2DEG concentration degrades with increasing the radiation dose. This behavior was expected and has been already have been shown in heterojunctions. Exploatation of these results will be done later where a charge control model will be employed. From the Ns-V characteristics the 2DEG degradation parameter was found to be about $7.5x10^{-14}cm^2$ being in good agreement with the previous one

DLTS measurements have been also performed in HEMTs. As already mentioned no other trap with a concentration comparable to that of the DX center was detected. In some cases a

minority-like carrier trap, associated with the DX center, was detected in some HEMTs after irradiation. In other devices this trap was present before irradiation and its concentration was increased after radiation. This trap, in literature, is attributed to interface states at the heterojunction and always emerges or its concentration increases after thermal or current stressing [19].

Mobility degradation

In order to obtain a better insight on the HEMT degradation, the efficiency of the screening effect on carrier scattering was investigated. So the dependence of the device drift mobility on the sheet carrier concentration was determined for various radiation doses. The mobility was determined by applying both methods the geometrical magnetoresistance method [10,11] and the I_{DS}-V_{GS} characteristics in the linear region [12]. Due to excess noise in the magnetoresistance measurements, espetially at low current levels we adopted the second method. For the application of this method the determination of the sum of the HEMT series resistances $R_{SD}=R_S+R_D$ was needed. In general the source-drain resistance R_T of any field effect transistor is the sum of the intrinsic channel resistance R_C and the series ones R_{SD}. Furthere the channel intrinsic resistance can be expressed in terms of sheet carrier concentration and average mobility. The latter in the case of HEMTs includes some contribution from the AlGaAs donor layer when parasitic conduction occurs. The total resistance can be written in a simple way as:

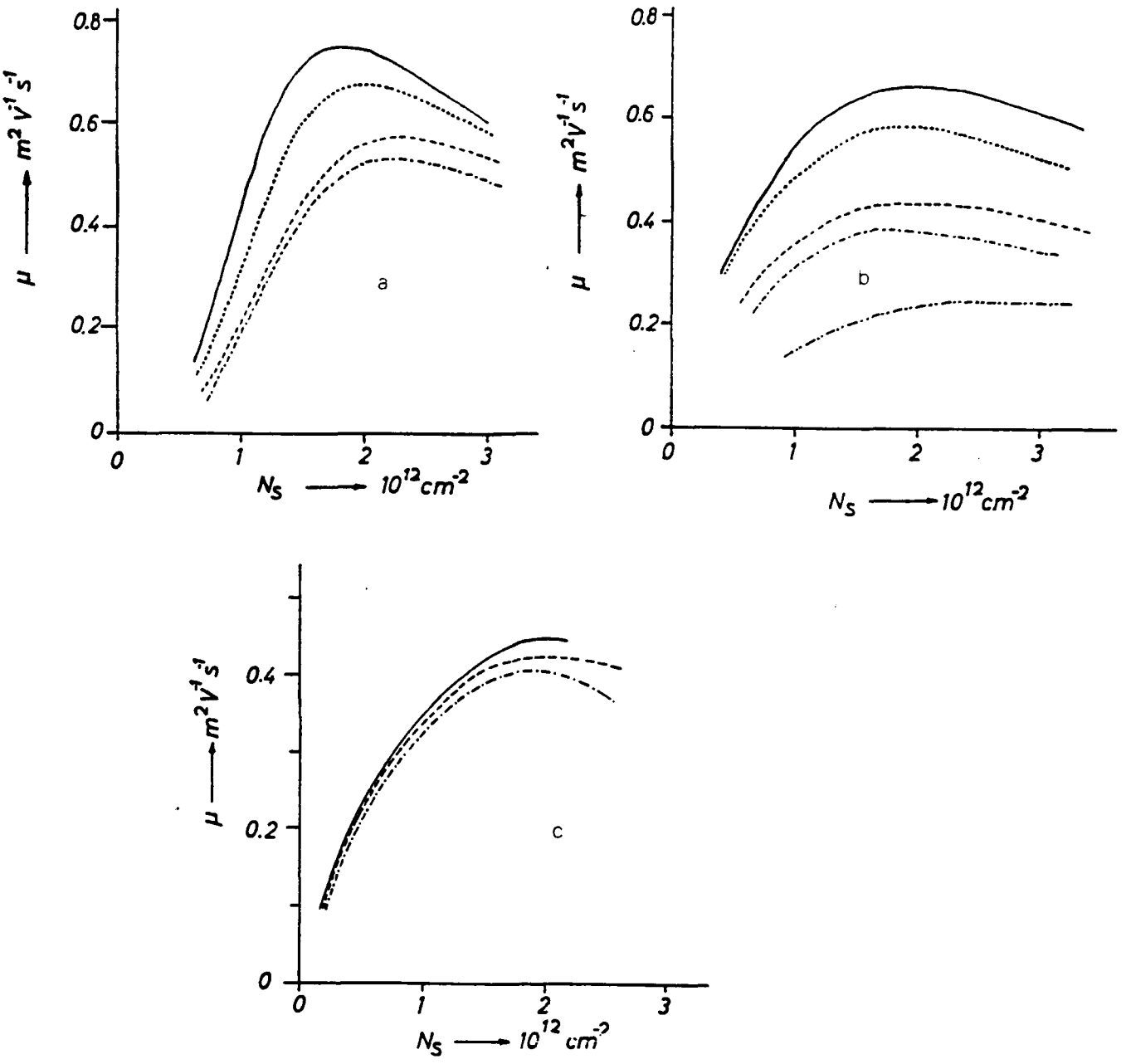

Fig.18 Dependence of mobility on sheet carrier concentration of:
(a) structure A (——) before irradiation, (···) after a dose of $10^{12}cm^{-2}$, (- - -) after a dose of $2x10^{12}cm^{-2}$ and (-·-·-) after a dose of $3x10^{12}cm^{-2}$
(b) structure B (——) before irradiation, (···) after a dose of $10^{12}cm^{-2}$, (- - -) after a dose of $3x10^{12}cm^{-2}$, (-·-·-) after a dose of $4.5x10^{12}cm^{-2}$ and (-··-··-) after a dose of $5.7x10^{12}cm^{-2}$.
(c) structure C (——) before irradiation, (- - -) after a dose of $1.5x10^{12}cm^{-2}$ and (-·-·-) after a dose of $3x10^{12}cm^{-2}$.
In all cases the mobility drop above $n_s=2x10^{12}cm^{-2}$ is due to parallel conduction in the AlGaAs donor layer

$$R_T(N_s) = R_{SD} + R_c$$

and the average mobility can be calculated from

$$\mu(Ns) = \frac{L_g}{q \cdot Ns \cdot W} \quad \frac{1}{R_T(Ns) - R_{SD}}$$

The total series resistance R_{SD} was found to depend strongly on the device geometry and manifacturer. The channel carrier concentration Ns was determined from the C_{GS}-V_{GS} characteristics.

All structure μ-Ns characteristics, obtained for several radiation doses are persented in Fig.18. A common feature of the μ-Ns characteristics is that the mobility increases with increasing Ns and this is due to the effect of gradual increase of screening. The mobility then attains a maximum which corresponds to a carrier concentration of about $2x10^{12}cm^{-2}$ beyond which it starts to decrease due to parallel conduction in AlGaAs.

Radiation decreases the mobility due to the introduction of ionized centers in the spacer and buffer layer and the increase of interface roughness. The results from HEMTs with conventional buffer layers (fig.18a) and those with an additional AlGaAs buffer layer (fig.18b) show that the introduction of the additional buffer layer does not improve the device radiation hardnes from the point of view of carrier mobility. In contrast the devices with the low temperature growth AlGaAs donor layers (fig.18c) show an improved radiation hardness although they are of inferion material quality.

That is because of the larger concentration of defects in the spacer layer and at the interface which reduces, before any radiation, the 2DEG mobility. Low radiation doses do not alter significantly the population of these defects. Therefore much larger doses are needed to increase the concentration of the background defects and hence to reduce the mobility. The dependence of the normalized mobility, to its pre-irradiation value, on the radiation dose is shown in Fig.19. In both structures A and B the corresponding degradation parameter is the same, $\beta_\mu = 1.1 \times 10^{-13} cm^2$, indigating again that the insertion of an additional AlGaAs buffer layer does not improve the total dose radiation hardnes of a HEMT. Finally the degradation parameter of structure C is much lower than that

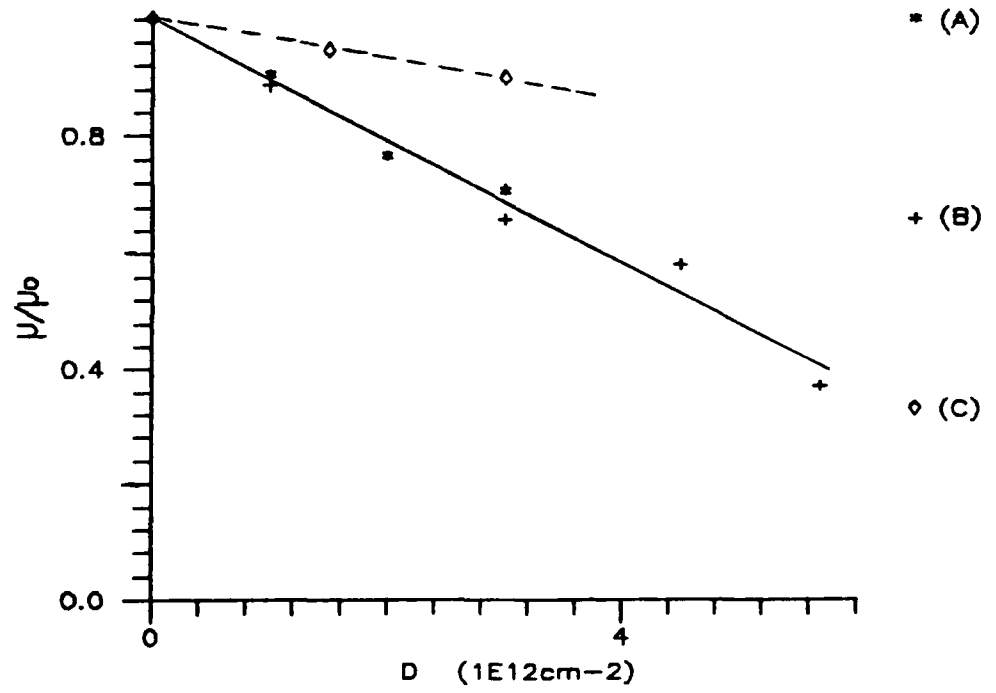

Fig.19 Dependence of the normalized mobility, to its pre-irradiation value, on the radiation dose.

of structures A and B, $\beta_\mu = 3.4 \times 10^{-14} cm^2$, thus supporting all previous results obtained from other parameters. The conclusion to which we are lead is that from the point of view of radiation tolerance a compromise can be done between regarding the material quality.

Series Resistance degradation

Many models have been preoposed to describe the HEMT d.c. characteristics. The majority of these models treat the parasitic series resistances as a constant fitting parameter. This assumption is partially justified for low drain currents such as in the linear region, where the interelectrode spacing may be considered to exhibit an ohmic behavior, hence to be approximated by simple transmission line model [23,24]. In general the parasitic series resistances are non ohmic. They are modulated by both the surface potential and the potential difference between the gate and the source or drain electrods [25,26]. In our case we assumed that the series resistances were ohmic and the study was limited on the data of the linear region. On the other hand due to large dispersion in the Rs values among various devices and structures (Rs=5-15ohm) we studied the variation of their normalized magnitude with the radiation dose. For the determination of Rs we assumed that all devices were symmetrical, that is $R_S = R_D = R_{SD}/2$, and we applied the method proposed by M.S. Shur in Ref.22. The variation of the normalized source resistance of each structure used in this project is presented in Fig.20. From there

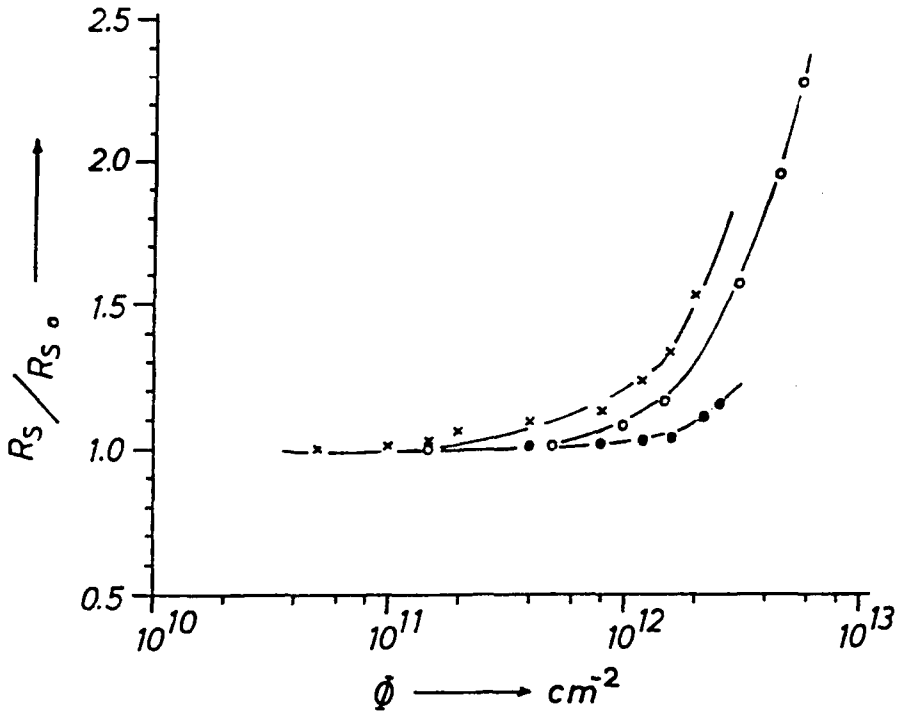

Fig.20 Variation of the normalized Rs /Rs o, to their values before radiation, parasitic resistances vs radiation dose for: (x) structure A, (o) structure B and (o) structure C.

it becomes obvious that structure C exhibits a higher radiation hardness relatively to the other structures. The series resistance degradatiopn can be attributed mainly to the decrease of the 2DEG carrier concentration since the degradation of the mobility is much lower to justify that. Another reason for the fast dagradation is the specific structure of the series resistances which contain a GaAs/AlGaAs heterojunction which tunneling resistance can be affected by the damage introduced by He ion radiation.

Charge Control Model

When an AlGaAs layer is grown on top of an undoped GaAs layer a two-dimensinal electron gas is formed at the interface owing to the difference in the electron affinity of the two layers (fig.21). The distribution of electrons in the subbands can be obtained analytically assuming an infinite barrier height on the AlGaAs side and a linear potential energy on the vicinity of the heterointerface.

$$V = qF_s x$$

where F_s is the surfacez electric field (triangular potential well approximation). This approach yields a satisfactory solution for the surface carrier density as a function of the Fermi level. In this model the relation between the subbands energy and the electric field is given by

$$E_i = \left(\frac{h^2}{2m}\right)^{1/3}\left[\frac{3}{2} qF_s\left(i+\frac{3}{4}\right)\right]^{2/3}$$

The surface field is related to the surface carrier density N_s by Gauss's law

$$\varepsilon F_s = q(N_s + N_A)$$

where N_A is the net acceptor density per unit area in the GaAs buffer layer, which typically is of the order of 10^{13}-$10^{15}\,cm^{-3}$. Substituting the latter into the previous equation we obtain the energies of the first two subbands

$$E_o = a_o (N_s + N_A)^{2/3}$$

$$E_1 = a_1 (N_s + N_A)^{2/3}$$

The values of the parameters a_o and a_1 are [22]

$$a_o = 2.5\times10^{-12}\ eV\ m^{4/3}$$

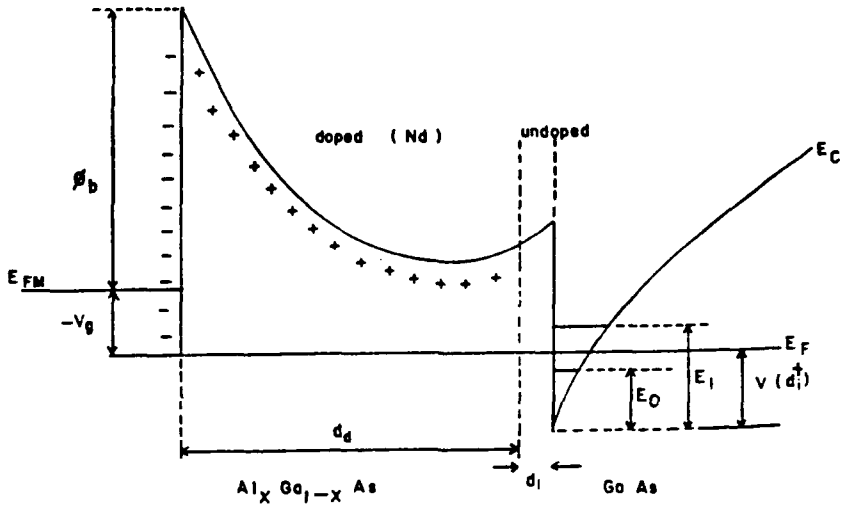

Fig.21 Band diagram of a modulation doped layer.

$$a_1 = 3.2\times10^{-12}\ eV\ m^{4/3}$$

A satisfactory approximation is achieved, in most practical cases, if only two subbands are considered. Then the carrier concentration is given by

$$N_s = D\frac{kT}{q}\ln\{[1+\exp(\frac{E_F-E_0}{kT})][1+\exp(\frac{E_F-E_1}{kT})]\}$$

where D is the density of states of the 2DEG which is determined from cyclotron effective mass measurements [27]

$$D=3.24\times10^{17}\ m^{-2}\ V^{-1}.$$

In the presence of the Schottky gate the surface carrier concentration is given by [27]

$$N_s(V_{GS}) = \frac{\epsilon}{qd_t}[V_{GS}-(\Phi_b-V_P+V(d_i)-\Delta E_c)]$$

where $V(d_i)$ is the Fermi potential, that is the distance of the Fermi level from the bottom of the triangular quantum

well and ΔE_c for simplicity is measured in volts. From the above equations we can determine the relationship between the Fermi potential and the concentration of carriers in the 2DEG assuming that E_o and E_1 are measured from the bottom of the conduction band of GaAs at the heterointerface. This leads to a quadratic equation with respect to $\exp[qV(d_i)/kT]$.

The charge control model is further simplified if we assume that only one subband is populated with electrons. This assumption has been also adopted by R.J. Krantz et. al. [2] and by B.K. Janousek et. al. [1] for the study of neutron radiation effects in HEMTs. This assumption, in fact, is not far from reality for a HEMT biased close to the threshold. In this case we arrive, after some algebric calculations, to a non linear relation between the gate voltage and the carrier concentration

$$V_{GS} = \frac{qd_t N_s}{\varepsilon} + (\Phi_b - \Delta E_c - V_P) + \frac{kT}{q} \ln\left[\exp\left(\frac{qN_s}{DkT}\right) - 1\right] + \frac{a_o}{q} (N_s + N_A)^{2/3}$$

This relation offers a satisfactory approximation for carrier concentrations bellow about $5 \times 10^{11} cm^{-2}$ and allows the calculation of three parameters: the thickness of the AlGaAs donor layer, the pinch-off voltage and the net acceptor concentration in the buffer layer. Here it must be pointed out that the interface states introduced by irradiation are accounted in the variation of the donor layer pinch-off voltage, thus

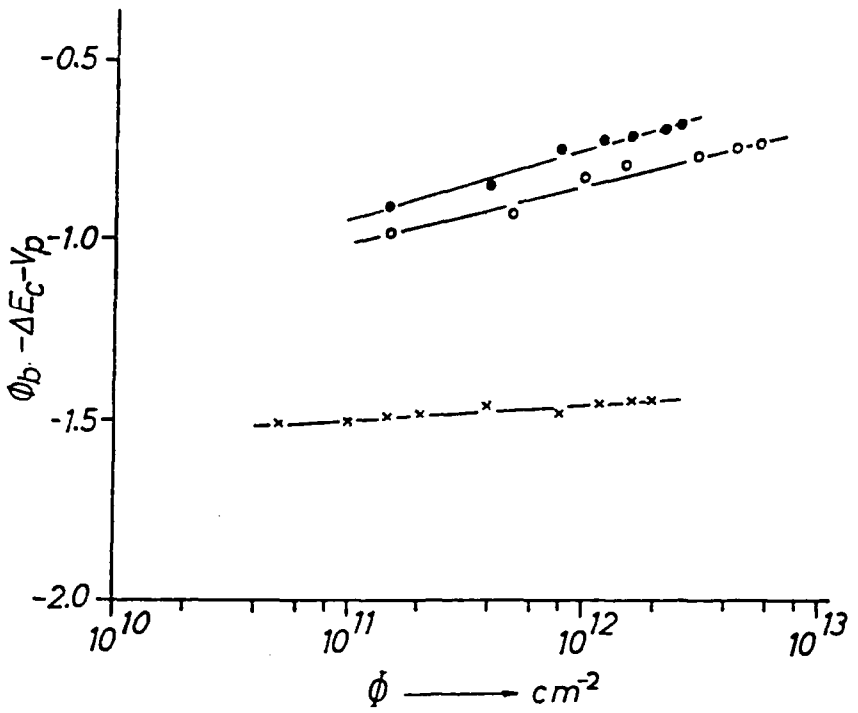

Fig.22 Dependence of the $\Phi_b - \Delta E_c - V_P$, which represents the AlGaAs pinch-off voltage, on the radiation dose of (●) structure A, (o) structure B and (x) structure C.

in the net donor concentration of the AlGaAs layer.

The procedure followed in our case was to define before irradiation the parameters d_t; $(\Phi_b - \Delta E_c - V_P)$ and N_A. Next for all radiation doses the thickness of the AlGaAs layer was kept constant and the other were determined. The experimental data were fitted to the last equation using a least square method. The effect of alpha particle radiation dose on $(\Phi_b - \Delta E_c - V_P)$ and the buffer layer net acceptor concentration are presented in Fig.22 and Fig.23 respectively.

The parameter $(\Phi_b - \Delta E_c - V_P)$ is directly related to the net donor concentration of the AlGaAs donor layer, since all the other parameters are not affected by radiation. In all HEMTs this parameter was found to vary almost logarithmically with the radiation dose. Here it must be noted that the dif-

ness of the AlGaAs donor layer due to different recess depth in each device. The logarithmic dependence of V_P on the dose clearly indicates that the variation of the pinch-off voltage with the radiation dose is not caused only by the carrier removal in the AlGaAs layer. The last would lead to a linear relation of V_P with the radiation dose, since the pinch-off voltage is given by $V_P = qN_D d_t^2/2\varepsilon$. So the almost logarithmic relation, which in fact is a sublinear one, must be attributed to other effects such as the introduction of interface states at the AlGaAs/GaAs heterojunction and deep traps in the AlGaAs spacer. Attempting to determine the carrier removal in the AlGaAs we can first consider the low radiation doses where the variation of V_P can be assumed to be linear. From there the degradation parameter was found to have an average value of about $3\times10^{-14}\,cm^2$ in the conventional HEMTs and on those with an AlGaAs buffer layer and about $10^{-14}\,cm^2$ in those with a LT donor layer. Further taking into account the results from the heterojunctions radiations we may try to estimate the dependence of the degradation parameter on the AlGaAs doping level. For this, only two doping levels were used that is $2\times10^{16}\,cm^{-3}$ and $2\times10^{18}\,cm^{-3}$. The relationship between β_{AlGaAs} and the doping level was found to be

$$\beta_{AlGaAs}(cm^2) = 7.7\times10^{-12}N_D^{-0.13}$$

which in fact is of the same order of magnitude with that of GaAs and shows a similar power law dependence.

The net acceptor concentration in the GaAs buffer layer

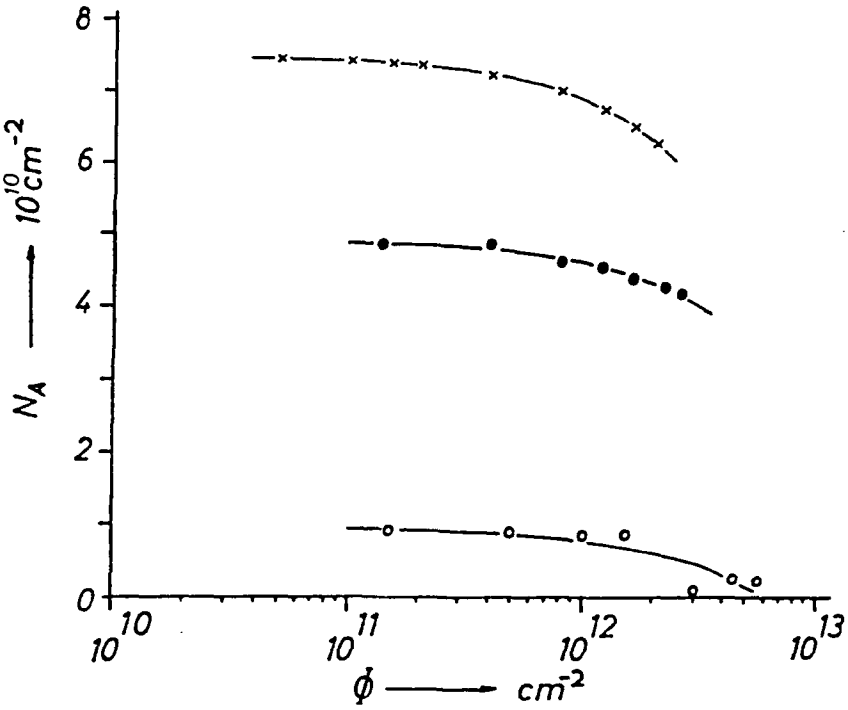

Fig.23 Buffer layer, equivalent, net acceptor concentration N_A per unit area vs radiation dose for: (x) structure A, (o) structure B and (o) structure C.

is presented, as already mentioned, in Fig.23. The acceptor concentration decreases with radiation due to introduction of of deep donors which turn the lightly p-type buffer layer into a more intrinsic one. The introduction rate of deep donors, assuming the following relation:

$$dN_A = \beta_A \cdot dD$$

was found to be about 0.003 for structure A, about 0.004 for B and 0.0008 for structure C.

The reduction of the net acceptor concentration layer results into an increase of the depletion region in the GaAs buffer layer because the Fermi level, at large distances from the radiated area, remains at the same level. So the electric field at the heterointerface decreases and this causes a lowering of the subbands into the quantum well. If we assume

that at threshold the concentration of the 2DEG is equal to the negative of the acceptors over the quantum well width N_A^* [2], the first subband the lowering is approximated by

$$dE_o = \frac{2}{3} E_o \frac{dN_A}{N_A}$$

The subband lowering must lead to an increase of 2DEG if the distance of the Fermi level from the quantum well bottom remains constant with radiation.

This problem is complicated due to the simultaneous introduction of defects in both the donor and buffer layer. In a more general way the degradation of the 2DEG can be studied by using the relation

$$V_{GS} = \frac{qd_t N_s}{\varepsilon} + (\Phi_b - \Delta E_c - V_P) + \frac{kT}{q} \ln[\exp(\frac{qN_s}{DkT}) - 1]$$

$$+ \frac{a_o}{q} (N_s + N_A)^{2/3}$$

Under an arbitrary constant gate bias, well above threshold where $N_s >> N_A^*$, the radiation will decrease the 2DEG concentration. The change in N_s will be obtained from

$$0 = \frac{qd_t}{\varepsilon} dN_s - dV_P + \frac{kT}{q} d\{\ln[\exp(qN_s/kTD)]\} + dE_o$$

which after some further calculations leads to

$$[q(\frac{d_t}{\varepsilon} + \frac{1}{D} \frac{\exp(qN_s/kTD)}{\exp(qN_s/kTD) - 1}) + \frac{2}{3N_s} E_o] \, dN_s = dV_P$$

where

$$dV_P = - V_P \beta_{Al_1Ga_{As}} dD$$

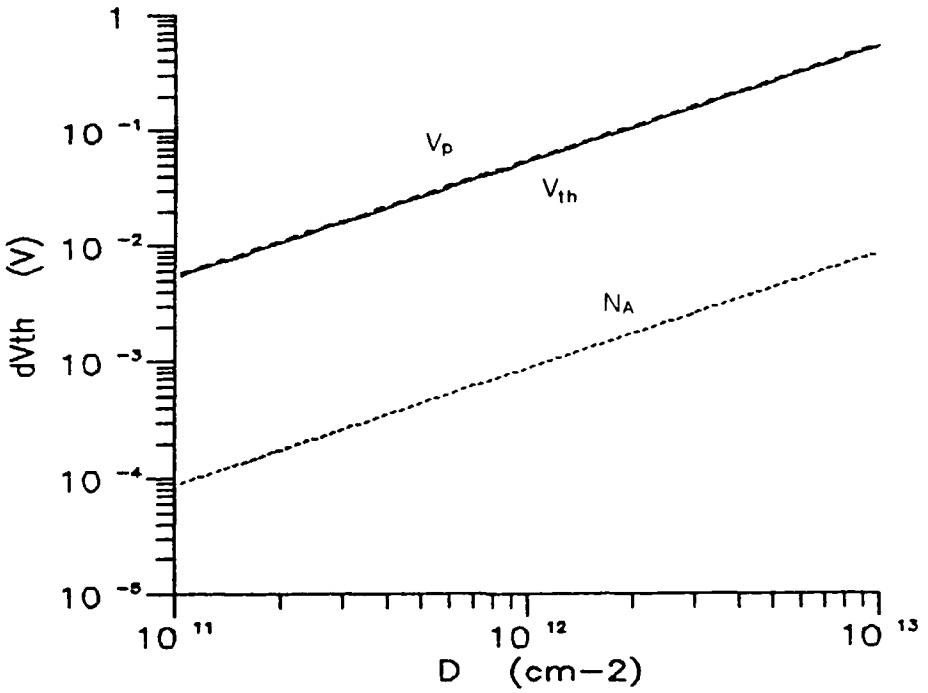

Fig.24 Variation of threshold voltage and the contributions of each parameter versus the He ion dose

which denotes that above threshold the degradation of 2DEG originates from the decrease of the AlGaAs donor layer pinch-off voltage. In order to determine the degradation of V_{th} we may assume that at threshold the channel charge density is equal to the local acceptor charge density N_A [2]. Then the shift of the gate voltage for threshold condition ($V_{Gst}=V_{th}$) is given, after some simplifications, by

$$dV_{Gst} = \{-[\frac{kT}{q} + \frac{2}{3} E_o] \frac{\beta_A}{N_A} + V_P \beta_{AlGaAs}\} dD$$

The term in the brackets is always positive and denotes an increase of threshold voltage with the radiation dose. The variation of the threshold voltage, the pinch-off voltage of

AlGaAs donor layer and the shift of first subband towards the bottom of the quantum well versus the radiation dose are plotted in Fig.24.The parameters used in Fig.24 were d_t=350A, N_D=2x10^{18}cm^{-3}, N_A=3x10^{10}cm^{-2}, β_A=0.0035 and β_{AlGaAs}=3x10^{-14} cm^2. The comparison of the contribution of each parameter clearly shows that the second parameter in the bracket previous equation is the dominant one.

Table 6. MESFET pinch-off voltage and degradation parameters

Structure	V_{po}(V)	β^*(x10^{-14}cm^2)	β_R(10^{-13}cm^2)
MBE GaAs buffer	3.12	29.6	0.74
MBE AlGaAs buffer	2.64	49.8	0.68
Ion Implanted	1.70	35.6	3.46
MBE LT buffer	2.48	10.4	0.38

3.4 Comparison with MESFETs

The effect of He ion radiation on HEMTs was further compared to that on MESFETs. In order to compare the radiation hardness of the 2D and the 3D devices, MESFETs with conventional, AlGaAs and LT GaAs buffer layers were fabricated. In addition ion implanted devices were used.

The comparison of the radiation hardness of the MESFETs and the HEMTs was limited, in our case, on the variation of the threshold voltage and the source series resistance with the radiation dose, sice these parameters affect significantly the device performance.

In the case of MESFETs the pinch-off voltage, V_P, was found to decrease linearly with the radiation dose. The va-

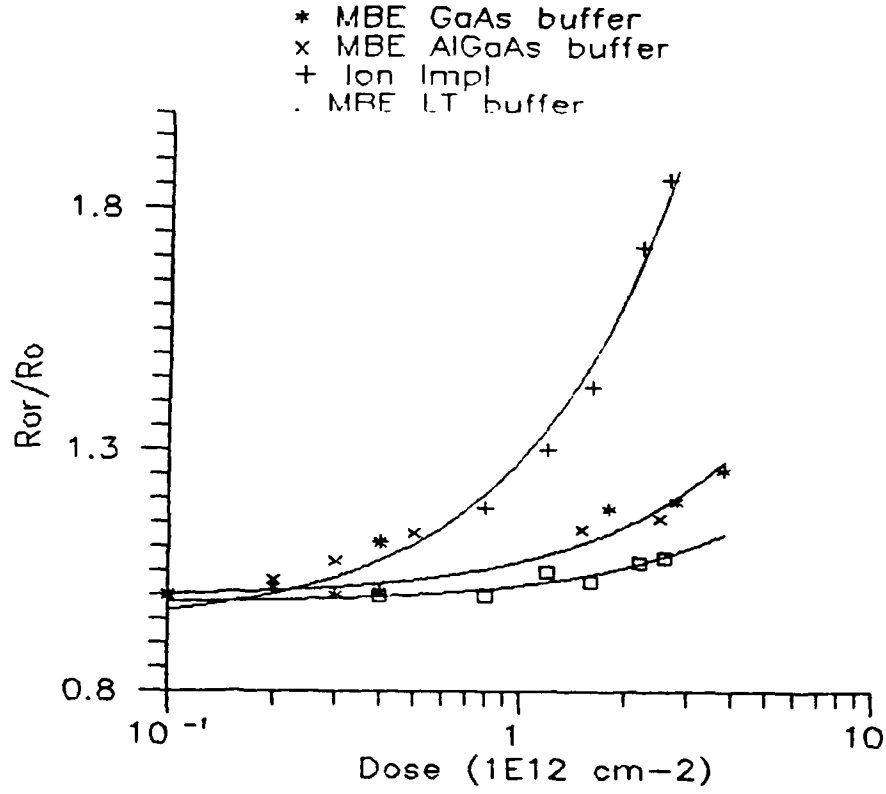

Fig.25 Variation of pinch-off voltage with radiation dose in different structure MESFETs

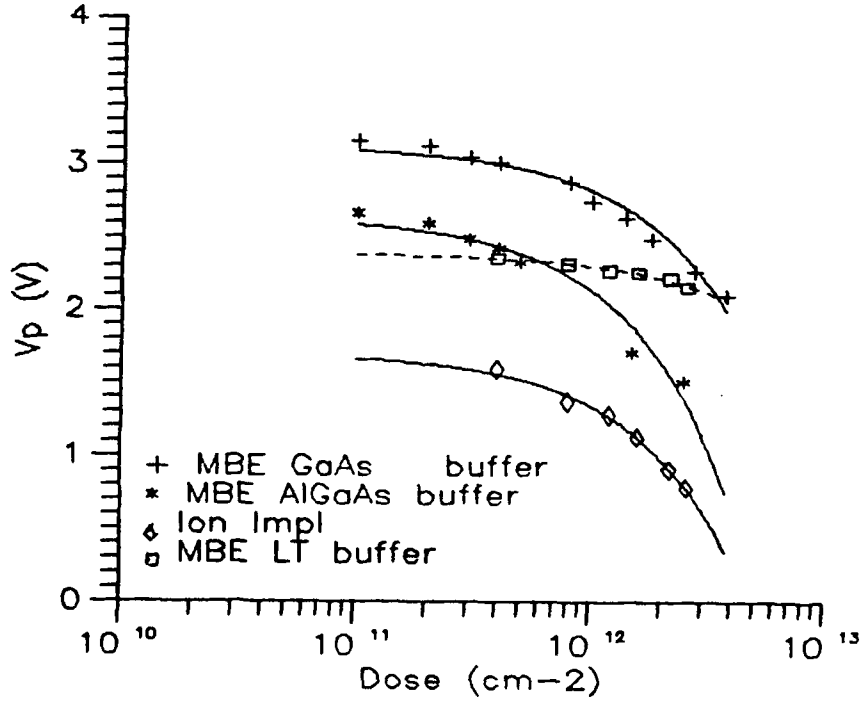

Fig.26 Variation of source series resistance with the radiation dose

riation of V_P with the He ion dose may be approximated by [28]

$$V_P = V_{Po} (1-\beta^* D)$$

The variation of pinch-off voltage with the radiation dose is presented in Fig.25 for different structure MESFETs. For the same structures, both V_{Po} and β^* are presented in Table 6. On the other hand the variation of the normalized source series resistance with the radiation dose is shown in Fig.26, for different MESFET structures. The series resistance increases linearly with the radiation dose the corresponding degradation parameters β_R are presented also in Table 6.

In the case of HEMTs it was shown that the parameter $(\Phi_b - \Delta E_c - V_P)$, which is almost equal to the threshold voltage, varies almost linearly with the radiation dose. It was also shown that the corresponding degradation parameter is about $3x10^{-14} cm^2$ for all structures with high temperature AlGaAs donor layer and $10^{-14} cm^2$ for those with low temperature donor layer. In the case of MESFETs the degradation parameter of the threshold voltage (table 6) is in general one order of magnitude larger than that of HEMTs. Only in the case of the MESFETs with low temperature buffer layers the degradation parameter is comparable to that of the HEMTs. From the point of view of radiation hardness of source series resistance, MESFETs (fig.26), excluding the ion implanted ones, show a slightly better performance over HEMTs (fig.20). This difference is attributed to the complex structure of the series resistance of HEMTs which includes two heterojunctions,

one between the contact and donor layer and the other between the donor and the buffer layer.

Comparing these results we can conclude that the radiation hardness of HEMTs is higher than that of MESFETs excluding the MESFETs which are fabricated on low temperature buffer layers. These devices exhibit a performance comparable to that of HEMTs.

3.5 Conclusions

In conclusion the He ion radiation degradation of HEMTs is a composit effect. Radiation affects all layers of HEMT structure and the degradation of each layer contributes to the overall performance degradation. The main effects of radiation are summarised bellow

* Radiation introduces interface states or increases the density of the already existing ones, which are introduced by MBE growth [29,30]. In addition the displaced atoms increase the heterointerface roughness. These effects are detected by
  - DLTS assessment method and
  - sublinear increase of $\Phi_b - \Delta E_c - V_P$ parameter.

  The introduction of interface states due to limited analysis is unavoidably incorporated in the degradation of the donor layer effective doping
* Radiation shifts decreases the 2DEG density due to decrease of donor layer effective doping and
* shifts the device threshold voltage due to

- decrease of effective acceptor density in the buffer layer and
- decrease of donor layer effective doping

* Radiation degrades both the 2DEG mobility and saturation velocity due to
  - increase of charged defects in the buffer and spacer layers and
  - increase of heterointerface roughness
* The device performance is significantly degraded by the increase of the series parasitic resistances.This effect is attributed to the complex nature of the series resistance and becomes important at He ion radiation doses above $2x10^{12}cm^{-2}$.
* The introduction of an AlGaAs buffer layer does not improve significantly the device radiation hardness
* The use of a low temperature grown (LT) AlGaAs donor layer improves significantly the device radiation hardness, although the pre-irradiation performance is inferior to that of conventional HEMTs.
* Finally a comparison of radiation hardness shows that HEMTs are more resistant than MESFETs. Comparable performance to that of HEMTs show the MESFETs which are fabricated on low temperature buffer layers.

4 NEUTRON RADIATION

4.1 Radiation Effects in GaAs Layers

The effect of neutron radiation in GaAs epitaxial and ion implanted layers has been studied extensively during the last two decades [31-37]. The carrier removal rate and its dependence on the background doping was determined by Bethe and Zuleeg [31]. The relation connecting the damage factor and the concentration of background doping N_D is

$$\beta(cm^2) = 7.2 \times 10^{-4} N_D^{-0.77}$$

A different relation was proposed recently in [38] for ion implanted GaAs layers. In the present work we shall use the one of Bethe and Zuleeg.

Another issue is the electron traps that are introduced by neutron radiation. Since the literature on this area is limited [39,40] we have investigated the traps that are introduced in GaAs and attempted to discriminate them from those which are introduced in AlGaAs.

The samples used in this investigation were MESFETs fabricated on MBE grown layers with channel carrier concentrations ranging from $10^{17} cm^{-3}$ to $10^{18} cm^{-3}$. This doping level range was chosen because at lower ones the samples become semi-insulating at relatively low radiation doses [40]. Defect characterisation was performed by means of drain current DLTS measurements in MESFETs with gate lengths of 8μm to 20μm and widths of 250μm.

The trap concentration before irradiation, in all sam-

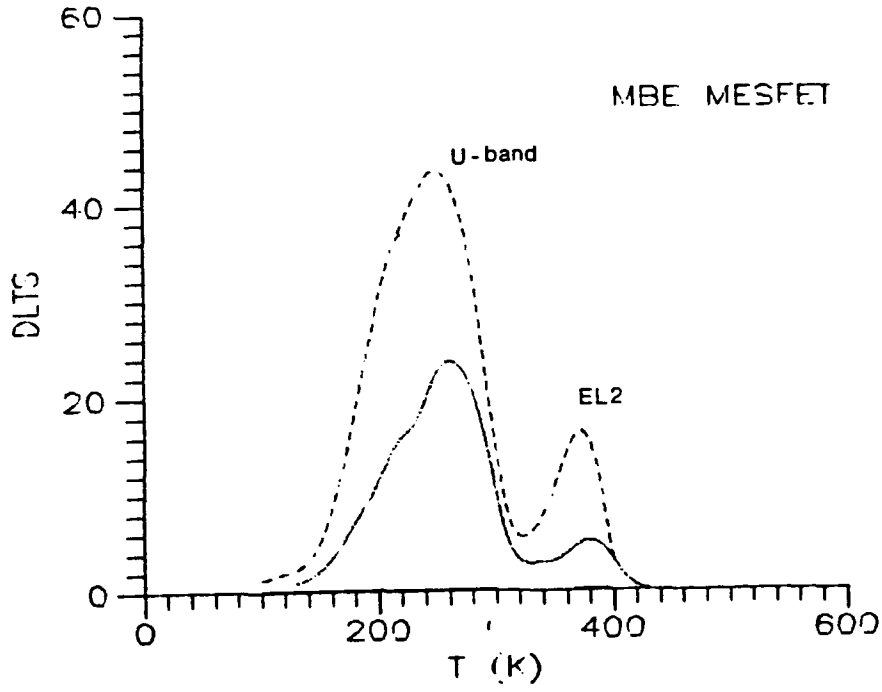

Fig.27 DLTS spectra of neutron irradiatd MESFETs. The continuous line is the spectrum before irradiation, the doted line after a dose of $3x10^{15}$ n/cm^2 and the dashed line after a dose of 10^{16} n/cm^2

ples, was within the detection limits of the DLTS system. The DLTS spectra (fig. 27) became clear at radiation doses above 10^{15}cm^{-2} and showed the presence of a feature centered around 240K and a normal peak at 375K, for a rate window of 63s^{-1}. These two traps are the U-band at low temperatures, which consists of many electron traps and exhibits several shoulders, and the EL2 at high temperatures [39,40].

4.2 Radiation Effects in AlGaAs Layers

In the case of AlGaAs layers the effect of neutron radiation was determined from HEMTs. Devices with same geometry like that of MESFETs were employed. The carrier removal rate

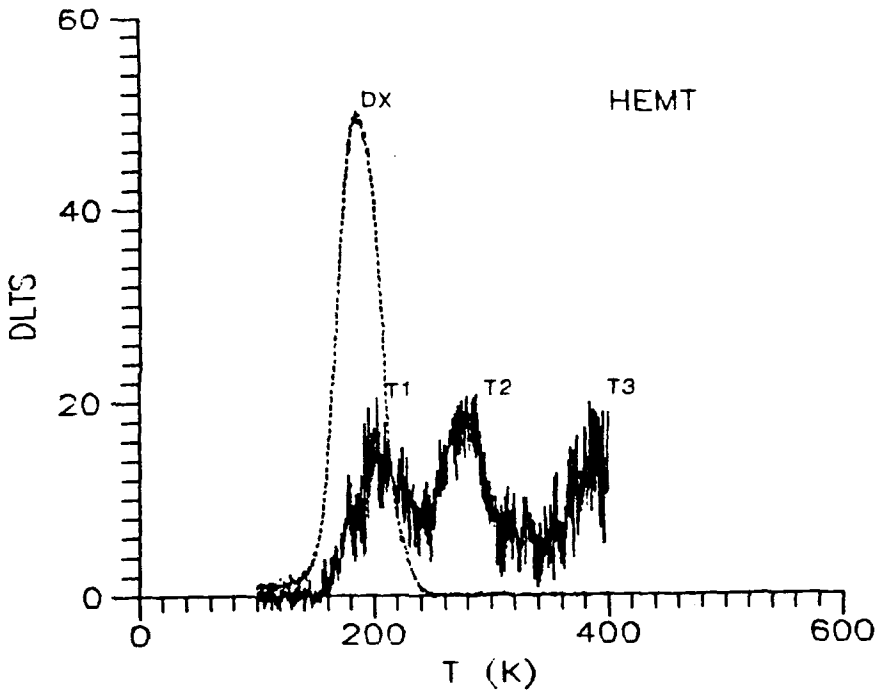

Fig.28 DLTS spectra of a HEMT. Doted line is before irradiation and continuous line after a dose of 10^{16} n/cm^2

was determined from the variation of the AlGaAs donor layer pinch-off voltage V_P and will be discussed later in the appropriate paragraph.

The neutron induced traps were studied by the drain current DLTS of long gate HEMTs and typical spectra are presented in Fig.28. A common feature of all spectra was the dominance of the DX centre at doses up to 10^{15} n/cm^2. Above this radiation level two new traps (T2 and T3) emerged gradually and the DX centre amplitude decreased due to the rapid decrease of the device transconductance. In order to determine the origin of the new traps the spectra were compared to those of MESFETs. The comparison showed no similarity which indicated that T2 and T3 are induced in the AlGaAs donor layer.

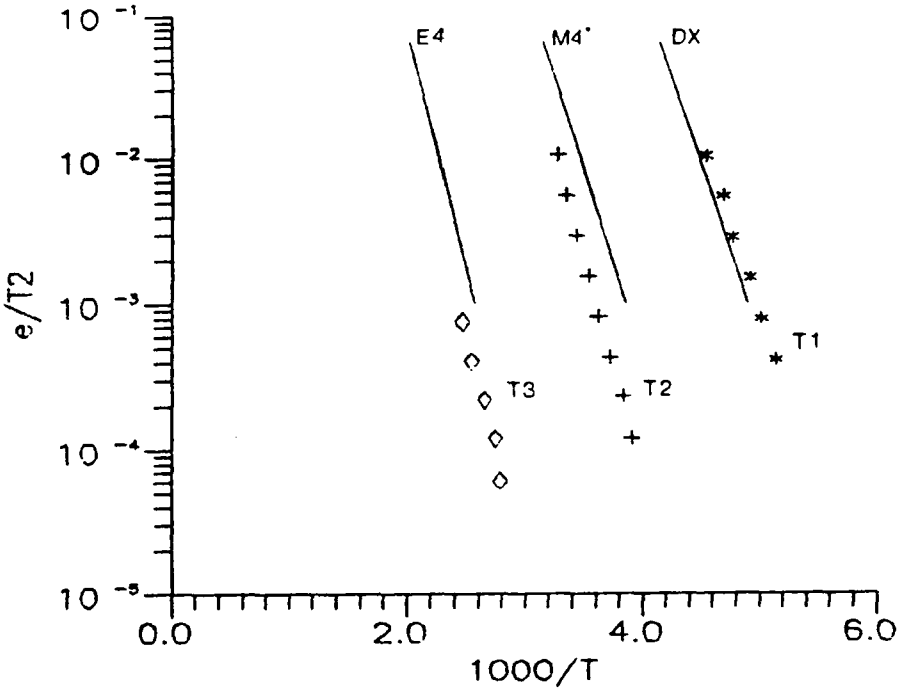

Fig.29 Arrhenious plots of traps T1-T3 and their nearest candidates

This is also supported by the fact that the electron traps in the buffer layer show their presence in the drain current DLTS spectra as minority carrier traps since only their capture process is monitored during the signal relaxation. The Arrhenious plots of the DLTS peaks and their nearest candidate are presented in Fig.29. A comparison of the signatures of T2 and T3 with those of E4 and M4*, which are detected in AlGaAs suggests that T3 may be related to E4 while there in no relation between the T2 and M4*. It was not possible to draw any information about the introduction rate of T2 and T3 because the drain current transient is directly related to the device transconductance [41] which degrades rapidly above 10^{15} n/cm^2.

4.3 Radiation Effects in HEMTs

Neutron radiation gives rise displacenment defects. In GaAs these defects are complex and are attributed to the As_{Ga} antisite [42] and its interaction with other lattice defects. In AlGaAs the displacement defects can reach concentrations as largre as that of the DX centre (fig.28) as revealed by DLTS assessment. The simultaneous introduction of defects in the donor and the buffer layers of a HEMT decreases the 2DEG concentration and mobility so the device performance degrades rapidly. In order to investigate the neutron irradiation effects in HEMTs and finally to compare the neutron and ion radiation effects we shall follow the same procedure a in the case of He ion radiation. The structures employed in the study of neutron radiation were the structure A and B. No structure C was available.

I-V Characteristics

The effect of neutron irradiation on the I_{DS}-V_{DS} characteristic, of 1μm gate length devices, is shown in Figs.30a and 30b for structure A and B respectively. The evolution of the I-V characteristcs with the radiation dose indicates that the device performance is not significantly affected for radiation doses bellow 10^{14} n/cm^2. Beyond this level the devices degradation rate becomes significant and the drain saturation current (fig.31) drops to almost 50% of its pre-irrradiation value at a total dose of about $3x10^{15}$ n/cm^2 in all structures, independently whether they contain or not an AlGaAs buffer

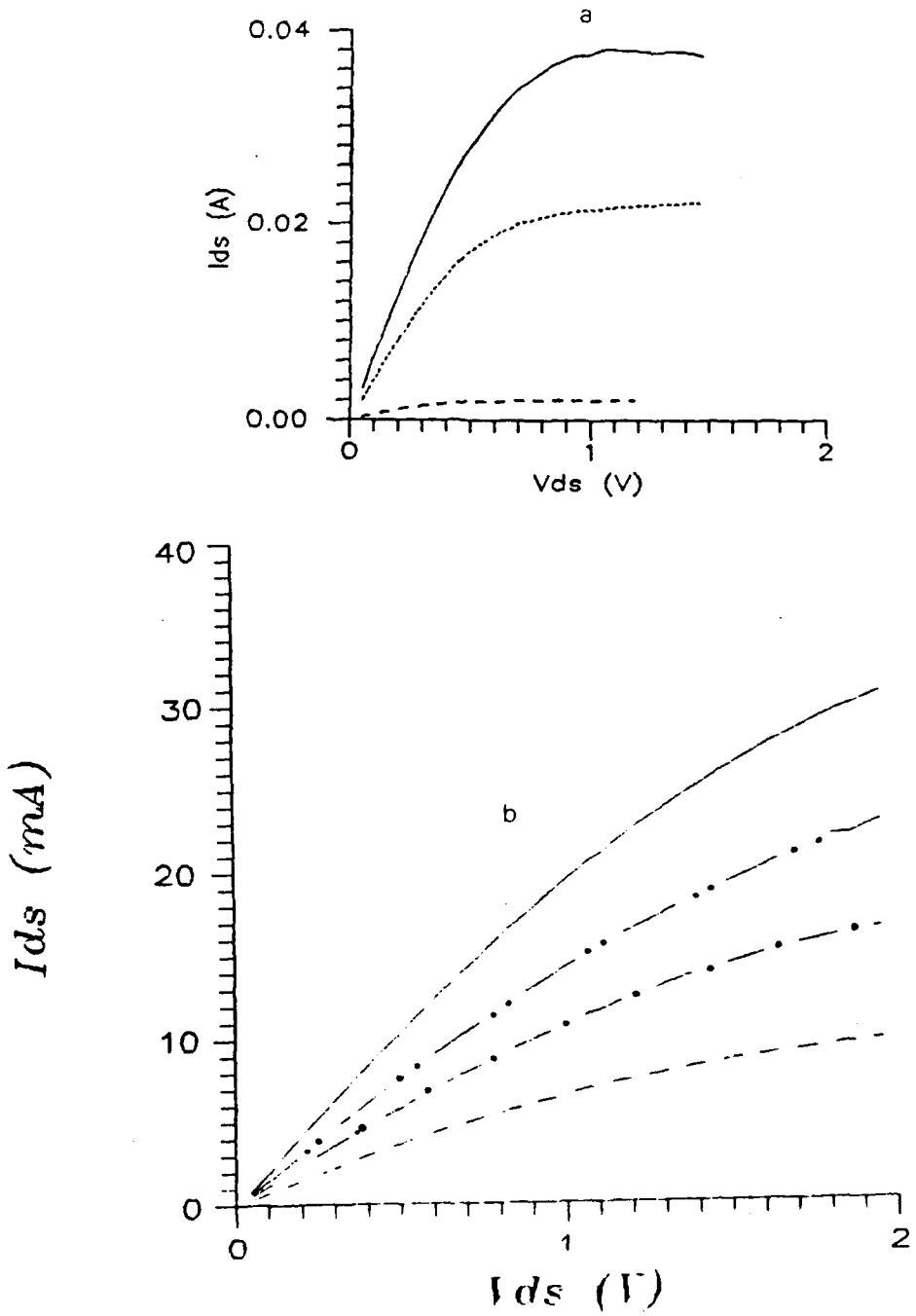

Fig.30 Dependence of I_{DS}-V_{DS} (V_{GS}=0V) characteristics on the radiation dose
a. Conventional HEMT (——) before irradiation, (· · ·) after a dose of 10^{15} n/cm^2 and (- -) after a dose of 1.7×10^{16} n/cm^2
b. HEMT whith AlGaAs buffer layer (——) before irradiation, (-· · -) after a dose of 6×10^{14} n/cm^2, (-· -) after a dose of 3×10^{15} n/cm^2 and (- -) after a dose of 6×10^{15} n/cm^2

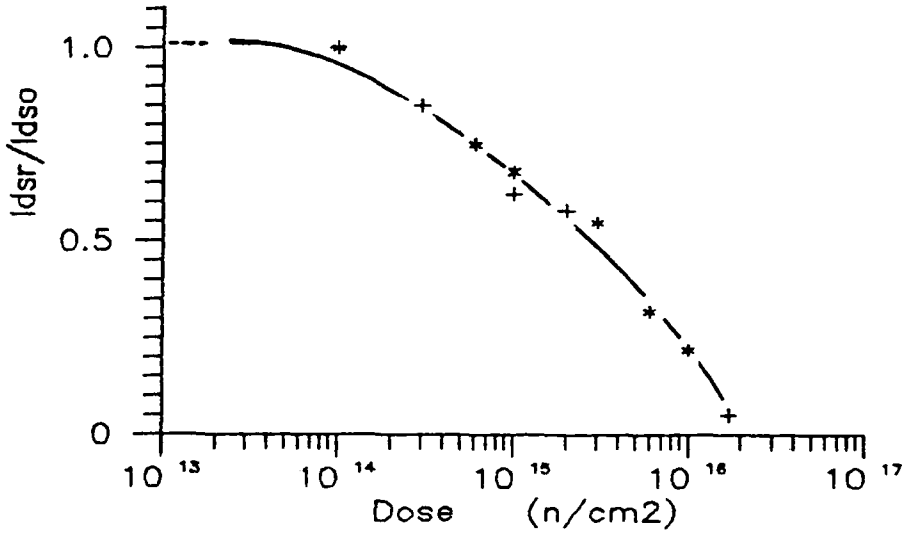

Fig.31 Dependence of the drain saturation current on the radiation dose of (*) conventional and (+) AlGaAs buffer layer HEMTs.

layer. A comparison of the degradation rates of these structures leads to the conclusion that the presence of an AlGaAs buffer layer seems to play a minor role on the device radiation hardness.

As already mentioned in the study of He ion radiation, the degradation of the I_{DS}-V_{DS} characteristics may result from:

a) the decrease of the 2DEG carrier concentration

b) the decrease of the mobility or saturation velocity, when the device operates in the linear or saturation region

c) the increrase of the threshold voltage

d) the increase of the source series resistance.

The effect of radiation on the I_{DS}-V_{GS} characteristics become more evident by studying the transconductance ones

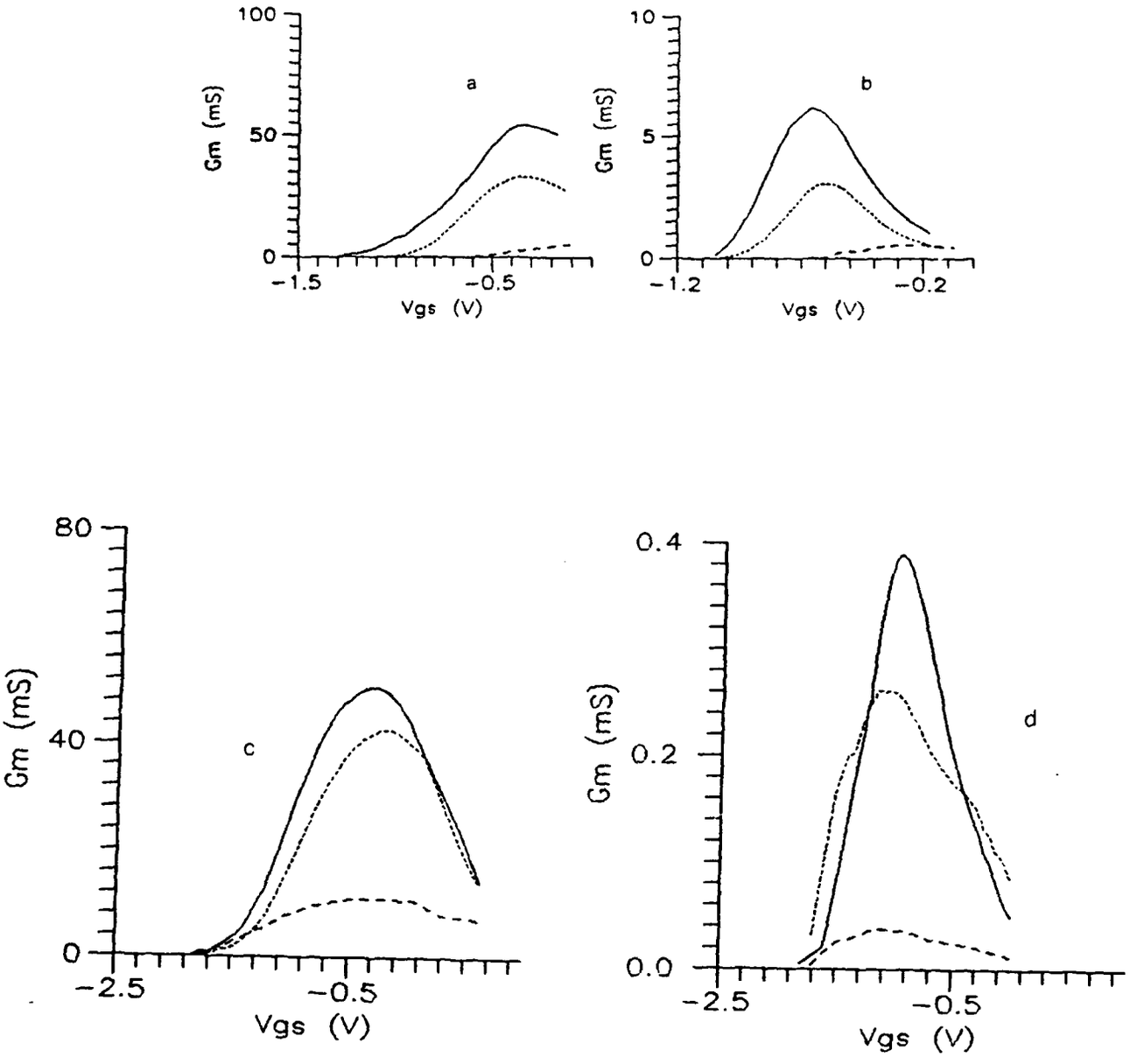

Fig.32 Effect of neutron irradiation on the transconductance characteristics

* Conventional HEMT in (a) the saturation and (b) the linear region of operation. (——) before irradiation, (· · ·) after 10^{15} n/cm^2 and (- -) after 1.7×10^{16} n/cm^2
* HEMT with AlGaAs buffer layer in (c) the saturation and (d) the linear region of operation. (——) before irradiation, (· · ·) after 6×10^{14} n/cm^2 and (- -) after 10^{16} n/cm^2

(fig.32). The transconductance characteristics in the linear region of operation (fig.32b and d) show that neutron radiation causes in both structures, A and B, an increase of threshold voltage, a decrease of the charge control efficiency and the 2DEG mobility. The gate bias for Gm maximum remains constant for doses not exceeding $3x10^{15}$ n/cm^2 while the Gm magnitude decreases with the increasing dose. So in the case of neutron radiation, as in the case of He ions, the maximum efficiency of charge control of the 2DEG does not shift with radiation. Above this radiation level the Gm charactersistics shift to more positive gate voltages and the transconductance collapse at doses larger than 10^{16} n/cm^2. Here it must be pointed that the threshold voltage of heavily irradiated devices lies very close to the gate bias of Gm maximum. This in connection with the very low Gm values indicates that the 2DEG charge control effitiency is very low or even absent, due to the absence of the 2DEG itself. The last suggest that at large radiation doses the devices do not operate like HEMTs but rather like MESFETs and the measured I-V and Gm characteristics originate from the AlGaAs parasitic MESFET. Similar conclusions are drown from the Gm characteristics of the saturation region (fig.32a and c).

At saturation the peak transconductance decreases also due to increase of channel roughness. This is because the 2DEG are scattered mainly by the channel roughness which increases with radiation. The effect of increase of channel roughness has been studied through the variation of the satu-

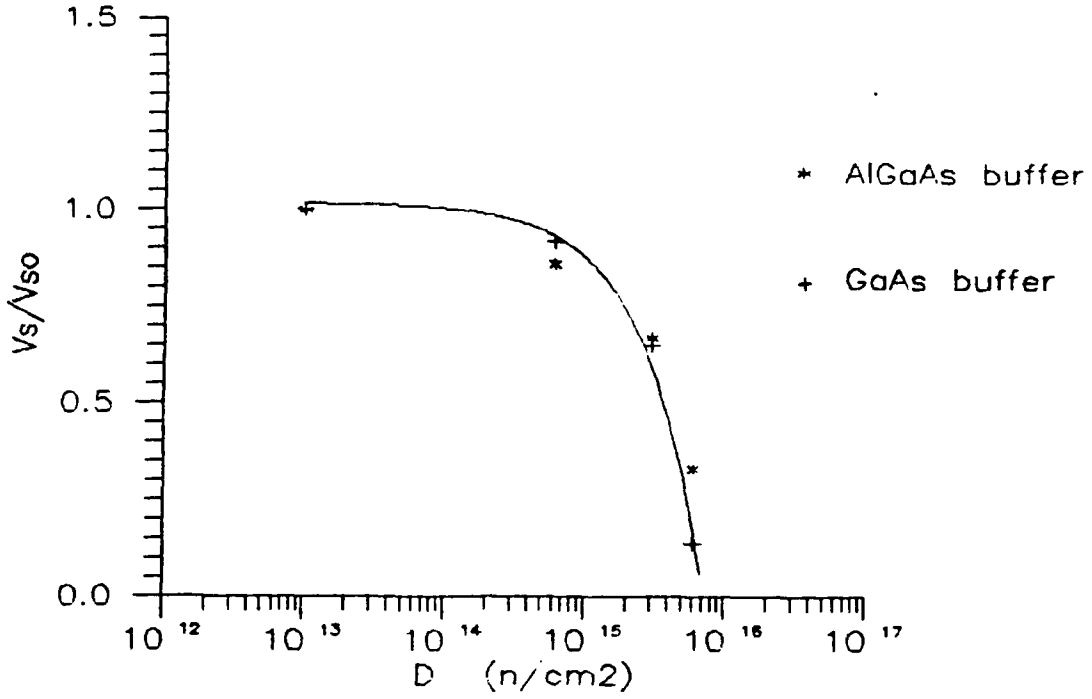

Fig.33 Dependence of the ratio of saturation velocity to its pre-irradiation value on the radiation dose

ration velocity with the radiation dose. The ratio of the velocity after irradiation to its pre-irradiation one (v_s/v_{so}) is plotted for both structures in Fig.33. The increase of the of the hetero-junction interface roughness is caused by neutron induced atom displacement. The interface roughness was not followed by an increase of density of interface states as in the case of He ion radiation (fig.17). This may be attributed to the fact that at the same temperatures an electron trap, T2 in Fig.28, emerges and covers the minority-like spectrum of the interface traps.

The other parameters that affect the I-V and Gm characteristivs, like the threshold voltage shift and the decrease of AlGaAs pinch-off voltage, will be discussed further in the charge control section.

I-T Characteristics

In HEMTs the drain current increases when the temperature decreases. In these structures the dominant scattering mechanism is on phonons which leads to a significant increase of mobility and hence the conductivity when the temperature decreases (fig.34 curve a). The latter is valid if the 2DEG does not vary significantly with temperature. At room temperature the leading scattering mechanism is on phonons, so there the effect of radiation is less prominent. The introduction of lattice defects in the buffer and spacer layers,with radiation, increases the concentration of charged centers which in turn increase the scattering on ionized impurities that decrease the 2DEG mobility and carrier concentration by traping at low temperatures. Both mechanisms lead to a decrease of device current at low temperatures. At low radiation doses (fig.34 curve b) these effects are less prominent and the device current collapses at low temperatures mainly due to the presence of the DX center. At large radiation doses (fig.34 curve c) the lattice defects are the leading ones and the device drain current vanishes gradually with the temperature decreasing. The effect of carrier traping is the dominant mechanism at high radiation doses, above $6x10^{15} n/cm^2$, and this is supported by the fact that the temperature dependence of the drain current shows two slopes (fig.34 curve c) thus indicating two trapping mechanisms. Taking into account that at these large radiation doses the devices behave like an AlGaAs MESFETs we estimated the activation erergies of the

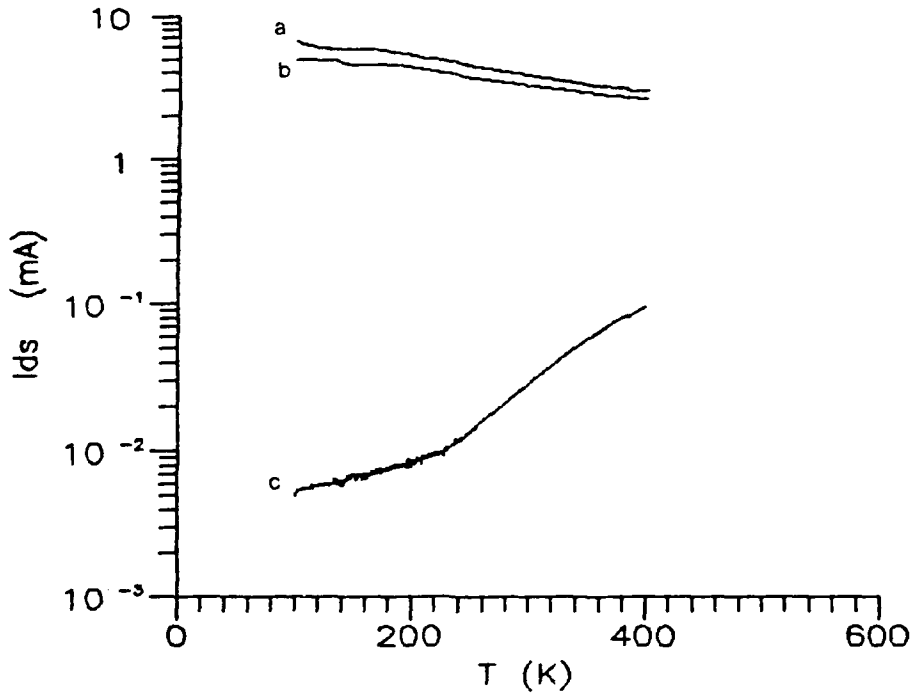

Fig.34 Temperature dependence of drain current (a) before irradiation and after a doses of (b) $6x10^{14}$ n/cm^2 (c) $1.7x10^{16}$ n/cm^2

MESFET channel conductance. In the high temperature region the activation energy was found to be about 0.18eV which coincides with that of trap E1 (0.19eV) that is introduced in AlGaAs by radiation. In the low temperature region the activation energy was found to be about 0.05eV. No such trap was found in the literature since its DLTS spectra might be located at temperatures well bellow that of liquid nitrogen.

Ns-V Characteristics

The concentration of the 2DEG was calculated from C-V measurements of FATFET gate capacitance. Experimental results are presented in Fig.35. In the lower part of each Ns-V characteristic the concentration is determined by the 2DEG while

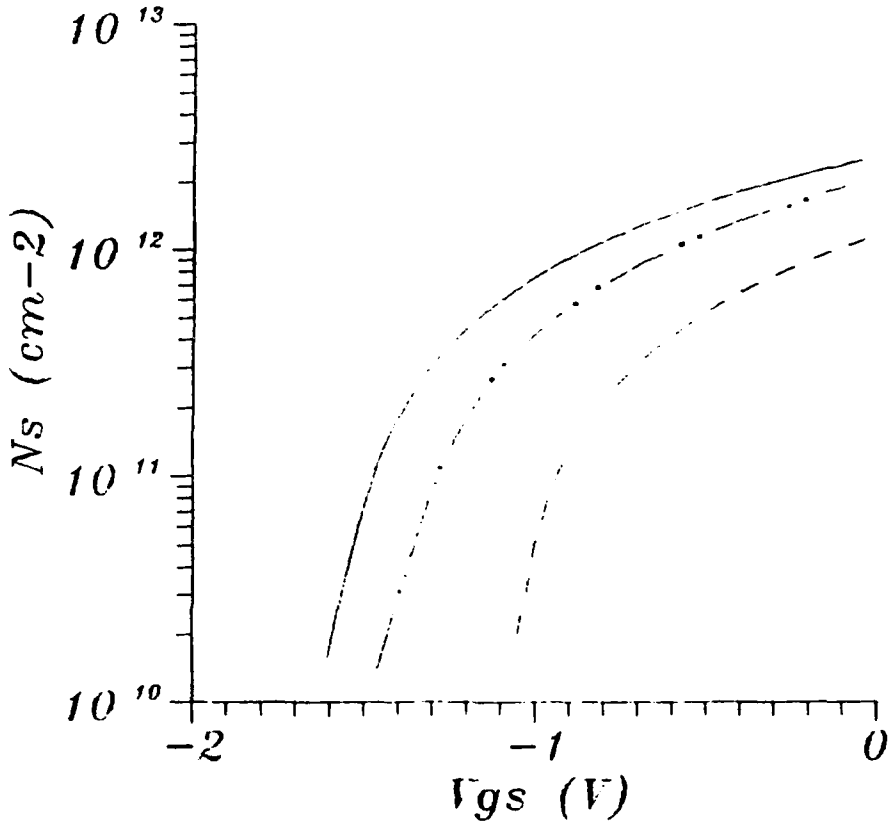

Fig.35 Sheet carrier concentration, including that of the AlGaAs donor layer, vs gate bias (—) before irradiation, (-·-·-) after a dose of $6x10^{14}$ n/cm^2 and (- - -) after a dose of 10^{16} n/cm^2

in the upper part there is always a contribution from the AlGaAs donor layer. The 2DEG concentration degrades with increasing the radiation dose. Exploatation of these results will be done later in the charge control model section. From the Ns-V characteristics the 2DEG degradation parameter was estimated to be about $6x10^{-17}$ cm^2.

Mobility degradation

In order to obtain a better insight on the neutron induced degradation in HEMTs, the efficiency of the screening effect on carrier scattering was further investigated. So the dependence of the device drift mobility on the sheet carrier

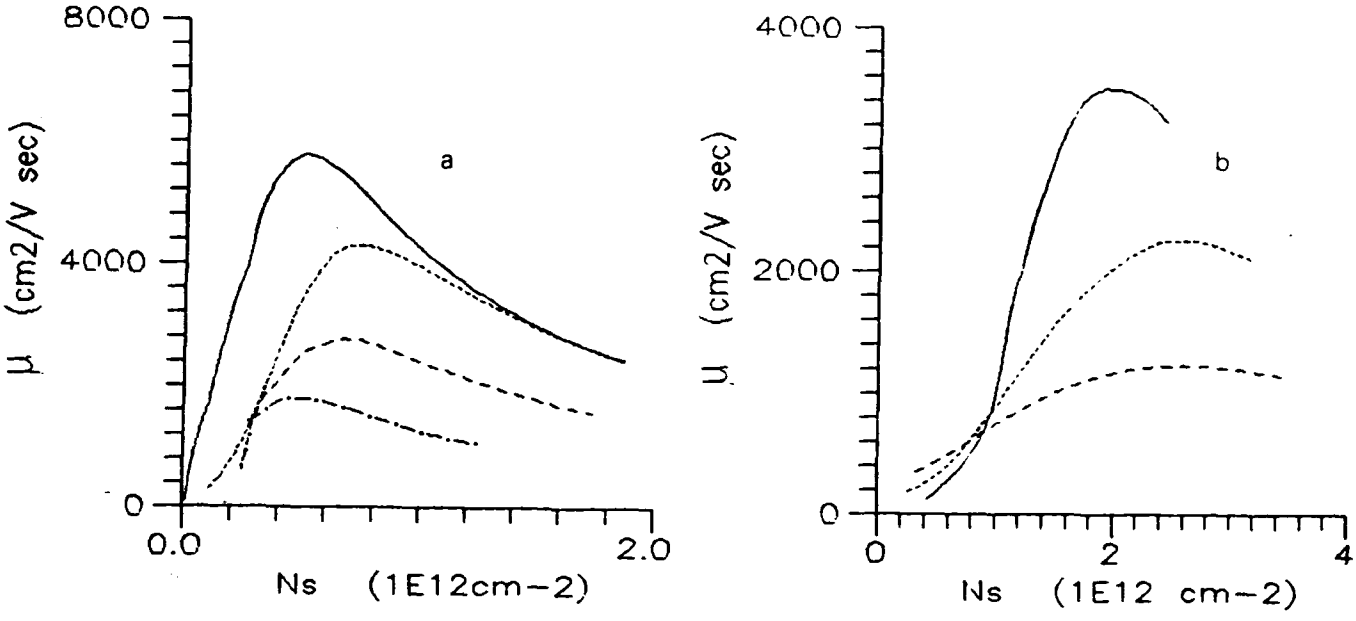

Fig.36 Dependence of mobility on sheet carrier concentration of:
(a) structure A (——) before irradiation, (···) after a dose of $6x10^{14}$ n/cm^{-2}, (- - -) after a dose of $3x10^{15}$ n/cm^{-2} and (-·-·-) after a dose of $6x10^{15}$ n/cm^{-2}
(b) structure B (——) before irradiation, (···) after a dose of $6x10^{14}$ n/cm^{-2}, (···) after a dose of $3x10^{15}$ n/cm^{-2} and (- - -) after a dose of $6x10^{15}$ n/cm^{-2}
In all cases the mobility drop above $n_s=2x10^{12}$ cm^{-2} is due to parallel conduction in the AlGaAs donor layer

concentration was determined at various radiation doses. The mobility was determined by applying the previously described method.

Typical μ-Ns characteristics, obtained for several radiation doses are persented in Fig.36. A common feature of the μ-Ns characteristics is that the mobility increases with increasing Ns and this is due to the effect of gradual increase of screening. The results from HEMTs with conventional

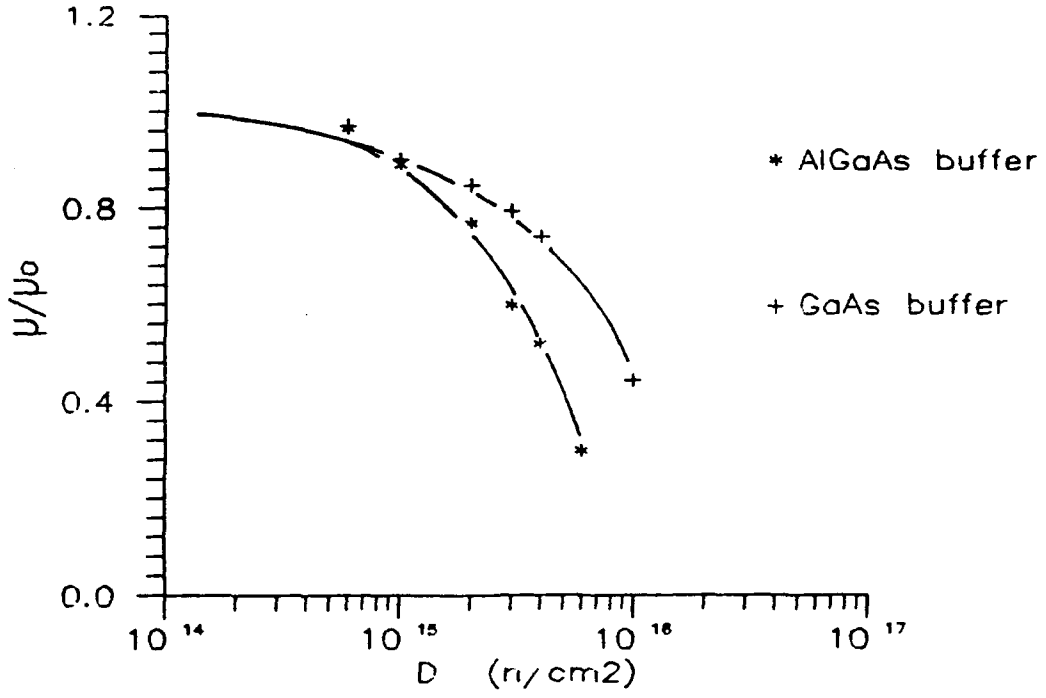

Fig.37 Dependence of the normalized mobility, to its pre-irradiation value, on the radiation dose.

buffer layers (fig.36a) and those with an additional AlGaAs buffer layer (fig.36b) show that the introduction of the additional buffer layer does not improve the device neutron radiation hardnes from the point of view of carrier mobility.

The dependence of the normalized mobility, to its pre-irradiation value, on the radiation dose is shown in Fig.37. In both structures the mobility decreases linearly with the radiation dose. The very low mobility values above $6x10^{15}$ n/cm^2 must be attributed to a partial contribution from the AlGaAs donor layer due to low concntration of 2DEG. The corresponding degradation parameter in structures A and B was found to be $5x10^{-17}$cm^2 and $1.2x10^{-16}$cm^2 respectively, indicating again that the insertion of an additional AlGaAs buffer layer does not improve the device total dose radiation hard-

ness.

Series Resistance degradation

In the present study we have assumed that the series resistances of HEMTs are ohmic and the study is limited on the data obtained from the linear region of operation. For reasons described in the chapter of He ion radiation we studied the variation of series resistance normalized magnitude with the radiation dose. The variation of the normalized source resistance of each structure used in this project is presented in Fig.38. From there it becomes obvious that the introduction of an AlGaAs buffer layer does not affect the neutron radiation hardnes of HEMTs.

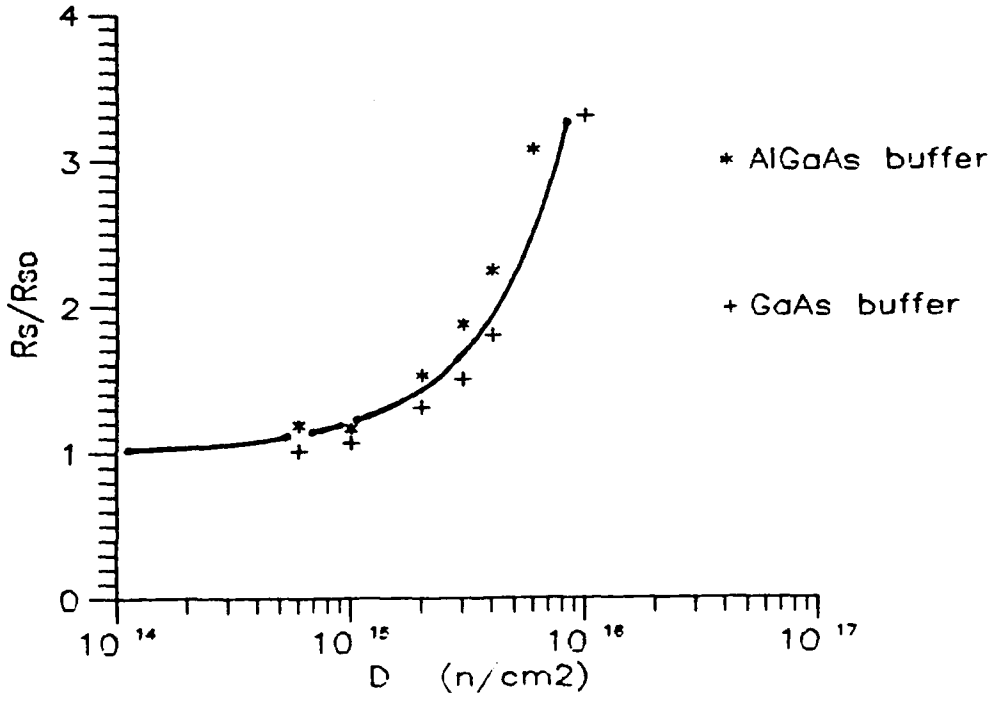

Fig.38 Variation of the normalized R_{SD}/R_{SDo}, to their values before radiation, parasitic resistances vs radiation dose: (+) for structure A and (*) for structure B.

The series resistance increases linearly with the neutron dose. The large value of degradation parameter, about $3x10^{16}cm^{-2}$, is attributed to the simoultaneuous decrease of the 2DEG carrier concentration and the degradation of the mobility. Another reason for the fast dagradation is the specific structure of the series resistances which contain a heterojunction which tunneling resistance can be strongly affected by the damage introduced by neutrons.

Charge Control Model

In order to study the neutron radiation effects in HEMTs we have applied the charge control model described in the previous chapter. As already mentioned the 2DEG carrier concentration is given by

$$N_s(V_{GS}) = \frac{\varepsilon}{qd_t}\,[V_{GS}-(\Phi_b-V_P-\Delta E_c)-V(d_i)]$$

where the meaning of each parameter is known.

The charge control model is further simplified, after some algebric calculations, leads to

$$V_{GS} = \frac{qd_tN_s}{\varepsilon} + (\Phi_b-\Delta E_c-V_P) + \frac{kT}{q}\ln[\exp(\frac{qN_s}{DkT})-1] + \frac{a_o}{q}(N_s+N_A)^{2/3}$$

which works satisfactory for carrier concentrations bellow about $5x10^{11}cm^{-2}$. A fitting of the experimental N_s-V_{GS} data to the above equqtion alows the calculation of three parame-

meters, that is: the thickness of the AlGaAs donor layer, the pinch-off voltage and the net acceptor concentration in the buffer layer. The interface states introduced by irradiation are accounted in the variation of the donor layer pinch-off voltage, thus in the net donor concentration of the AlGaAs layer.

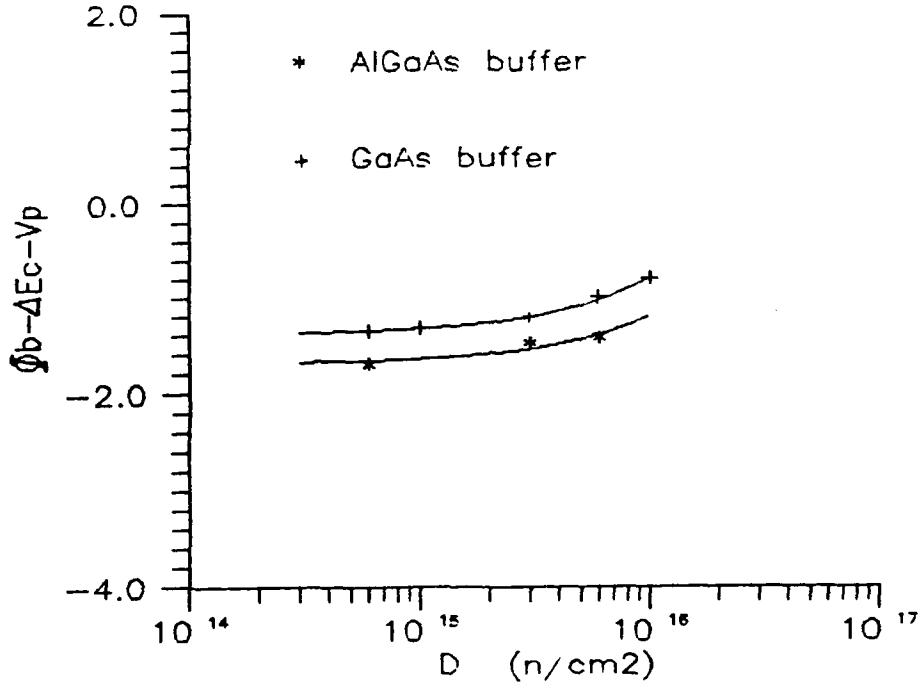

Fig.39 Dependence of the $\Phi_b - \Delta E_c - V_P$, which represents the AlGaAs pinch-off voltage, on the radiation dose of (+) structure A and (*) structure B.

The effect of alpha particle radiation dose on ($\Phi_b - \Delta E_c - V_P$) and the buffer layer net acceptor concentration N_A are presented in Fig.39 and Fig.40 respectively.

The parameter ($\Phi_b - \Delta E_c - V_P$) is directly related to the net donor concentration of the AlGaAs donor layer, since all the other parameters are not affected by radiation. In all HEMTs this parameter was found to vary linearly with the radiation dose. The linear dependence of V_P agrees well with

the results presented by R.J. Krantz et al in [2] and clearly indicates that the variation of the pinch-off voltage with the radiation dose is caused mainly by the carrier removal in the AlGaAs layer. From this the degradation parameter of the AlGaAs donor layer was found to have an average value of

$$\beta_{AlGaAs-n} = 10^{16}\,cm^{-2}$$

with a dispersion of about $\pm$25% which did not depend on the device structure.

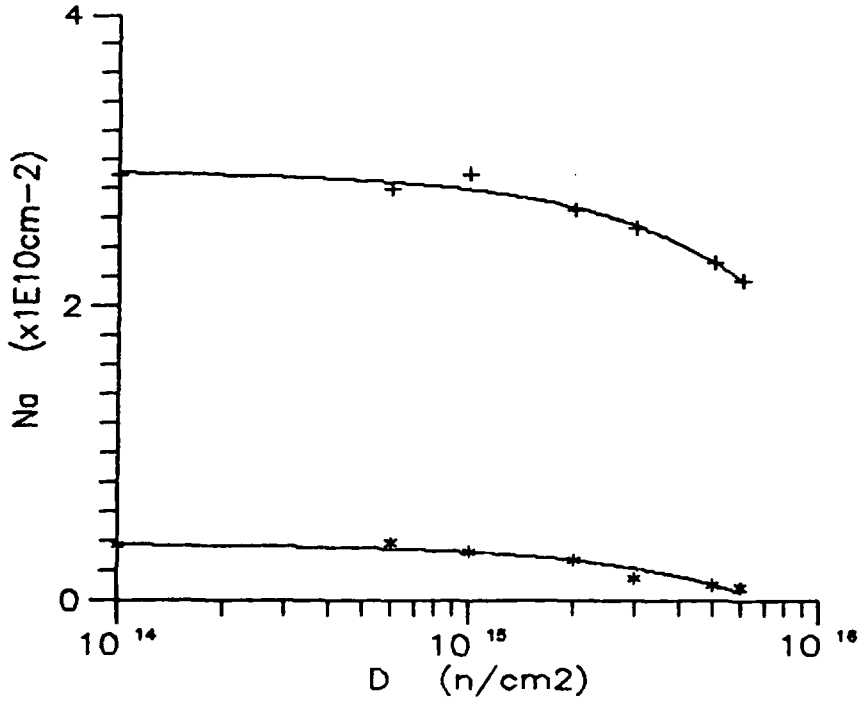

Fig.40 Buffer layer, equivalent, net acceptor concentration N_A per unit area vs radiation dose: (+) for structure A and (*) for structure B.

The net acceptor concentration in the GaAs buffer layer is presented, as already mentioned, in Fig.40. The acceptor concentration decreases with radiation due to introduction of of deep donors which turn the lightly p-type buffer layer into a more intrinsic one. The introduction rate of deep do-

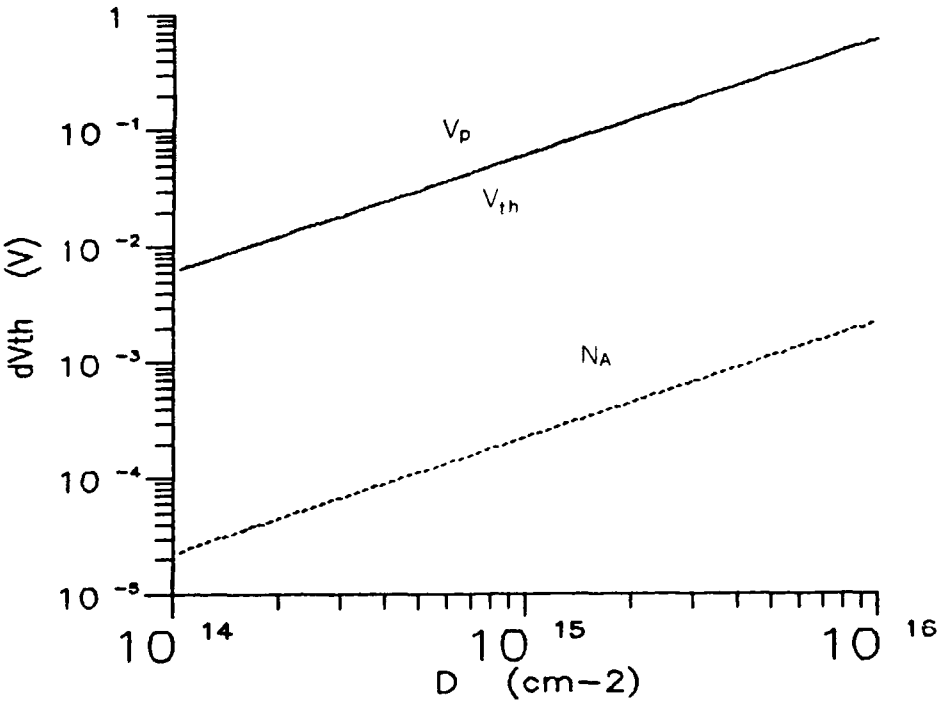

Fig.41 Variation of threshold voltage and the contributions of each parameter versus the He ion dose

nors, assuming the following relation:

$$dN_A = \beta_A \cdot dD$$

was found to be about 1.2×10^{-6} for structure A and about 5.4×10^{-7} for structure B. The smaller carrier removal rate, observed in structures B, may be attributed to the negative charge that is accumulated at the GaAs/AlGaAs heterojunction of the buffer layers.

The variation of the threshold voltage, the pinch-off voltage of AlGaAs donor layer and the shift of first subband towards the bottom of the quantum well versus the radiation dose are plotted in Fig.24. The parameters used in Fig.41 were d_t=350A, $N_D=2\times10^{18}cm^{-3}$, $N_A=3\times10^{10}cm^{-2}$, $\beta_A=1.2\times10^{-6}$ and $\beta_{AlGaAs}=10^{-16}cm^{-2}$. The comparison of the contribution of

each parameter clearly indicates that the donor layer pinch-off voltage is is the dominant one.

Table 7. MESFET and HEMT threshold voltage and series resistance degradation parameters

Structure	Ref	β^* (10^{-16} cm^2)	β_R (10^{-16} cm^2)
HEMT			
GaAs buffer	*	1.3	3.0
AlGaAs buffer	*	0.8	3.0
SL buffer	1	1.4	-
GaAs buffer	2	2.0	-
MESFET			
MBE GaAs buf.	*	0.9	5.2
MBE AlGaAs buf.	*	1.2	8.4
Ion Implanted	*	1.2	1.5
Ion Implanted	43	1.7	-
Ion Implanted	44	2.5	-
Ion Implanted	45	3.5	-
Ion Implanted	46	3.8	-
VPE	47	5.0	88

* Data from present work

4.4 Comparison with MESFETs

The effect of neutron radiation on HEMTs was further compared to that on MESFETs. The comparison of radiation hardness of 2D and 3D devices included devices with GaAs and AlGaAs buffer layers. Additional ion implanted ones were used

as also data from literature. The comparison of the radiation hardness of the MESFETs and the HEMTs was limited on the variation of the threshold voltage and the source series resistance with the radiation dose, sice these parameters affect significantly the device performance. The results are summarised in Table 7.

Comparing these results we can conclude that the radiation hardness of HEMTs from the point of view of threshold voltage is slightly higher than that of MESFETs. From the point of view of series resistance the radiation hardness of HEMTs is similar to that of MESFETs.

4.5 Conclusions

In conclusion the neutron radiation degradation of HEMTs is a composit effect. Radiation affects all layers of HEMT structure and the degradation of each layer contributes to the overall performance degradation. The main effects of radiation is summarised bellow

* The neutron displaced atoms increase the heterointerface roughness. The introduction of interface states due to limited analysis is unavoidably accounted for the degradation of the donor layer effective doping
* Radiation decreases the 2DEG density due to the decrease of the donor layer effective doping
* Neutron irradiation shifts the device threshold voltage.
  - The contribution of the buffer layer to the shift of the threshold voltage is attributed to the decrease of

effective acceptor density due to introduction of deep electron traps such as the EL2 and U-band levels

- The contribution of the donor layer to the shift of the threshold voltage is attributed to the decrease of decrease of donor layer effective doping due to introduction of four electron traps. Two of them, the deeper ones, are assigned as the E4 and M4* while the presence of the shallower ones can be detected from the temperature dependence of the device drain current

* Radiation degrades both the 2DEG mobility and saturation velocity due to
  - increase of charged defects in the buffer and spacer layers, that is the increase of ionized impurity scattering and the
  - increase of heterointerface roughness which decreases the saturation velocity
* The device performance is significantly degraded from the increase of the series parasitic resistances.This rapid increase may be attributed to the complex nature of the series resistance and becomes important at neutron radiation doses larger than 10^{15} n/cm^2.
* The introduction of an AlGaAs buffer layer does not seem to cause an important improve of radiation hardness
* Finally a comparison of radiation hardness shows that HEMTs are slightly more resistant than MESFETs to neutron radiation.

5 GAMMA RAY RADIATION

The gamma rays generate electron-hole pairs, photoelectric effect, or interact with electrons through Compton effect or give rise to pair production according to their photon energy. The three types of photon interactions in function of the absorbing material and the photon energy is presented in Fig.42.

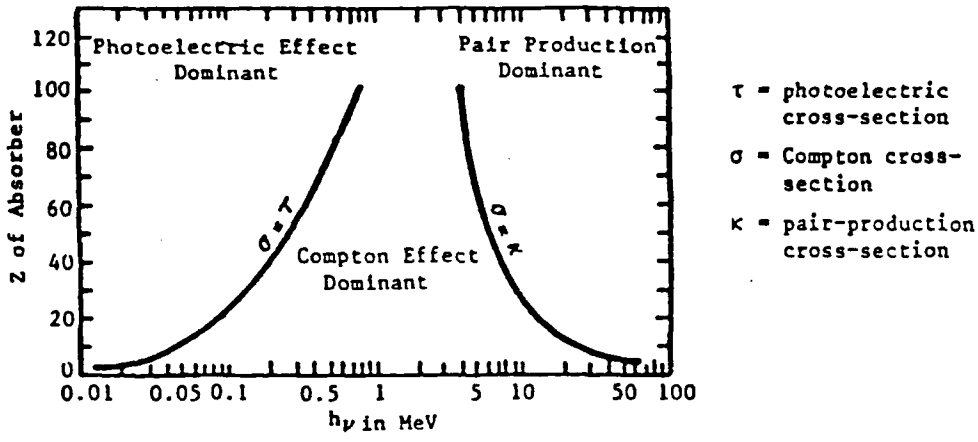

Fig.42 Gamma rays interactions in function of the absorbing material and the photon energy

5.1 Radiation Effects in GaAs Layers

The effect of gamma ray radiation in GaAs, bulk and epitaxial layers, has been studied extensively during the last two decades [48-52]. The Co60 gamma ray Compton electrons have energies of about 0.6MeV that lies above the threshold enerdy for displacement damage in GaAs [53]. Low dose gamma rays induce in GaAs a very shallow donor which lies

about 20meV bellow the conduction band while at higher doses a deep acceptor is induced which lies about 0.13eV from the conduction band [36]. The introduction of this shallow donor is in good agreement with the 1MeV electron radiation induced donor [54,55], 30meV bellow the conduction band, and the often reported improvement of device performance which have been subjected to low gamma ray radiation doses [44]. In practice the effect of Co60 gamma ray radiation in GaAs is hardly noticeable at doses bellow 10^7 rad in epitaxial layers, while there is a synergetic effect in post neutron irradiated [44] or ion implanted ones [15] layers. The carrier removal in MBE GaAs layers may be described by the empirical equation [52]

$$\Delta N(cm^{-3}) = 9.92 \times 10^5 \; D^{1.17}$$

which does not depend on the initial carrier concentration N_o as long as no synergetic effects occour. In the other cases the degradation rate is higher.

In order to determine the traps that are induced by gamma rays irradiation, MESFETs were irradiated with doses up to 3×10^7 rad. The DLTS measurements performed on the irradiated devices revealed the introduction of the E3 [57,58] trap with an activation energy of 0.35eV, which is in good agreement with the 0.32eV dominant trap reported by Aono et.al. [56]. On the other hand MCTS measurements revealed the introduction of the H4 hole trap [57]. Finally a slight increase, within error limits, of EL2 concentration was observed. The latter was observed in ion implanted MESFETs [15] and it may be

attributed to interactions with other already existing background defects.

5.2 Radiation Effects in AlGaAs Layers

In the case of AlGaAs layers the effect of gamma ray radiation was investigated from the HEMT donor layers. Devices with same geometry like that of MESFETs, 20μm gate length and 250μm gate width, were assessed with DLTS method. The spectra before and after irradiation are presented in Fig.43 and shows no difference thus denoting that the concentration of induced traps is extremely low. Such a behavior can be justified if a similar equation for carrier removal holds in AlGaAs like in GaAs where the carrier removal is independent of the background doping [51].

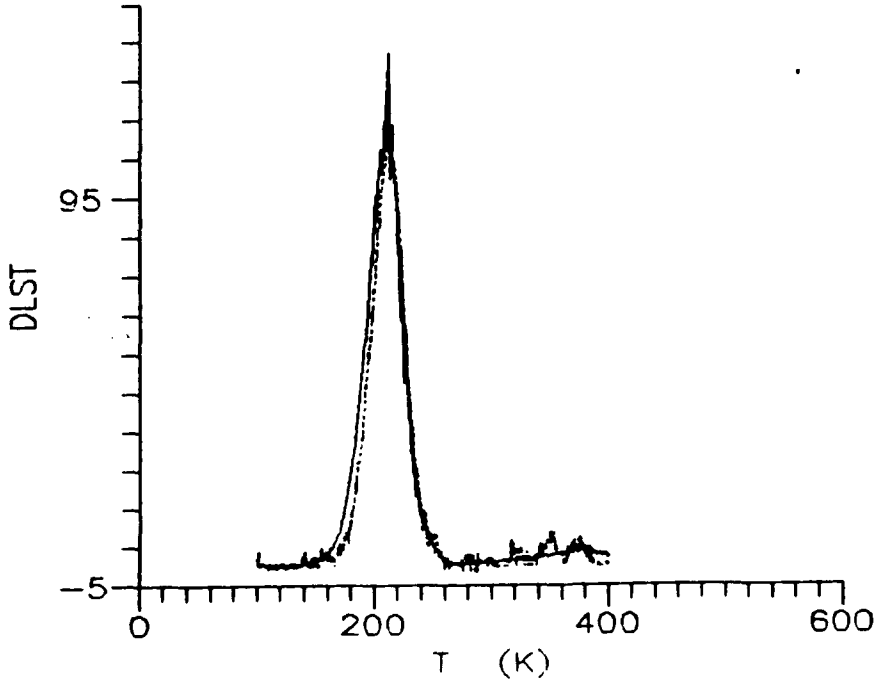

Fig.43 DLTS spectra of a HEMT. Continuous line is before radiation and doted line is after a dose of $3x10^7$ rad.

The carrier removal rate was furhter investigated from the variation of the AlGaAs donor layer pinch-off voltage V_P and that will be discussed later in the appropriate paragraph.

5.3 Radiation Effects in HEMTs

Gamma rays give rise displacenment defects through Compton electrons, which in GaAs are point defects. In the AlGaAs donor layer the displacement defects were not detected at doses up to $3x10^7$ rad. The simultaneous introduction of defects in the donor and the buffer layers of a HEMT affects the 2DEG concentration and mobility so the device performance degrades. In order to investigate the ef-fect of gamma rays in HEMTs we followed the same procedure as in the previous cases. The structures employed in this study were the A and B ones.

I-V Characteristics

The effect of gamma ray irradiation on the I_{DS}-V_{DS} characteristic HEMTs is shown in Figs.44a and 44b for structure A and B respectively. In these devices no significant change was observed bellow 10^6 rad so the pre-irradiadion and the highest dose post-irradiation characteristics are presented. The evolution of the I-V characteristcs with the radiation dose indicates that the device performance dagrades by about 12% for structure A and 9% for structure B at a dose of 10^7 rad. The results in Fig.44 are in good agreement with those of O'Loughlin [3]. Also our experiments show a much

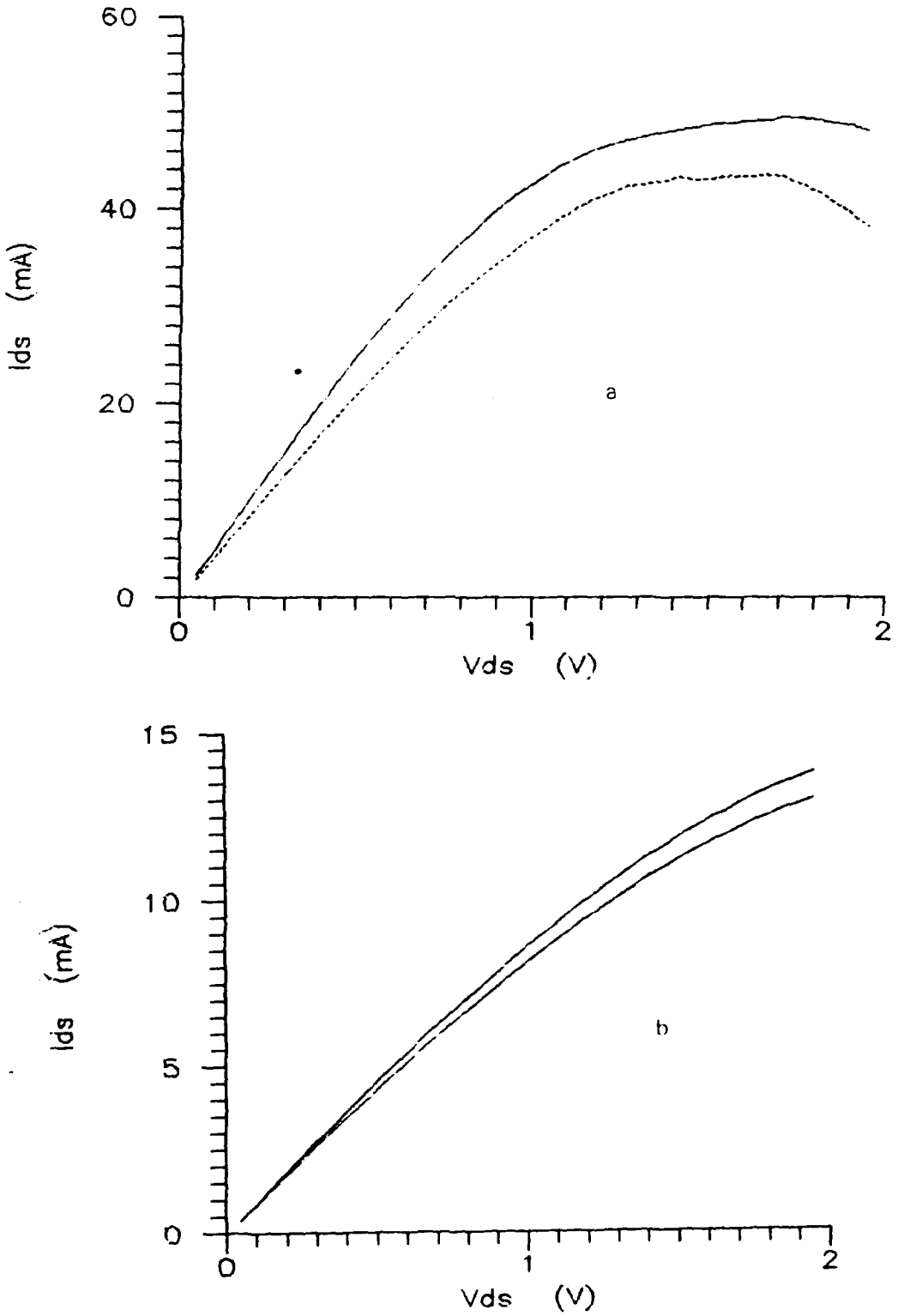

Fig.44 Dependence of I_{DS}-V_{DS} (V_{GS}=0V) characteristics on the radiation dose
a. Conventional HEMT (——) before irradiation and (· · ·) after a dose of 10^7 rad
b. HEMT whith AlGaAs buffer layer (——) before irradiation and (· ·) after a dose of 10^7 rad

higher degradation than the one reported by Listvan, Vold and Arch in [4].

A comparison of the degradation rates of these structures leads to the conclusion that the presence of an AlGaAs buffer layer seems to improve the device radiation hardness. This conclusion is also supported by the fact that X-ray flash experiments performed by Anderson et.al. [59] showed that HEMTs with AlAs/GaAs superlattice buffer layers exhibited a radiation hardness of two order of magnitude higher than conventional ones with structures similar to that of A in the present report.

The effect of radiation on the I_{DS}-V_{GS} characteristics become more evident by studying the Gm-V_{GS} ones (fig.45). The transconductance characteristics in the linear region of operation decreases by about 13% in structure A and 9% in B at a dose of 10^7 rad. In addition Fig.45 shows that gamma radiation causes an increase of threshold voltage of structures B. So the gate bias for Gm maximum remains constant with radiation in structure A while it shifts towards more negative gate bias levels in structure B, the shift being about 0.1Volt for a dose of 10^7 rad. The decrease of transconductance maximum is be attributed to a decrease of 2DEG concentration and mobility. Similar is the behavior of the saturation transconductance characteristics. There for radiation doses up to 10^7 rad we did not observe in structure A any shift of transconductance peak towards more positive gate bias levels while in structure B devices the shift was about 0.1Volt. This effect can be

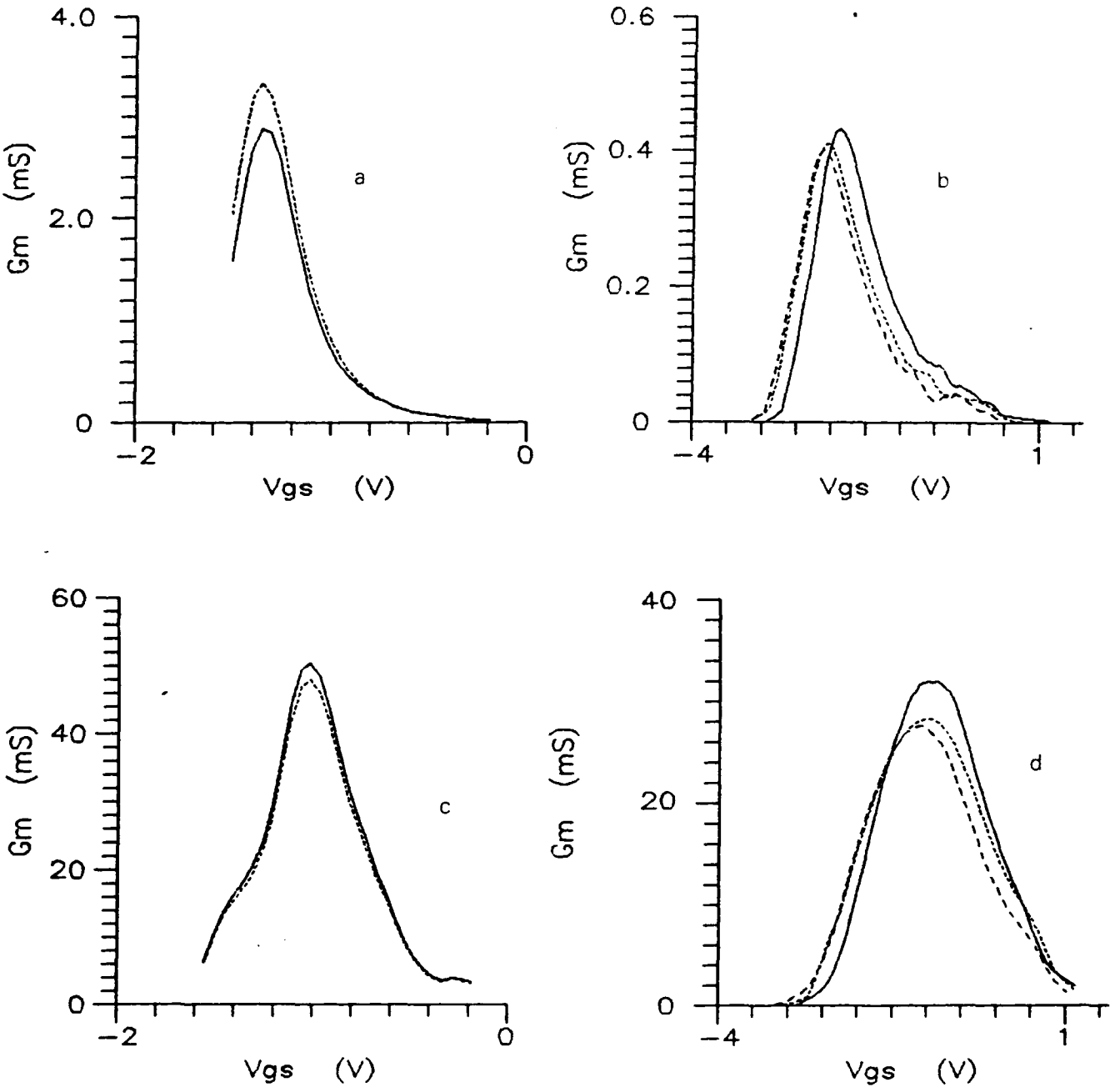

Fig.45 Effect of gamma ray irradiation on the transconductance characteristics

* Conventional HEMT in (a) the saturation and (b) the linear region of operation. (···) before irradiation and (——) after 10^7 rad
* HEMT with AlGaAs buffer layer in (c) the saturation and (d) the linear region of operation. (——) before irradiation, (···) after 3×10^6 rad and (- -) after 10^7 rad

explained by an increase of electron concentration in the 2DEG which may be related with the the presence of the AlGaAs buffer layer in structure B.

I-T Characteristics

In HEMTs the drain current increases when the temperature decreases because due to spatial separation of donors and carriers the dominant scattering mechanism is on phonons which leads to a significant increase of mobility and hence the conductivity when the temperature decreases. The latter is valid if the 2DEG does not vary significantly with temperature. The introduction of lattice defects in the buffer and spacer layers,with radiation, increases the concentration of charged centers which in turn increase the scattering on ionized impurities that decrease the 2DEG mobility and carrier concentration by traping at low temperatures. Both mechanisms lead to a decrease of device current at low temperatures. The effect of gamma ray radiation in HEMT is presented in Fig.46a for structure A and Fig.46b for structure B, before and after a totoal dose of 10^7 rad. In both figures the gamma ray radiation decreases slightly, by about 3%, the device current while it does not affect the current-temperature slope. To a first approach the decrease of current can be atributed to a simultaneous decrease of 2DEG concentration and mobility. On the other hand the absence of change in the slope of the I-T

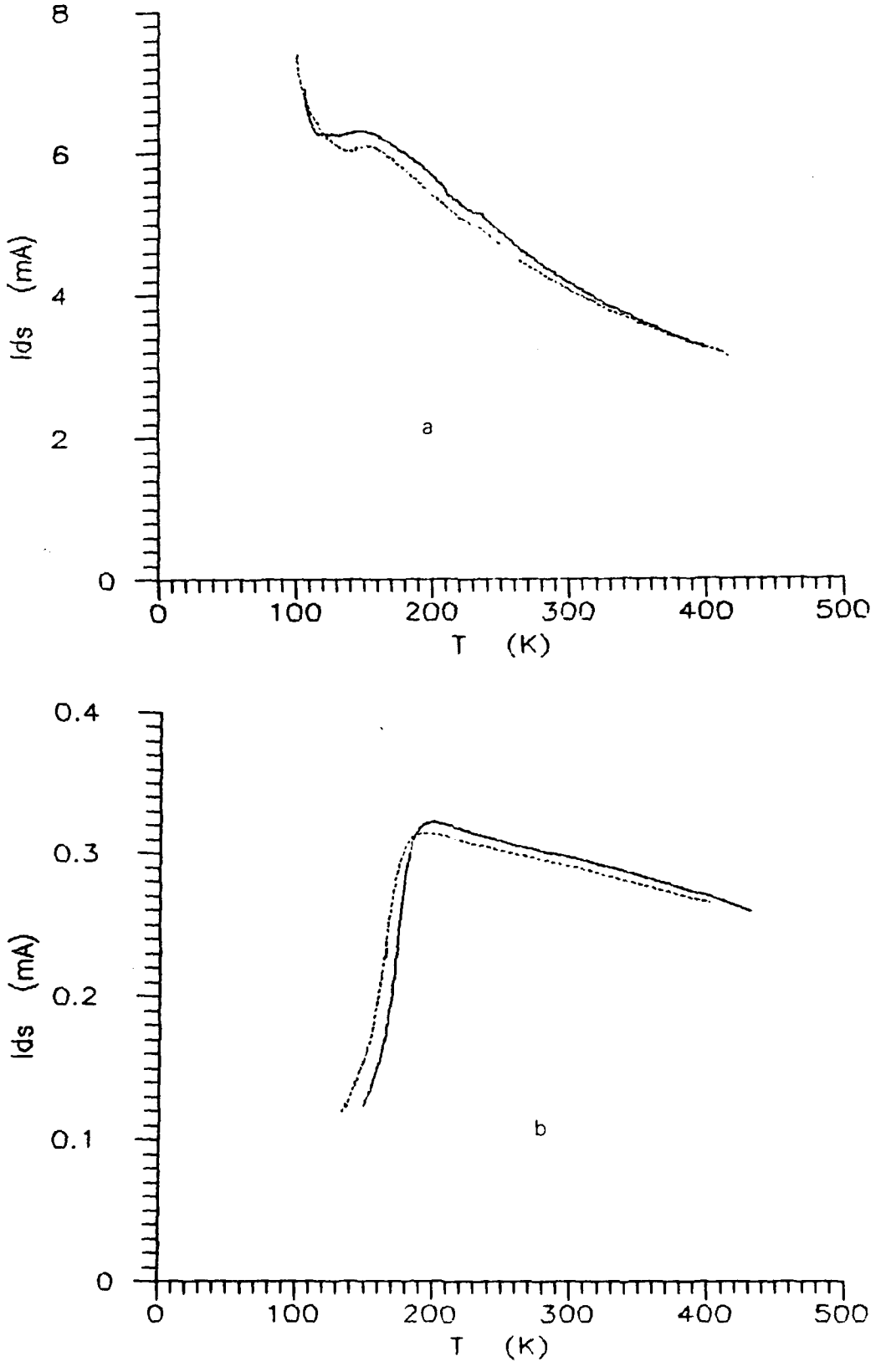

Fig.46 Temperature dependence of drain current (—) before irradiation and (···) after a doses of 10^7 rad for (a) structure A and (b) structure B devices.

characteristics suggests that the increase of ionized impurity scattering is still low and the decrease of current may be attributed to rather a decrease of carrier concentration. This is supported from the evolution of N_s-V and μ-N_s characteristiques with the radiation as will be shown later.

Ns-V Characteristics

The concentration of the 2DEG was calculated from C-V measurements of FATFET gate capacitance. Typical experimental results are presented in Fig.47. At a gate bias where Gm attains maximum the 2DEG concentration decreases by about 30% for a total dose of 10^7 rad. This decrease of N_s is very large and it can be justified if we assume that dose enhancement occurs [50] due to high Z materialsused for the gate, source

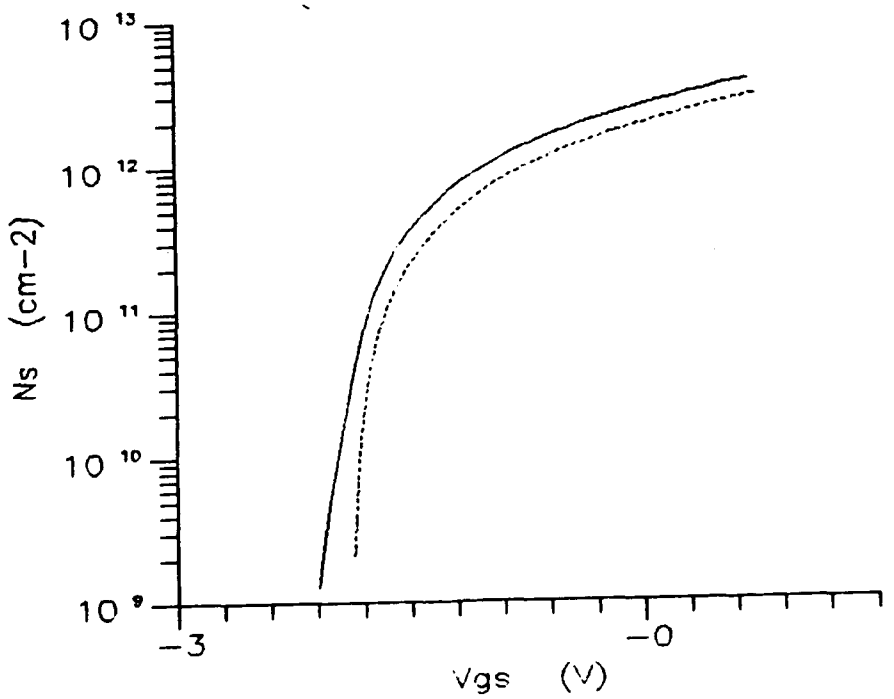

Fig.47 Sheet carrier concentration, including that of the AlGaAs donor layer, vs gate bias (—) before irradiation and (··) after a dose of 10^7 rad gamma rays

and drain contacts. The enhancement factor can be as high as 21 [55]. The decrease of N_s is much larger than the one observed in the I-V and I-T characteristics, about 11% and 3% respectively. Another feature of the N_s-V characteristics is the shift of the threshold voltage towards more positive values which is in contradiction with the shift of the HEMT threshold voltage.

Mobility degradation

The efficiency of the screening effect on carrier scattering was further investigated. The dependence of the device drift mobility on the sheet carrier concentration was determined at various radiation doses.

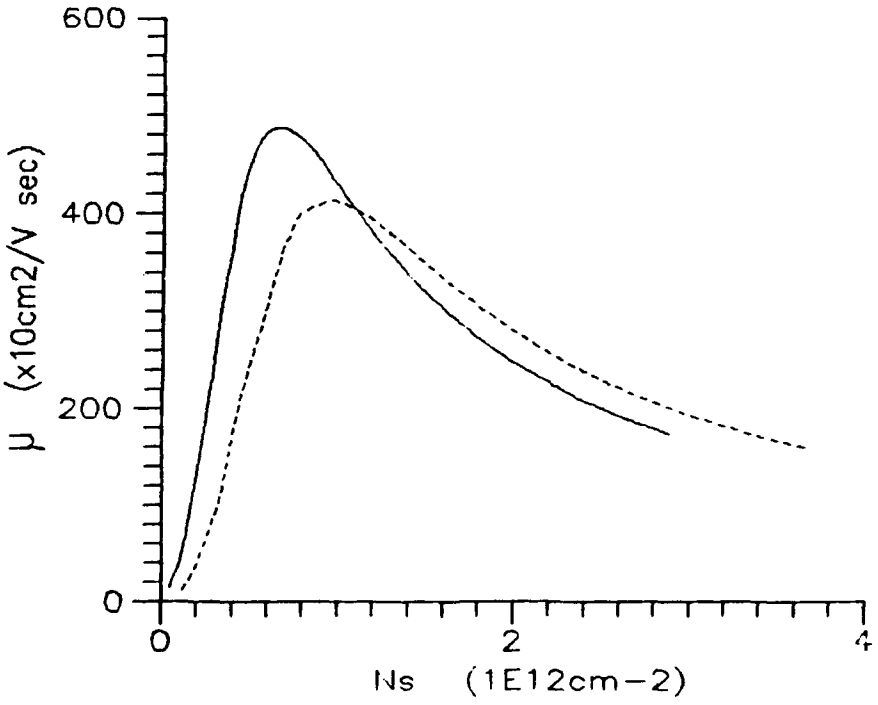

Fig.48 Dependence of mobility on sheet carrier concentration (——) before irradiation and (···) after a dose of 10^7 rad γ-rays

Typical μ-Ns characteristics, obtained for several radiation doses are persented in Fig.48. A common feature of the μ-Ns characteristics is that the mobility increases with increasing Ns and this is due to the effect of gradual increase of screening. The results from HEMTs with conventional buffer layers showed an average decrease of about 16% at μ_{max} and from those with an additional AlGaAs buffer layer a decrease of about 19% at μ_{max}. This indicates that the introduction of an additional AlGaAs buffer layer does not improve the device radiation hardnes from the point of view of carrier mobility.

The variation of carrier mobility and concentration with radiation dose leads to the conclusion that for a total radiation dose of 10^7 rad the device channel conductance would decrease by more than 35%. This discrepancy may be attributed to an increase of surface states which further increase the device surface leackage. This is supported by the fact that the drain-gate leackage cvurrent does not increase linearlly with the V_{DS} bias hence the surface current is more prominent when the device operates in the linear region. In addition the modulation efficiency of the surface leackage current is low so its contribution to the Gm characteristics is also low. The effect of increase of surface leackage current with the radiation dose is expected to increase even more in passivated devices due to charge traping in the insulating coating.

Series Resistance degradation

As already mentioned we assume that the series resistances of HEMTs are ohmic and the study is limited on the data obtained from the linear region of operation. The variation of the normalized source resistance of each structure used in this project was found to vary almost logarithmicaly with the radiation dose and described by an empirical equation

$$\frac{\Delta R_s}{R_{so}} = m \cdot D^{0.21}$$

where m is a factor (-0.0032) which exact value depends on the device growth and process. The power law relation indicates that the dominant mechanism of the series resistance degradation is rather the carrier removal than the decrease of mobility. Here it must be pointed that the large value of power law factor, relatively to those of V_P and N_A as will be presented bellow, must be attributed to the complex structure of the two underlying heterojunctions.

The above empirical equation fits well to the experimental data, reported by O'Loughlin (fig.4 of Ref.3), of the series resistance variation with radiation dose. In these data the radiation dose was extended up to about 10^8 rad and the empirical equation becomes

$$\frac{\Delta R_s}{R_{so}} = 0.0039 D^{0.20}$$

which is extremely good agreement with the above one. Therefore we can conclude that the degradation of series resistance in HEMTs, upon γ-ray irradiation and up to 10^8 rad, is go-

verned by a power law relation.

Charge Control Model

In order to study the gamma rays radiation effects in HEMTs we have used again the charge control model described in the previous chapters and which which works satisfactory for carrier concentrations bellow about $5x10^{11}cm^{-2}$. A fitting of the experimental data allows the calculation of two radiation dependent paramemeters, that is: the pinch-off voltage and the net acceptor concentration in the buffer layer. Any radiation induced charges in tha spacer layer or the hetero-

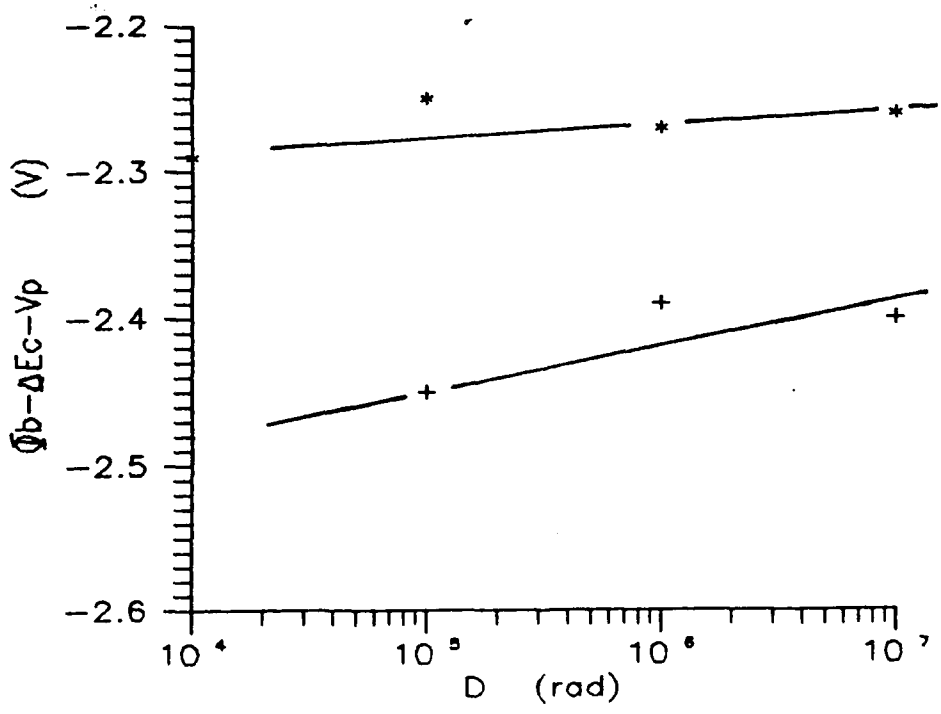

Fig.49 Dependence of the $\Phi_b-\Delta E_c-V_P$, which represents the AlGaAs pinch-off voltage, on the radiation dose of (+) structure A and (*) structure B.

junction interface are accounted in the pinch-off voltage.

The effect of alpha particle radiation dose on ($\Phi_b-\Delta E_c-$

V_P) and the buffer layer net acceptor concentration N_A are presented in Fig.49 and Fig.50 respectively.

The parameter ($\Phi_b - \Delta E_c - V_P$) is directly related to the net donor concentration of the AlGaAs donor layer, since ΔE_c and Φ_b, are not affected by γ-ray radiation. In all devices the $\Phi_b - \Delta E_c - V_P$ parameter was found to increase non linearly with the radiation dose. If we assume that a similar power law equation holds for the carrier removal in the AlGaAs donor layer, we find

$$\frac{\Delta N}{N_o} = 3 \times 10^{-3} \; D^{0.113}$$

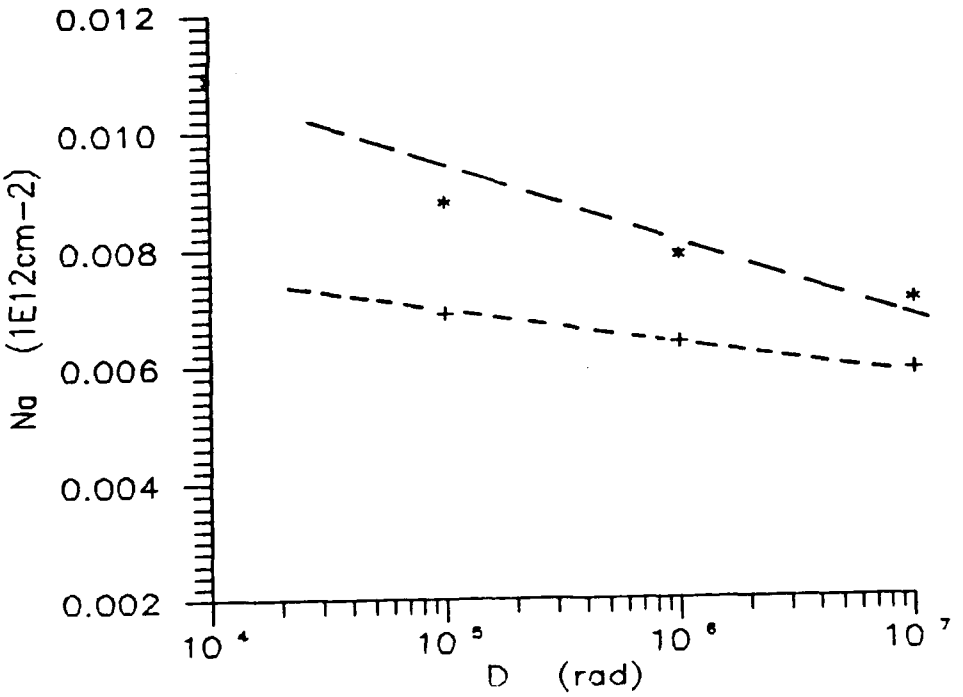

Fig.50 Buffer layer, equivalent, net acceptor concentration N_A per unit area vs radiation dose: (+) for structure A and (*) for structure B.

where N_o is the background doping which in in our case is about $2 \times 10^{18} cm^{-3}$. The above empirical relation denotes a very

slow varying carrier removal with the radiation dose. This behavior may be attributed to introduction of a shallow donor level such as in the case of GaAs. Therefore the simultaneous doping with the carrier removal in both the donor and the spacer layers causes a smaller decrease of net donor concentration. At a radiation dose of 10^7 rad the net donor concentration decreases by about 2%, so the shift of threshold voltage level must be attributed to the decrease of net acceptor concentration in the buffer layer and the shift of the Fermi level.

The net acceptor concentration in the GaAs buffer layer is presented in Fig.50. The acceptor concentration decreases with radiation due to introduction of of deep donors which turn the lightly p-type buffer layer into a more intrinsic one. The net acceptor removal in the GaAs buffer layer was found to be described by the empirical equation

$$\Delta N_A (cm^{-2}) = 1.06 \times 10^{10} \; D^{0.18}$$

while in the case of structure B where an AlGaAs buffer layer was used, the empirical equation is

$$\Delta N_A (cm^{-2}) = 1.84 \times 10^{10} \; D^{0.06}$$

which shows the effect of the buffer layer structure on the radiation hardness of the HEMT. The smaller power law factor in the case of structure B can be attributed to an increase of negative hetero-interface charge in the buffer layeras observed in the case of He ion radiation.

The adopted charge control model results show a decrease of both donor and acceptor concentrations thus supporting the

hypothesis that the apparent increase of I-V characteri-stics threshold voltage is caused by surface leackage curren. This is because the $\Phi_b - \Delta E_c - V_P$ and N_A parameters were obtained from the C-V characteristics measured at 1MHz where the lea-kage current does not affect the measurements. Effects originating from the surface during γ-ray radiation have been reported by M.J. O'Linghin [3] who ascribed the anomalous degradation of some HEMT devices to surface chemical reactions induced by radiation.

5.4 Comparison with MESFETs

The effect of γ-ray radiation on HEMTs was further compared to that on MESFETs. The comparison of radiation hardness of 2D and 3D devices included devices with GaAs and AlGaAs buffer layers. The comparison was limited on the variation of the threshold voltage and the source series resistance with the radiation dose, sice these parameters affect significantly the device performance. All MESFETs were found to follow the general empirical equation

$$\frac{\Delta X}{X_o} = m \cdot D^b$$

where the parameter Xis either the series resistance or the threshold voltage and m and b are fitting parameters.

In MBE MESFETs, studied in our laboratory [15], the fitting parameters were found to be $m_R = 1.5 \times 10^{-4}$ and $b_R = 0.397$ for the series resistance and $m_{th} = 9.8 \times 10^{-5}$ and $b_{th} = 0.373$ for the threshold voltage. A comparison of the power law factors

shows that in MESFETs they are much larger than in HEMTs ($m_R=3.2\times10^{-3}$, $b_R=0.21$, $m_{th}=3\times10^{-3}$, $b_{th}=0.113$) thus indicating that HEMTs are more radiation hard than MESFETs when they are subjected to γ-ray radiation.

5.5 Conclusions

The gamma ray induced degradation of HEMTs is almost negligible compared to that of He ions and neutrons. The main effects of γ-ray radiation can be summarised bellow

* Gamma ray radiation generates 0.6MeV Compton electrons which displace atoms in HEMT layers.
* The atom displacement increases of heterointerface roughness that degrades both the 2DEG mobility and saturation velocity
* The main electron traps induced in GaAs by γ-rays are the E3 one and a shallow donor about E_c-20meV. In a similar way a shallow donor and deep traps seems to be introduced in the AlGaAs layer although that was not detected by DLTS or other method.
* Radiation decreases the 2DEG density due to the decrease of the donor layer effective doping
* Gamma ray irradiation shifts the device threshold voltage.
  - The contribution of the buffer layer to the shift of the threshold voltage is attributed to the decrease of effective acceptor density.
  - The contribution of the donor layer to the shift of

the threshold voltage is attributed to the decrease of donor layer effective doping.

* The device performance is degraded due to increase of series parasitic resistances. The variation of series resistance with radiation dose seems to obey a power law relation
* The introduction of an AlGaAs buffer layer seems to improve the device radiation hardness
* Gamma ray radiation increase surface leakage in some devices resulting in an apparent increase of threshold voltage.
* Finally a comparison of radiation hardness shows that HEMTs are more resistant than MESFETs to gamma rays radiation.

6 CONCLUDING REMARKS

The present report investigates the effect of radiation on HEMTs. Both particle and electromagnetic radiations were used. The particle radiation consisted of either He ions or neutrons while the electromagnetic one consisted of gamma rays. Several structure HEMTs we employed in order to determine the best one for optimum radiaiton hardness. The study was furthere extended on MESFETs in order to compare the radiation hardness of the 2D and 3D electron gass devices. The radiation effects in HEMTs can be summarised bellow:

* Radiation induces defects due to atom displacement. The defects are complex ones in the case of He ion and neutron radiation while they are point defects in the case of gamma ray irradiation. The defects can be easily detected in GaAs by means of DLTS method while in AlGaAs this is possible under neutron radiation.
* The defects remove free carriers decreasing the net doping concentration in all layers thus turning them into more intrinsic ones and shifting the Fermi level towards midgap. This effect decreases the electric field intensity at heterointerface and lowers the subbands in the triangular quantum well. The simultaneous lowering of the subbands and the Fermi level throughout the structure leads to a decrease of electron density in the quantum well which in the case of a HEMT causes a shift of threshold voltage towards more positive voltages.

* The introduction of an AlGaAs buffer layer does not seem to improve significantly the structure radiation hardness because the threshold voltage is mainly determined by the shift of the AlGaAs donor layer pinch-off voltage.
* The introduction of a low temperature grown AlGaAs donor layer increases significantly the structure radiation hardness due to the presence of background defects introduced during growth.
* Radiation increases the density of heterointerface states and the interface roughness which furthere increases the scattering rate and decreases both the carrier mobility and saturation velocity.
* The introduction of a low temperature grown AlGaAs donor layer, although it degrades the carrier mobility and saturation velocity, decreases significantly the mobility and saturation velocity degradation, almost by a factor of two in the case of He ion radaition.
* An important degradation parameter in HEMTs is the parasitic series resistance. This depends strongly on the AlGaAs donor layer and quantum well heterointerface quality so the use of a low temperature grown AlGaAs donor layer enhances the series resistance radiation tolerance while the buffer layer structure doe not affect it.
* Finallly MBE MESFETs are less radiation hard than HEMTs excluding those which structure consists of a highly doped cahnnel grown on a LT buffer layer which are as hard

as HEMTs.

In conclusion the radiation hardness of HEMTs does not seem to depend on the buffer layer structure. The buffer layer structure deminishes the device response to ionizing radiation transients. An important parameter that increases the HEMT radiation hardness is the replacement of the conventional AlGaAs buffer layer with one grown at temperatures similar to these used in GaAs PM-HEMTs. This, independently of its consequences on the device initial performance, seems to enhance the devices radiation tolerance by a factor of two to four. A similar effect is observed in MBE MESFETs when their channel is hifghly doped and grown on a LT buffer layer. These structures exhibit a radiation hardness similar to that of HEMTs.

7 REFERENCES

1. B.K. Janousek, R.J. Krantz, W.L. Bloss, W.E. Yamada S. Brown, R.L. Remke and S. Witmer, IEEE Trans. Nuclear Science NS-36, 2223, (1989)
2. R.J. Krantz, W.L. Bloss and M.J. O'Loughin, IEEE Trans. Nuclear Science NS-35, 1438, (1988)
3. M.J. O'Linghin, IEEE Trans. Nuclear Science NS-34, 1808, (1987)
4. M.A. Listvan, P.J. Vold and D.K. Arch, IEEE Trans. Nuclear Science NS-34, 1664, (1987)
5. W.T. Anderson, M. Simons, W.F. Tseng, J.A. Herb and S. Bandy, IEEE Trans. Nuclear Science NS-34, 1669, (1987)
6. W.T. Anderson et. al., IEEE Trans. Nuclear Science NS-37 2065, (1990)
7. W.T. Anderson, A.R. Knudson, A. Meulenberg, H-L Hung, J. A. Roussos and G. Kiriakidis, IEEE Nuclear Science NS-37, 2065, (1990)
8. D. Pons, A. Mircea and J. Bourgoin, J Appl. Phys. 51, 4150, (1980)
9. D.V. Lang and L.C. Kimerling, Inst. Phys. Conf. Ser. 23, 581, (1975)
10. D.V. Lang, R.A. Logan and L.C. Kimerling, Phys. Rev. B15, 4874, (1977)
11. D. Pons, P.M. Mooney and J.C. Bourgoin, J Appl. Phys. 51, 2038, (1980)
12. D. Stevenard, J.C. Bourgoin and D. Pons, Physica 116B, 394, (1983)
13. Y. Yuba, M. Matsuo, K. Gamo and S. Namba, 13th ICDS, Coronado CA USA, p.973, (1984)
14. A.F. Behle and R. Zuleeg, IEEE Trans. Electron Devices ED-19, 993, (1972)
15. G.J. Papaioannou, B. Ioannou-Sougleridis and M.J. Papastamatiou, Physica Status Solidi (a) 131, K1, (1992) and G.J. Papaioannou, unpublished data
16. W.T. Anderson, M. Simmons and W.F. Tseng, IEEE Trans. Nuclear Sci. NS-33, 1442, (1986)
17. A.B. Campbell et. al., IEEE Trans. Nuclear Sci. NS-33, 1435, (1986)
18. M. Missus and E.H. Rodrick, Sol. State Electr. 28, 233, (1985)
19. W.T. Anderson, M. Simons, W.F. Tseng, J.A. Herb and S. Bandy, IEEE Trans. Nuclear Science NS-34, 1669, (1987)
20. K. Lee, M.S. Shur, T.J. Drummond and H. Morkoc, IEEE Trans. Electr. Dev. ED-30, 207, (1983)
21. K. Lee, M. Shur, T.J. Drummond, S.L. Su, W.G. Lyons, R. Fisher and H. Morkoc, J. Vac. Sci. Technol. B 1, 186, (1983)
22. M.S. Shur in "GaAs Devices and Circuits", Ch.10, I. Brodie and J.J. Muray Eds, Plenum Press N.Y., 1986
23. M.D. Feuer, IEEE Trans. Electron Dev. ED-32, 7, (1985)
24. D.C. Look, IEEE Trans. Electron Dev. ED-35, 133, (1988)
25. P. Roblin, L. Rice, S. Bibyk and H. Morkoc, IEEE Trans.

Electron Dev. ED-35, 1207, (1988)
26. H. Hida, T. Itoh and K. Ohada, IEEE Trans. Electron Dev. ED-33, 1580, (1986)
27. D. Delagebeaudeuf and N.T. Ling, IEEE Trans. Electron Dev. ED-29, 955, (1982)
28. G J Papaioannou, "Radiation effects in GaAs layers and Devices", Hellenic GSRT contract No.87EΔ-71
29. D.C. Look, C.E. Stutz and K.R. Evans, Appl. Phys. Letters 56, 668, (1990)
30. D.C. Look, K.R. Evans and C.E. Stutz, IEEE Trans. Electron Dev. ED-38, 1280, (1991)
31. A.F. Behle and R. Zuleeg, IEEE Trans. Electr. Devices ED-19, 993, (1972)
32. J.L. Nicols and W.S. Ginell, IEEE Trans. Nuclear Science NS-17, 52, (1970)
33. L.W. Aukerman et. al., J. Appl. Physics 34, 3590, (1963)
34. H.J. Stein, J. Appl. Physics 40, 5300, (1969)
35. R. Zuleeg and K. Lehovec, IEEE Trans. Nuclear Science NS-27, 1343, (1980)
36. N.J. Berg and A.G Lieberman, J. Appl. Phys. 46, 3475, (1975)
37. B.K. Janousek, W.E. Yamada and W.L. Bloss, IEEE Trans. Nuclear Sci. NS-35, 1480, (1988)
38. A.B. Campbell et. al., IEEE Trans. Nuclear Sci. NS-33, 1435, (1986)
39. G.M. Martin, E. Esteve, P. Langlade and S. Makram-Ebeid, J. Appl. Phys. 56, 2655, (1984)
40. R. Magno, M.. Spencer, J.G. Geissner and E.R. Weber, 13th Intern. Conf. on Defects in Semiconductors (ICDS) Coronado 1984, Ed. L.C. Kimerling and J.M. Parsey Jr, p.981, (1984)
41. I.D. Hawkins and A.R. Peaker, Appl. Phys. Letters 48, 227, (1986)
42. R. Worner, U. Kaufman and J. Schneider, Appl. Phys. Letters 40, 141, (1982)
43. B.K. Janousek, W.E. Yamada and W.L. Bloss, IEEE Trans. Nuclear Sci. NS-35, 1480, (1988)
44. J.Y. Chang, M.H. Badawi and A. DeCicco, IEEE Trans. Nuclear Sci. NS-36, 2068, (1989)
45. B.K. Janousek, W.E. Yamada, R.J. Krantz an W.L. Bloss, J. Appl. Phys. 63, 1678, (1988)
46. A.B. Campbell et. al., IEEE Trans. Nuclear Sci. NS-33, 1435, (1986)
47. J. Borrego, R.J. Gutmann, S.B. Moghe and M.J. Chudzicki, IEEE Trans. Nuclear Sci. NS-25, 1436, (1978)
48. R. Zuleeg, J.K. Notthoff and G.L. Troeger, IEEE Trans. Nuclear Sci. NS-29, 1656, (1982) and NS-30, 4151, (1983)
49. W.T. Anderson and S.C. Binari, IEEE Trans. Nuclear Sci. NS-30, 4205, (1983)
50. J.C. Garth, E.A. Burke and S. Woolf, IEEE Trans. Nuclear Sci. NS-32, 4382, (1985)
51. M. Kitagawa and K. Nakamura, IEEE Trans. Nuclear Sci. NS-34, 1704, (1987)
52. M. Nishiguchi et. al., IEEE Trans. Nuclear Sci. NS-37,

2071, (1990)
53. A. Meulenberg et. al., IEEE Trans. Nuclear Sci. NS-34, 1745, (1987)
54. T.I. Kol'chenko and V.M. Lomako, Radiat. Eff. 37, 67, (1978)
55. J.W. Farmer and D.C. Look, Phys. Review B 21, 3389, (1980)
56. K. Aono et.al.,"Symp. GaAs and Related Compounds 1986", p.527, (1986)
57. M. Yamaguchi and C. Uemura, J. Appl. Phys. 57, 604, (1985)
58. D. Pons, P.M. Mooney and J. Bourgoin, J. Appl. Phys. 51, 2038, (1980)
59. W.T. Anderson, M. Simons, W.F. Tseng, J.A. Herb and S. Bandy, IEEE Trans. Nuclear Sci. NS-34, 1669, (1987)